Evaluation of climate change data for wind energy applications

SET3901: Thesis Project

T. Kashyap

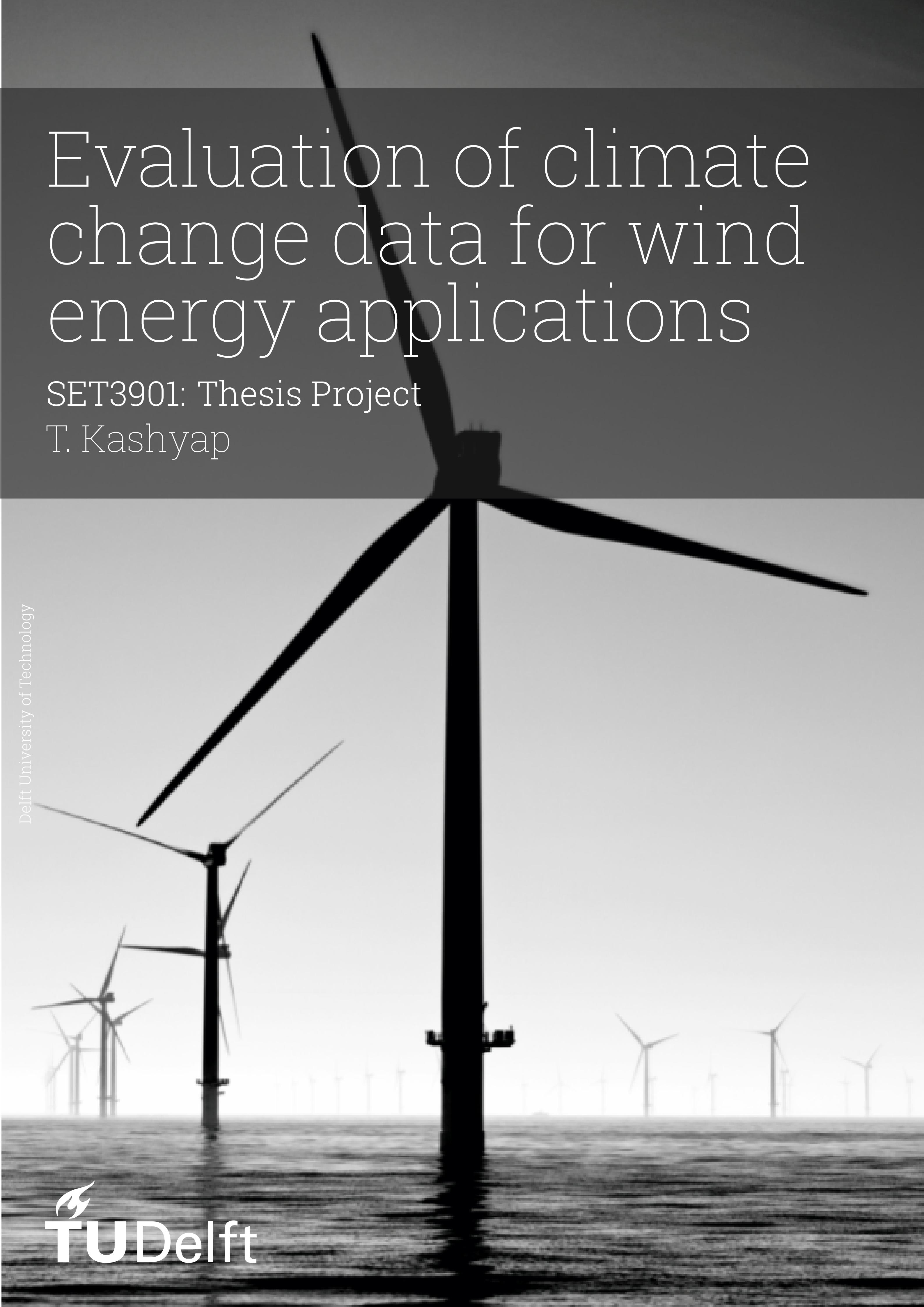

Delft University of Technology

TU Delft

Evaluation of climate change data for wind energy applications

by

Tanya Kashyap

to obtain the degree of:
Master of Science in Sustainable Energy Technology at Delft University of Technology
to be defended publicly in July 2024

RWE Offshore Wind, Netherlands
Faculty of Electrical Engineering, Mathematics and Computer Science, Delft University of Technology

Student number:	5689287
Thesis Committee:	Prof. Dr. S. J. Watson, TU Delft supervisor
	Dr. A. Sebastiani, RWE supervisor
	Dr. A. Meyers, TU Delft
Place:	Faculty of Aerospace Engineering, Delft University of Technology
Project Duration:	Dec, 2023 - July, 2024

TU Delft

Preface

As I write this last part of my thesis, I feel very honored and grateful. I worked on this research for 8 months and it makes me very proud to have learned so many things, not just academically but in life as well. I learned how to balance life.

I want to extend my gratitude to my daily supervisor, Dr. Alessandro Sebastiani, and my university supervisor, Prof. Dr. Simon Watson, who guided me, encouraged me at every stage, and were always there with their valuable feedback. I feel truly honored to have done my thesis under them and to have them in my thesis committee.

I also want to thank Dr. Angela Meyers for agreeing to assess my work by being a part of my thesis committee as well.

I moved to The Netherlands in August '22, leaving my home and my family behind. I feel extremely lucky to have met some of the nicest people here who made living alone easier. I want to thank all my friends who made my journey extremely special and I am happy to have grown together with them in life. Lastly, to my family, for being the pillar of my strength, especially my younger brother, Madhav, who called me every day even when we had nothing to talk about, thank you for everything. This is the end of a beautiful journey at TU Delft and I will always cherish each and every moment throughout my life.

T. Kashyap
Delft, July 2024

Summary

Climate change and wind energy are interlinked, with wind energy being crucial for reducing greenhouse gas emissions that drive climate change. Conversely, climate change poses a threat to the wind energy industry due to potential reductions in wind resources in key regions, although it may also enhance wind resources and profitability in other areas. This interplay underscores the connection between renewable energy adoption and climate adaptation strategies. The impact of climate change on wind energy is assessed using climate projections from Global Climate Models (GCMs) and Regional Climate Models (RCMs). GCMs have resolutions as low as 500 km, while RCMs can achieve resolutions of 10-50 km. To improve the resolution and capture smaller details, the process of downscaling is used, which can be either statistical (data-driven) or dynamical (physics-based).

This study investigates changes in mean wind speed variation at nine global sites using non-downscaled CMIP6 GCMs, statistically downscaled CMIP5/6 GCMs, and dynamically downscaled CMIP5 GCMs from CORDEX, under climate change scenarios with $4.5 W/m^2$ radiative forcing (RCP4.5 or SSP2-4.5, depending on data availability at the locations). Additionally, the study compares climate change scenarios RCP4.5/SSP2-4.5 and RCP8.5/SSP5-8.5 using the statistically downscaled CMIP GCMs. It examines impacts on wind resource availability, annual energy yield, sensitivity factor, and capacity factor, comparing these to historical data. Additionally, the research assesses revenue from Annual Energy Production (AEP) and compares historical projections from GCMs with reanalysis data, which integrates historical observations with advanced numerical models.

This research found that the non-downscaled CMIP6 GCMs and statistically downscaled GCMs exhibit the same trend and produce similar results when predicting the risk of wind speed decline at 8 out of the 9 sites analyzed. For the 9th site, a risk was predicted by 83% of the statistically downscaled GCMs, with a decline in wind speed variation of 99.9%, indicating a marginal difference. Given these findings, non-downscaled CMIP6 GCMs are effective for predicting wind speed declines and can be reliably used in place of statistically downscaled GCMs for most sites, eliminating the need for the more resource-intensive process of statistical downscaling. The CORDEX models indicate a significant influence of GCMs on mean wind speed projections, as different RCMs coupled with the same GCMs yield similar results. Consequently, to ensure a reliable analysis, it is recommended to include as many GCMs as possible.

To assess the impact of wind speed variation, two onshore and two offshore sites were selected. A larger decrease in AEP and consequently the capacity factor was observed at the onshore sites compared to the offshore sites, primarily due to the complex terrains of the onshore sites, which also resulted in higher sensitivity factors. The site with more complex terrain demonstrated higher sensitivity compared to the one with less complex terrain. Additionally, the revenue generated was adversely affected by the terrain, despite high mean electricity prices.

When comparing historical projections from non-downscaled CMIP6 GCMs and statistically downscaled GCMs with reanalysis data, higher percent bias, mean absolute percentage error (MAPE), and lower correlation were observed for onshore sites. This is primarily attributed to the complex terrains of these sites. Additionally, an analysis of the distance between GCM grid points and reanalysis data sites in relation to MAPE revealed no significant correlation, indicating that the metrics do not depend on spatial proximity. Several factors contribute to these discrepancies, including significant differences in the resolution of the datasets, topographical representation, temporal and spatial averaging, data assimilation processes, and the capture of internal climate variability. These differences lead to unreliable and inconsistent results when comparing historical data from GCMs with reanalysis data. Therefore, while GCMs are invaluable for understanding broad climate trends and making future projections, their direct comparison with reanalysis data for historical periods requires careful consideration. Understanding the limitations and appropriate methodologies for such comparisons is essential to avoid misleading conclusions.

Contents

Preface i

Summary ii

List of Figures vi

List of Tables vii

Nomenclature viii

1 Introduction 1

2 Background 3
- 2.1 Climate change and wind energy . . . 3
- 2.2 Data Types in Wind Resource Assessment . . . 5
- 2.3 Climate Change Scenarios . . . 9
- 2.4 Downscaling . . . 11
- 2.5 Data sources . . . 13
- 2.6 Wind Resource Assessment Parameters . . . 16
- 2.7 Fundamental Definitions . . . 19
- 2.8 Recent literature on climate change impact on wind resource assessment . . . 21

3 Methodology 25
- 3.1 Research Questions . . . 25
- 3.2 Sites in Analysis . . . 25
- 3.3 Data Collection and Preparation . . . 26
- 3.4 Design of Experiment . . . 28
- 3.5 Data Analysis . . . 32

4 Results and Discussion 36
- 4.1 Mean wind speed variation . . . 36
- 4.2 Annual Energy yield and Capacity factor . . . 59
- 4.3 Revenue . . . 63
- 4.4 Climate Models comparison with ERA5 . . . 64

5 Conclusion 70

References 72

A Appendix A 78
- A.1 Models list . . . 78

B Results 81
- B.1 CORDEX analysis . . . 81
- B.2 PDF for wind speeds at site NS2 and FR . . . 85
- B.3 Distance vs MAPE values . . . 87

List of Figures

2.1 Schematic for GCMs: Climate models represent complex systems of differential equations derived from fundamental principles of physics, fluid dynamics, and chemistry.[68]. 5
2.2 Schematic for RCMs[91] 6
2.3 Difference amongst the resolution of a GCM, RCM and satellite image [62] 7
2.4 Schematic of Reanalysis process [36] 7
2.5 Schematic showing Equivalence between SSP and RCP scenarios [91] 10
2.6 Schematic for Downscaling[94] 11
2.7 CMIP6 experiments schematic 14
2.8 EURO-CORDEX Domain[27] 15
2.9 Power curve of NREL 5 MW reference wind turbine [32] 17
2.10 Graphical representation of Energy yield equation 2.4 18

3.1 Maps of USA and Europe showing the sites analysed in this report 26
3.2 Datasets used in this work 28
3.3 Number of models utilised for each dataset and site under different climate change scenarios 29
3.4 Power curve of 5MW NREL reference wind turbine[32] 33
3.5 Shift in the Weibull curve upon decreasing the wind speed by a constant factor 34

4.1 Normalised mean wind speed from the year 2006 to 2060 at Site: NS1 37
4.2 Normalised wind speed projections for different future time periods under RCP 4.5/SSP2-4.5 at site: NS1. Confidence intervals show the 83% and 17% quantiles, point in between shows the median of the models 38
4.3 Comparison between normalised wind speed projections under climate change scenarios RCP 4.5 and RCP 8.5 for different future time periods at site: NS1. Confidence intervals show the 83% and 17% quantiles, point in between shows the median of the models 39
4.4 Normalised mean wind speed from the year 2006 to 2060 at Site: NS2 40
4.5 Normalised wind speed projections for different future time periods under RCP 4.5/SSP2-4.5 at site: NS2. Confidence intervals show the 83% and 17% quantiles, point in between shows the median of the models 41
4.6 Comparison between normalised wind speed projections under climate change scenarios SSP2-4.5 and SSP5-8.5 for different future time periods at site: NS2. Confidence intervals show the 83% and 17% quantiles, point in between shows the median of the models 41
4.7 Normalised mean wind speed from the year 2006 to 2060 at Site: FR 42
4.8 Normalised wind speed projections for different future time periods under RCP 4.5/SSP2-4.5 at site: FR. Confidence intervals show the 83% and 17% quantiles, point in between shows the median of the models 43
4.9 Comparison between normalised wind speed projections under climate change scenarios SSP2-4.5 and SSP5-8.5 for different future time periods at site: FR. Confidence intervals show the 83% and 17% quantiles, point in between shows the median of the models 43
4.10 Normalised mean wind speed from the year 2006 to 2060 at Site: IT 44
4.11 Normalised wind speed projections for different future time periods under RCP 4.5/SSP2-4.5 at site: IT. Confidence intervals show the 83% and 17% quantiles, point in between shows the median of the models 45

4.12 Comparison between normalised wind speed projections under climate change scenarios SSP2-4.5 and SSP5-8.5 for different future time periods at site: IT. Confidence intervals show the 83% and 17% quantiles, point in between shows the median of the models . . . 45
4.13 Normalised mean wind speed from the year 2006 to 2060 at Site: UK1 . . . 46
4.14 Normalised wind speed projections for different future time periods under RCP 4.5/SSP2-4.5 at site: UK1. Confidence intervals show the 83% and 17% quantiles, point in between shows the median of the models . . . 47
4.15 Comparison between normalised wind speed projections under climate change scenarios SSP2-4.5 and SSP5-8.5 for different future time periods at site: UK1. Confidence intervals show the 83% and 17% quantiles, point in between shows the median of the models . . . 47
4.16 Normalised mean wind speed from the year 2006 to 2060 at Site: UK2 . . . 48
4.17 Normalised wind speed projections for different future time periods under RCP 4.5/SSP2-4.5 at site: UK2. Confidence intervals show the 83% and 17% quantiles, point in between shows the median of the models . . . 49
4.18 Comparison between normalised wind speed projections under climate change scenarios RCP 4.5 and RCP 8.5 for different future time periods at site: UK2. Confidence intervals show the 83% and 17% quantiles, point in between shows the median of the models . . . 49
4.19 Normalised mean wind speed from the year 2006 to 2060 at Site: UK3 . . . 50
4.20 Normalised wind speed projections for different future time periods under RCP 4.5/SSP2-4.5 at site: NS2. Confidence intervals show the 83% and 17% quantiles, point in between shows the median of the models . . . 51
4.21 Comparison between normalised wind speed projections under climate change scenarios RCP 4.5 and RCP 8.5 for different future time periods at site: NS2. Confidence intervals show the 83% and 17% quantiles, point in between shows the median of the models . . . 51
4.22 Normalised mean wind speed from the year 2006 to 2060 at Site: NA1 . . . 52
4.23 Normalised wind speed projections for different future time periods under RCP 4.5/SSP2-4.5 at site: NA1. Confidence intervals show the 83% and 17% quantiles, point in between shows the median of the models . . . 53
4.24 Comparison between normalised wind speed projections under climate change scenarios RCP 4.5 and RCP 8.5 for different future time periods at site: NA1. Confidence intervals show the 83% and 17% quantiles, point in between shows the median of the models . . . 53
4.25 Normalised mean wind speed from the year 2006 to 2060 at Site: NA2 . . . 54
4.26 Normalised wind speed projections for different future time periods under RCP 4.5/SSP2-4.5 at site: NA2. Confidence intervals show the 83% and 17% quantiles, point in between shows the median of the models . . . 55
4.27 Comparison between normalised wind speed projections under climate change scenarios RCP 4.5 and RCP 8.5 for different future time periods at site: NA2. Confidence intervals show the 83% and 17% quantiles, point in between shows the median of the models . . . 55
4.28 Long term mean wind speed during operational years by 11 CORDEX models under RCP4.5. Wind speeds with same colour represent same GCM used by different RCMs 59
4.29 PDF for wind speeds at site NS1 and IT before and after 10% decline . . . 61
4.30 Error metrics calculated between historical ERA5 reanalysis data and historical wind speed projections from CMIP6 GGCMs for NS1, NS2, FR and IT . . . 64
4.31 Correlation metrics calculated between historical ERA5 reanalysis data and historical wind speed projections from CMIP6 GGCMs for NS1, NS2, FR and IT . . . 65
4.32 Scatter plot of distance vs MAPE calculated for CMIP6 wind speed projections at sites FR, NS1, NS2 and IT. . . . 66
4.33 Error metrics calculated between historical ERA5 reanalysis data and historical wind speed projections from statistically downscaled CMIP GGCMs for NS1, NS2, FR and IT 67

4.34 Correlation metrics calculated between historical ERA5 reanalysis data and historical wind speed projections from statistically downscaled CMIP GGCMs for NS1, NS2, FR and IT 68

B.1 Mean wind speed projected by 11 CORDEX models at site: NS1 81
B.2 Mean wind speed projected by 11 CORDEX models at site: NS2 82
B.3 Mean wind speed projected by 11 CORDEX models at site: FR 82
B.4 Mean wind speed projected by 11 CORDEX models at site: IT 83
B.5 Mean wind speed projected by 11 CORDEX models at site: UK1 83
B.6 Mean wind speed projected by 11 CORDEX models at site: UK2 84
B.7 Mean wind speed projected by 11 CORDEX models at site: UK3 84
B.8 PDF for wind speeds at site NS1 and IT before and after 10% decline 85

List of Tables

2.1 Overview Climate Change Effects on Wind Energy 4
2.2 Shared Socioeconomic Pathways as per IPCC Sixth Assessment Report [49] 9
2.3 Representative Concentration Pathways and their Projected Impacts[48] 10
2.4 Comparison between Dynamical and Statistical Downscaling Methods 13

3.1 List of sites used in the project 25
3.2 Time Periods chosen to analyse wind speed variation 27
3.3 NREL 5MW wind turbine specifications[32] 27
3.4 CMIP6 models used in this report for raw data projections 30
3.5 CMIP6 and corresponding RCM models used in CORDEX downscaling 31
3.6 Datasets used for comparison with reanalysis data 35

4.1 Risk assessment based on 83% quantile for different sites under various climate models 56
4.2 Comparison between climate change scenarios RCP4.5/SSP2-4.5 and RCP8.5/SSP5-8.5 for the risk assessment using statistically downscaled CMIP GCMs during operational period (2030-2060). A risk is reported when 83% of the GCMs show a decline in the long term wind speed variation with respect to the historic projections. 57
4.3 Risk assessment for different future periods and datasets 57
4.4 Comparison between climate change scenarios RCP4.5/SSP2-4.5 and RCP8.5/SSP5-8.5 for the risk assessment using statistically downscaled CMIP GCMs in near, mid and far future. The mark 'x' represents a reported risk, d2a: RCP4.5/SSP2-4.5 and d2b: RCP8.5/SSP5-8.5. 58
4.5 AEP based on variation in wind speed (GWh) 60
4.6 Relative change in AEP based on variation in wind speed 60
4.7 Sensitivity Factor based on decrease in wind speed variation 60
4.8 Summary of relative changes in wind speed variation, AEP, and sensitivity factor by different datasets under different scenarios for site in Italy 61
4.9 Capacity Factor based on decrease in wind speed variation 62
4.10 Relative change in Capacity factor based on variation in wind speed 62
4.11 Summary of relative changes in wind speed variation, AEP, and capacity factor under different scenarios for site in Italy 62
4.12 Revenue (million Eur/year) based on decline in wind speed 63
4.13 Revenue (million Eur/year) generated at site IT based on decline in wind speed predicted by different datasets 63
4.14 Distances from Reference Point for Different Sites 69

A.1 List Downscaled CMIP 6 models used in this report 78
A.2 List of downscaled CMIP5 Models used in this study 79

B.1 Scale and shape factor and AEP values based on decline in wind speed 86
B.2 Comparison of Distance and Bias for Wind Speed Change Factors across Different Sites 87

Nomenclature

Abbreviations

Abbreviation	Definition
AEP	Annual Energy Yield
AMIP	Atmospheric Model Intercomparison Project
CDF	Cumulative Distribution Function
CDS	Climate Data Store
CMIP	Coupled Model Intercomparison Project
CMIP5	Fifth phase of Coupled Model Intercomparison Project
CMIP6	Sixth phase of Coupled Model Intercomparison Project
CORDEX	Coordinated Regional Climate Downscaling Experiment
DECK	Diagnostic, Evaluation and Characterization of Klima
ECMWF	European Centre for Medium-Range Weather Forecasts
ERA5	ECMWF Re-Analysis 5th generation
EURO-CORDEX	Coordinated Regional Climate Downscaling Experiment Europe domain
GCM	Global climate model
GHG	Green House Gas
IAM	Integrated Assessment Model
IEA	International Energy Agency
IPCC	Intergovernmental Panel on Climate Change
MBC	Multivariate quantile Mapping Bias Correction
MAPE	Mean Absolute Percent Error
MIP	Model Intercomparison Projects
NREL	National Renewable Energy Laboratory
PBIAS	Percentage Bias
PDF	Probability Distribution Function
PES	Price Elasticity of Supply
QDM	Quantile Fata Mapping
RCM	Regional Climate model
RCP	Representative Concentration Pathway
SSP	Shared Socioeconomic Pathway
WCRP	World Climate Research Project

Symbols

Symbol	Definition	Unit
A	Swept area of wind turbine	$[m^2]$
a	Scale factor	-
c_p	Coefficient of performance	-
E_y	Annual energy yield	[Wh]

Symbol	Definition	Unit
k	Shape factor	-
N	Total hours or days	[h] or [days]
o$_i$	Observed wind speed	[m/s]
P	Power harnessed from wind	[Watts]
p$_i$	Predicted wind speed	[m/s]
α	Wind shear exponent	-
$\bar{p}$	Mean of predicted wind speeds	[m/s]
$\bar{o}$	Mean of observed wind speeds	[m/s]
$\bar{u}$	Mean of wind speeds	[m/s]
$\bar{X}_t$	Central moving mean wind at time t	[m/s]
ρ	Density	[kg/m^3]
u	Wind speed	[m/s]
v(z)	Wind speed at height z	[m/s]
v$_{ref}$	Wind speed at reference height	[m/s]
z	Hub height	[m]
z$_{ref}$	Reference height	[m]
u_{era5}	Velocity	[m/s]

1 Introduction

As per the European Commission, the decade of 2011-2020 has been recorded to be the warmest decade in the history of time with the global average temperature that reached 1.1 °C above the pre-industrial levels in 2019. Human activities such as deforestation, burning fossil fuels, and farming livestock have been continuously influencing the climate and the earth's temperature. As a result, large amounts of greenhouse gases are accumulating in the atmosphere on top of the naturally existing ones leading to an increase in greenhouse effect and, ultimately, global warming. There is an increasing rate of 0.2°C per decade in global warming due to human activities in which carbon dioxide is the largest contributor. The CO_2 concentration in the atmosphere rose by 48% as compared to its pre-industrial levels (before 1750) by the year 2020. Other greenhouse gases like methane and nitrous oxide are emitted in smaller quantities. There are also natural causes like volcanic activities and solar radiation that have contributed about $\pm$ 0.1 °C to the warming between the years 1890 and 2010 [37].

The 2015 Paris Agreement aims to limit global warming to 1.5°C above pre-industrial levels and prevent it from exceeding 2 °C. This target is crucial as scientific studies indicate that surpassing it could lead to severe and irreversible effects on ecosystems and human societies [37]. Potential consequences include more frequent and intense extreme weather events, rising sea levels, loss of biodiversity, threats to food security, and disruptions to economic and social systems [54]. Several strategies exist to reduce greenhouse gas (GHG) emissions including enhancing energy efficiency across all sectors, adopting low-carbon and renewable energy technologies, utilizing carbon capture and storage, and modifying land use. Wind energy is becoming increasingly important in the global energy mix due to its environmental benefits, renewable nature, and economic viability. Recognized by the International Energy Agency (IEA), wind energy is the fastest-growing renewable energy source and contributed about 17% of global electricity generation in 2021, with this figure expected to rise. Wind energy projects vary in scale from community-based farms to large offshore installations.

Climate change and wind energy have a bidirectional relationship. Transitioning to wind energy is essential for reducing greenhouse gas emissions that contribute to climate change. Conversely, climate change is a threat to the wind energy industry as variations in the global climate might result in reductions of the wind resource in critical regions of interest [73]. However, it should be mentioned that variations of the global climate might also result in the increase of the wind resource, increasing the profitability of wind projects in certain regions[54]. This dynamic highlights the interconnection between renewable energy adoption and climate adaptation strategies [54].

The impact of climate change on wind energy can be investigated through climate projections obtained by climate models. Global climate models (GCMs) have a resolution as low as 500km and the Regional climate models can have a resolution of 10-50km [10]. The resolution of global climate models is often increased with the help of a process called downscaling which is typically of two types: Statistical and Dynamical. Statistical downscaling is data driven and uses historical data to establish relationships between global climate models and observations/reanalysis data[10, 41]. Dynamical downscaling is physics based and needs detailed data on topography and land use [4, 80].

This paper studies how these different datasets project the change in mean wind speed variation for 9 different sites across the world. It also presents the impact on Annual energy yield, capacity factor and electricity prices. A comparison is also made between the historical projections given by the Global climate models and the reanalysis data that is the integration between historical observations and advanced numerical models.

The structure of the report is as follows: chapter 2 provides a comprehensive background necessary to proceed with the research, starting with the effects of climate change on wind energy and detailing various data types used in wind resource assessment. It also covers climate change scenarios, downscaling methods, and data retrieval sources. Key parameters in wind resource assessment and fundamental definitions are explained, followed by a review of recent literature on climate change impacts. Chapter 3 outlines the research aims, site selection, data collection, and preparation processes, including the use of climate models and reanalysis data. The design of the experiment and data analysis methods are described to ensure a thorough evaluation of wind power generation potential, considering variations in wind speed, energy yield, and electricity pricing. Chapter 4 presents the results and discussion based on the methodology followed in chapter 3 and lastly, chapter 5 concludes this report.

2 Background

The assessment of the wind resource plays a crucial role in the development and optimization of wind energy projects. This chapter provides an overview of the essential components involved in wind resource assessment. It begins with Section 2.1, discussing the impact of climatically affected meteorological parameters on wind energy. Section 2.2 details the different types of datasets used in climate change assessment, including global and regional climate models and reanalysis data. Section 2.3 covers climate change scenarios and their implications, while Section 2.4 explains downscaling methods used to refine climate model outputs. Section 2.5 describes the sources for data retrieval. Section 2.6 examines key parameters in wind resource assessment, followed by Section 2.7, which defines fundamental concepts and metrics. Section 2.8 reviews recent literature on the impact of climate change on wind resources. The chapter concludes with a brief discussion on the energy system integration technologies to tackle the wind energy intermittency. This comprehensive background lays the groundwork for understanding the methodologies and analyses presented in the subsequent chapters.

2.1. Climate change and wind energy

As per the United nations organisation, climate change is defined as the shift in weather patterns and temperatures prevailing for long terms either due to natural causes like sun's activity, substantial volcanic eruptions or due to human activities. In fact, because of constant burning of fossil fuels, the latter has been the main reason for climate change since the 1800s [90]. This has led to increased green house gas emissions that trap sun's heat causing the temperatures to rise and resulting in global warming on the planet [88]. The increased global warming also has impacts on many parameters that link to wind energy production [73]. For example, changes in wind speed, wind direction, air density, icing, sea levels and wave heights can affect both production and consumption from wind energy systems [46].

The impact on wind energy can be negative or positive depending upon the geographical location since the climate change impacts vary from one region to another [46]. Table 2.1 below provides an overview of the impacts of various physical parameters on the wind energy production. It describes how different meteorological changes affect the operational conditions and potential wear of turbines, which could lead to either an increase or decrease in electricity generation. Factors such as increased wind speed improve wind conditions and may lead to higher electricity generation, while decreases in wind speed or adverse changes in wind patterns can worsen conditions and potentially reduce energy generation. The table also notes that changes in wave and tidal patterns can present challenges for accessibility and infrastructure stability.

Table 2.1: Overview Climate Change Effects on Wind Energy

Meteorological Change	**Impact on Wind Energy Resources**	**Impact on Electricity Generation**
Temperature variations [75, 74]	Could modify air density and wind flow, high temperatures can hinder turbine operations	Possible variation in energy production.
Wind speed increase [52, 63]	Generally favorable wind conditions	Potential for enhanced energy production, barring storms can decrease energy or lead to shut downs
Wind speed decline [52, 63]	Deterioration of wind conditions	Diminished energy production
Variability in wind patterns [92]	Affects air density and wind patterns	Could either enhance or reduce energy production
Change in seasonal or daily distribution of wind [9, 46]	Uncertain production of wind energy	Difficulty matching the wind energy input to grid and daily load demand.
Increased precipitation [63]	Potentially speeds up wear on turbine blades	Does not directly alter energy output
Reduced precipitation [63]	Not applicable to wind resource impact	No direct effect on power generation
Glacial thawing [74, 64]	Relevant only if associated with flooding	Could disrupt generation if flooding occurs and lead to decreased generation
Flooding events [46, 52]	Possible equipment damage	Potential interruptions in power supply
Storm surges [46, 52]	Possibility of harm to structures, more downtime	Decreased power availability due to damage
Oceanic tidal shifts [74]	Risk of exposing underwater cables due to scour increase	Possible disruptions in energy conveyance

From table 2.1 it can be noticed that whether climate change is a boon or bane for wind energy production is not certain. Depending upon the geographical location of the wind farms, the energy yield can be positively or negatively affected. The estimation of prediction regarding the impacts of climate change are derived from sophisticated mathematical models like, Global Climate Models (GCMs), Regional Climate Models (RCMs), and reanalysis datasets [70]. These models explore the extent to which natural causes, human activities or both of them together are responsible for climate change. The findings and future outlooks derived from these analyses offer critical insights that significantly enhance decision-making processes at various governance levels, including national, regional, and municipal. This information proves instrumental in guiding strategic planning and policy development across a broad spectrum of areas including the energy policies [70]. A detailed explanation of these models can be found in the following sections.

2.2. Data Types in Wind Resource Assessment

2.2.1. Global climate Models (GCMs)

GCMs are complex instruments that simulate the interactions among the atmosphere, ocean, cryosphere, and land surface. They are considered the most advanced tools currently available for predicting how the global climate system will respond to rising concentrations of greenhouse gases [51]. GCMs employ a mixture of mathematical equations that encapsulate the underlying physics governing circulation processes, alongside empirical calculations derived from observational data[30]. It should be noted that investigation of mathematical formulae involved in the modeling of GCMs is out of the scope of this work.

Because of the complexity and interdisciplinary nature of atmospheric and oceanic circulation phenomena, modeling these processes necessitates making numerous assumptions. This also leads to a large number of computations required to simulate all relevant processes accurately. Moreover, uncertainty arises due to the incomplete understanding of various processes involved [30].

Several factors, such as spatial and temporal resolution, as well as the level of detail in representing various processes, significantly influence the GCM's capacity to depict the entire planetary system and, consequently, determine the model's accuracy and performance across different aspects. Climate models work by partitioning the Earth globe into a three-dimensional grid composed of cells that correspond to particular geographic positions and altitudes.

By design, GCMs estimate numerous variables, including surface radiation, humidity, temperature, precipitation and wind speeds at their original spatial and temporal resolutions [30, 51].

Within this framework, each component: the atmosphere, land surface, ocean, and sea ice, is represented by equations computed across the global grid for various climate parameters like temperature, wind speeds. Moreover, beyond simply calculating the evolution of each component over time, these models facilitate the exchange of water, heat, and momentum fluxes among the different parts. This allows them to function as a coupled system, with each component influencing and being influenced by the others [70].

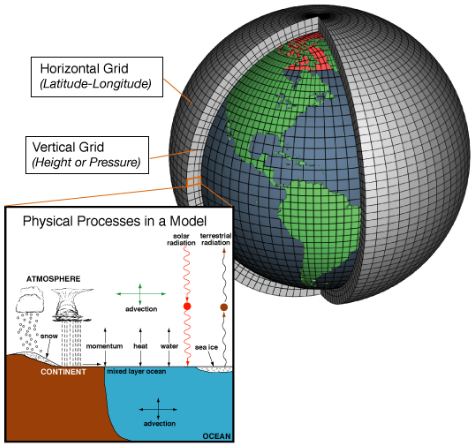

Figure 2.1: Schematic for GCMs: Climate models represent complex systems of differential equations derived from fundamental principles of physics, fluid dynamics, and chemistry.[68].

Model Resolution

GCMs, with spatial resolutions ranging from 100 km to 500 km, incorporate numerous vertical layers to accurately represent atmospheric and oceanic dynamics[30]. These models divide the Earth's surface into a three-dimensional grid of cells. Within this grid, processes simulated in each cell interact with neighboring cells, enabling the exchange of matter and energy over time. The resolution of the model is determined by the size of these grid cells: smaller cells correspond to higher model detail. However, finer-resolution models require more grid cells, thereby demanding greater computational resources for their execution [71].

Limitations

While there may be some divergence among climate models, these models are rooted in established physical principles, whether directly for simulated processes or indirectly for parameterized processes. The outcomes of model experiments undergo extensive scrutiny from a global community of modelers and researchers, such as those associated with the Intergovernmental Panel on Climate Change (IPCC), which helps mitigate uncertainty[70]. Nevertheless, GCMs have some limitations to them:

- GCMs face challenges in accurately reproducing real-world climate observations due to various sources of uncertainty, including the magnitude of future greenhouse gas emissions, computational constraints, incomplete understanding of atmospheric processes, and the inherently chaotic nature of the atmosphere [34].
- GCMs often have coarse spatial resolution and limited skill in representing daily and monthly

rainfall and temperature, necessitating additional computational steps before their use in impact studies or adaptation planning. This post-processing typically involves bias correction to mitigate known systematic errors and downscaling to generate output with higher spatial and temporal resolution.

- Temporal downscaling is necessary because GCMs often lack realistic daily climate data. Spatial downscaling is essential because the coarse resolution of GCMs prevents them from accurately representing features like topography, land use, and land cover, which influence local climate [34].

GCMs are limited in their ability to capture the detailed spatial variations in atmospheric and land surface processes that define the unique regional climate patterns. If future large-scale weather patterns interact differently with local terrain and coastlines compared to current patterns, the resulting changes at the local level could deviate significantly from the broad-scale projections generated by global models [13]. This is where regional climate models come into play. A detailed explanation has been provided in the subsection below:

2.2.2. Regional Climate Models (RCMs)

Regional climate models explicitly simulate the interactions between the large-scale weather patterns predicted by global models and the specific local characteristics of the region, providing more accurate insights into potential regional climate changes [13]. It is a computational tool used for predicting climate patterns within a specific geographic area. The rationale behind RCMs stems from the principle of 'downscaling'[69] which is further explained in section 2.4. RCMs operate by simulating atmospheric and land surface processes, incorporating high-resolution topographical data, land-sea contrasts, surface characteristics, and other Earth-system components. These models are driven by lateral and oceanic conditions obtained from either a GCM or observation-based datasets (reanalysis) [1]. Since RCMs are designed to cover limited geographical domains, they require explicit specification of boundary conditions, which are typically derived from the results of coarser GCMs or reanalysis datasets. RCMs are initialized with initial conditions and driven by time-variable conditions along their lateral-atmospheric boundaries and lower-surface boundaries. In essence, RCMs serve to refine and downscale global reanalysis or GCM simulations, enabling the simulation of climate variability with greater regional detail[1].

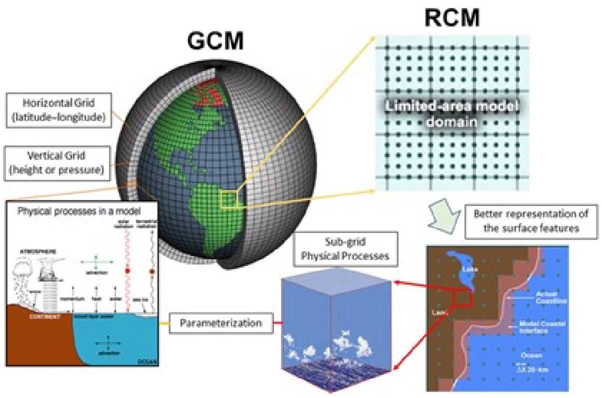

Figure 2.2: Schematic for RCMs[91]

Model Resolution

Regional models are occasionally labeled as thorough, coherent, and physically grounded interpolators or, in more vernacular language, as "zoom lenses" and can have a resolution of 10-50 km [65, 69, 62]. These benefit from being closer in scale to real-world observations, incorporating detailed information about topography, land cover, and soil types, all of which play significant roles in shaping the climate system. Consequently, regional climate models can utilize more real-life data compared to global models, resulting in simulations that are generally more accurate [62].
Figure 2.3 provides a visual to the difference amongst a GCM of resolution of 2° of latitude and longitude, an RCM with a resolution of 50km in comparison to a satellite image.

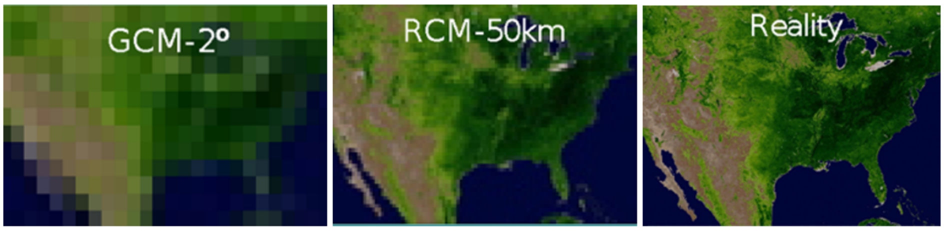

Figure 2.3: Difference amongst the resolution of a GCM, RCM and satellite image [62]

When exploring the capabilities the GCMs and the RCMs, it is crucial to realise the importance of observational data in validating these models.While these models provide projections based on law of physics, the observed climate variables help us assess the accuracy of these models and refine them. Here, the Reanalysis data comes into play. It assimilates large set of observations, from satellites to weather stations, into a coherent climate model framework and delivers a synthesized estimate of the state of the atmosphere at different scales [36]. The following section now details the process of making reanalysis datasets, their applications in climate science, and the role it plays in predictions of GCMs and RCMs by anchoring them to the reality of observed climate.

2.2.3. Reanalysis Data

Climate reanalyses integrate historical observations with advanced numerical models to produce comprehensive time series of diverse climate parameters. Widely embraced across the geophysical sciences, these datasets offer detailed insights into observed climate trends over recent decades [23]. By synthesizing various datasets into a uniformly spaced grid, reanalysis methods facilitate efficient comparison of observations while preserving the integrity of the original data collection model. This approach ensures that the historical record remains untainted by artificial factors [67]. Reanalyses represent the most exhaustive record available of past weather and climate, amalgamating observations with historical short-range weather forecasts re-run using modern forecasting models. With global coverage and temporal consistency, they are often regarded as 'maps without gaps', facilitating a thorough understanding of past climate conditions [36]. A very popular reanalysis data provider is European Centre for Medium-Range Weather Forecasts (ECMWF) delivering ERA5 reanalysis hourly data on several atmospheric, land-surface as well as sea-state parameters together including estimates of uncertainty [23]. The figure 2.4 depicts the schematic of the reanalysis data.

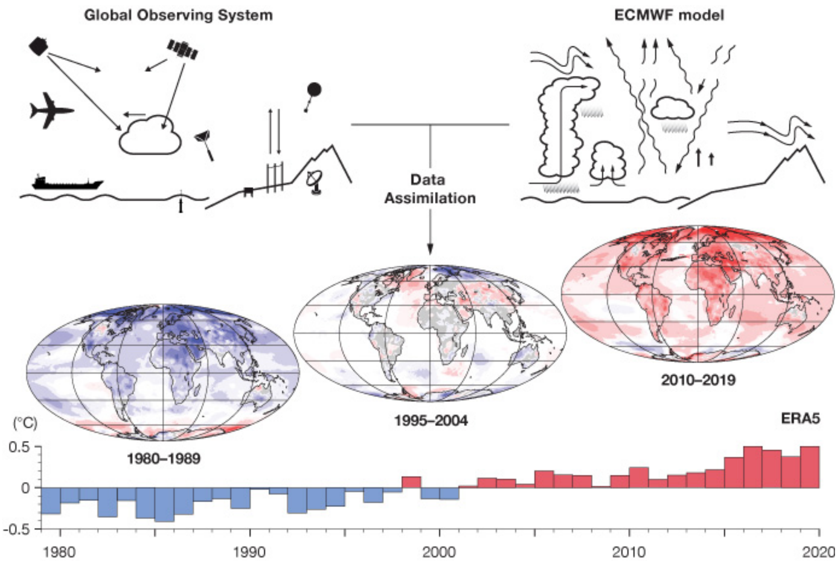

Figure 2.4: Schematic of Reanalysis process [36]

Reanalysis integrates model data with observations from around the globe, creating a globally complete and consistent dataset through the application of physics-based principles known as data assimilation.

This method, akin to that used in numerical weather prediction centers, involves combining previous forecasts with newly available observations to produce updated estimates of atmospheric conditions, termed analyses [24]. While similar to daily weather forecasting, reanalysis operates at a reduced resolution, enabling the generation of datasets spanning several decades. ERA5 offers global estimates at an hourly frequency with a horizontal resolution of approximately 31 kilometers and 137 vertical levels [25]. Unlike timely forecasts, reanalysis allows more time for the collection of observations and incorporation of improved versions of original data, enhancing the quality of the reanalysis product over time. Rigorous quality control measures are implemented throughout the reanalysis process to ensure accuracy, including the comparison of results with those from other organizations.[36].

Reanalysis data use in climate modeling

Reanalysis data plays a crucial role in a lot of aspects as mentioned below:

- High-Resolution Baseline Data: The detailed level of information provided by ERA5 due to higher spatial and temporal resolution makes it an ideal foundational dataset for examining climate variability and trends with greater detail than most GCMs can provide [36].
- Bias Correction Reference: ERA5 data serves as a valuable reference for correcting biases in climate model simulations, particularly for regional climate models (RCMs) or empirical statistical downscaling methods. By comparing model outputs with ERA5 data, researchers can detect and adjust systematic biases in temperature, precipitation, and other meteorological variables[1].
- Boundary Conditions for RCMs: In dynamical downscaling approaches, where RCMs are employed to generate higher-resolution climate projections for specific regions, ERA5 data offers crucial initial and boundary conditions. These conditions are necessary for driving the RCM simulations and ensuring consistency with observed global climate patterns [44].
- Evaluation and Calibration: ERA5 data is utilized to assess the performance of downscaling models by comparing the downscaled data with ERA5's observed climatic features. This comparison aids in fine-tuning the downscaling models to enhance their accuracy and reliability.

Despite the wide use of reanalysis data, there are certain drawbacks to it. ECMWF Copernicus identifies four main limitations [21] as mentioned below:

- The observational system: The quality of a reanalysis is inherently tied to the quality and density of the observational data it relies on. Reanalysis uses a combination of weather models and available observations to estimate the atmospheric state at specific times. Consequently, a reanalysis can only extend back to a certain historical point before it becomes unreliable. Typically, reanalyses are most reliable from 1979 onwards due to the extensive data provided by the satellite era, which began around that time and greatly enhances the quality of reanalysis data. ERA5, for example, extends back to 1950 because substantial data sources are available from that period. While some reanalyses extend further back, they rely on fewer observational sources, resulting in a lower number of well-represented variables.
- The weather model: The quality of the weather model significantly impacts the reanalysis. A more accurate model requires fewer observations to correct inherent errors. These errors arise from the model's simplified representation of reality, which is limited by spatial resolution and incomplete modeling of all real-world processes and interactions.
- The spatial representation: Reanalysis products are gridded, meaning they provide data for larger regions rather than specific points like weather stations. For example, ERA5 has a spatial resolution of about 30x30 km, so the data for a city within this grid will represent the combined environment of the entire grid area rather than the city itself. This implies that temperature values from the reanalysis might not accurately reflect the city's actual temperature but rather an average of the grid's diverse landscapes. Additionally, reanalysis accuracy varies globally, as observational data becomes sparser further back in time and coverage differs across regions.
- Varying degree of realism depending on the variable considered: Reanalyses generate numerous output variables, and the quality and representativeness of these measurements vary depending on the specific variables considered.

The Climate models are executed across various greenhouse gas emissions scenarios defined by IPCC, each depicting diverse potential outcomes for the future. In order to proceed further it is beneficial to take an overview of the climate change scenarios presented in the next section.

2.3. Climate Change Scenarios

Climate change scenarios describe how changes in the atmosphere due to factors like greenhouse gas emissions, air pollutants, and land use affect the energy balance of the global climate system [50]. The IPCC's AR5 report outlines four Representative concentration pathways (RCPs) based on their impact on the Earth's energy balance, showing different atmospheric compositions expected by the end of the 21st century [50]. The latest Assessment Report by IPCC, AR6 introduced the Shared Socioeconomic Pathways (SSPs) which are a further refinement to the RCPs depicting variations in population, economic growth, education, urbanization, and technological advancement that could influence future greenhouse gas emissions without even a climate policy [49, 93]. SSPs and RCPs are characterized by numerical designations such as RCP 4.5 or SSP5-8.5, which signify the anticipated alteration in radiative forcing from 1750 to the conclusion of the 21st century, in 2100 [49, 48]. Radiative Forcing is pivotal in dictating the alteration in globally-averaged temperature due to adjustments in the energy budget, whether induced by natural or human activities [20].An overview of the SSPs and RCPs has been presented in the table 2.2 and 2.3 below:

Table 2.2: Shared Socioeconomic Pathways as per IPCC Sixth Assessment Report [49]

SSP Scenario	Description	Approximated warming (2041–2060)	Approximated warming (2081–2100)	Very likely range in °C (2081–2100)
SSP1-1.9	Very low GHG emissions: CO2 emissions net zero by 2050	1.6 °C	1.4 °C	1.0 – 1.8
SSP1-2.6	Low GHG emissions: CO2 emissions net zero by 2075	1.7 °C	1.8 °C	1.3 – 2.4
SSP2-4.5	Intermediate GHG emissions: CO2 stable until 2050, then fall	2.0 °C	2.7 °C	2.1 – 3.5
SSP3-7.0	High GHG emissions: CO2 doubles by 2100	2.1 °C	3.6 °C	2.8 – 4.6
SSP5-8.5	Very high GHG emissions: CO2 triples by 2075	2.4 °C	4.4 °C	3.3 – 5.7

The SSP-based scenarios have been used in the latest set of climate model experiments, called CMIP6 or Sixth Phase of the Coupled Model Intercomparison Project. CMIP models play a crucial role in climate change analysis. Their outcomes have given a solid foundation to the AR6 for the robust evaluations of historical and projected climatic variations [15]. Similarly, RCPs have been incorporated in the CMIP5 that is the 5th phase of CMIP and aided the climate change assessment in the AR5 of IPCC [48]. Given below in figure 2.5 is a schematic presenting the equivalence between the SSPs and RCPs.

Table 2.3: Representative Concentration Pathways and their Projected Impacts[48]

RCP	Forcing	Temperature	Emission Trend
1.9	1.9 W/m^2	∼1.5°C	Very Strongly Declining Emissions
2.6	2.6 W/m^2	∼2.0°C	Strongly Declining Emissions
4.5	4.5 W/m^2	∼2.4°C	Slowly Declining Emissions
6.0	6.0 W/m^2	∼2.8°C	Stabilising Emissions
8.5	8.5 W/m^2	∼4.3°C	Rising Emissions

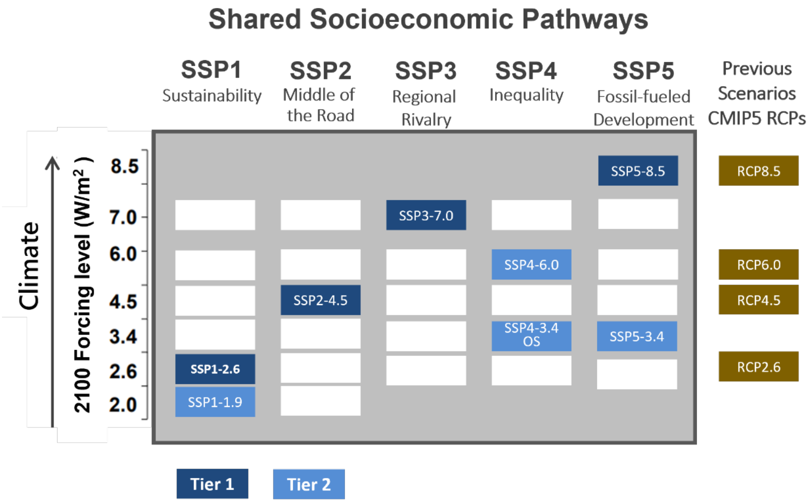

Figure 2.5: Schematic showing Equivalence between SSP and RCP scenarios [91]

The scenario simulation design is categorized into two phases, Tier 1 and Tier 2, based on priority. Each cell within the design represents a socioeconomic development path along with a corresponding feasible radiative forcing in the Integrated Assessment Model (IAM). Cells shaded in dark blue denote the first-phase climate model scenarios, those in light blue denote the second phase, while the brown cells on the right represent past RCP scenarios devoid of socio-economic elements, serving as a reference point [47].
In the above sections, the role of General Circulation Models (GCMs) in providing broad-scale climate projections and the broad capabilities of these models in capturing the essence of climate systems on a global scale was examined. Moreover, the utility of Regional Climate Models (RCMs) and reanalysis data for enhancing the understanding of climate dynamics at a regional level was discussed. However, there exists an imperative to further localize this information for it to be effectively used in local climate impact studies:Downscaling.

Downscaling techniques serve as a crucial methodological bridge, narrowing the resolution gap by employing statistical or dynamical methods to produce high-resolution climate data from the relatively coarser-resolution models [16]. Such detailed climate data are essential for assessing climate change impacts on localized phenomena. Moreover, downscaling is pivotal in the context of climate change adaptation and mitigation planning. It provides stakeholders and decision-makers with the detailed information needed for anticipating changes in climate at scales pertinent to local infrastructure, like watersheds, cities, and agricultural areas.

The use of downscaling techniques marks the convergence of large-scale patterns delineated by GCMs and RCMs with the granular details required for a comprehensive understanding and preparation for climate change at the community level[57]. The following section will explore the concept of downscaling, dissecting both the dynamical downscaling approach, which leverages high-resolution RCMs, and the statistical downscaling approach, which utilizes statistical techniques to refine GCM and RCM outputs into local climate projections [45].

2.4. Downscaling

The process of deriving local to regional-scale information, typically spanning 10 to 100 kilometers, from larger-scale modeled or observed data is commonly referred to as downscaling[10].While Global Climate Models (GCMs) offer valuable scientific insights into climate system dynamics over various time scales, their raw output may not always meet the interdisciplinary needs of stakeholders. The spatial resolution of GCMs may not match the requirements of end-use applications. Various landscape elements, including mountains, water bodies, infrastructure, land cover, and climate components like convective clouds and coastal breezes, exhibit scales much smaller than the typical 100–500 kilometers represented in Global Climate Models (GCMs). These finer-scale heterogeneities hold significance for decision-makers seeking information on potential impacts at scales ranging from 10 to 50 kilometers[10, 41]. Moreover, GCM output often contains biases compared to observational data, making it unsuitable for direct use in downstream applications[41].That is why downscaling the GCMs is a sensible approach.

The downscaling process enhances the coarse output of Global Climate Models (GCMs) by incorporating additional information to achieve a more realistic representation at a finer scale. This involves capturing sub-grid scale differences and variations. Downscaling can address both spatial and temporal aspects of climate projections. Spatial downscaling involves methods to generate finer-resolution spatial climate data from coarser-resolution GCM output, such as refining from a 500 kilometers grid cell to a 20 kilometers resolution or even specific locations. Temporal downscaling, on the other hand, focuses on deriving detailed temporal information from coarser-scale temporal GCM output, such as extracting daily rainfall sequences from monthly or seasonal rainfall data [10].Figure 2.6 illustrates the schematic of downscaling. The top layer shows the low-resolution grid of a GCM, which is then refined into a higher-resolution grid of an RCM, showing an increase in the details. As the scale is more localized, the models start incorporating complex features such as hydrology, soil layers, vegetation, and topography. The process integrates human social systems and links large-scale climate processes to local impacts and responses [94]. Downscaling is also crucial step in wind resource assessment but the question rises why?

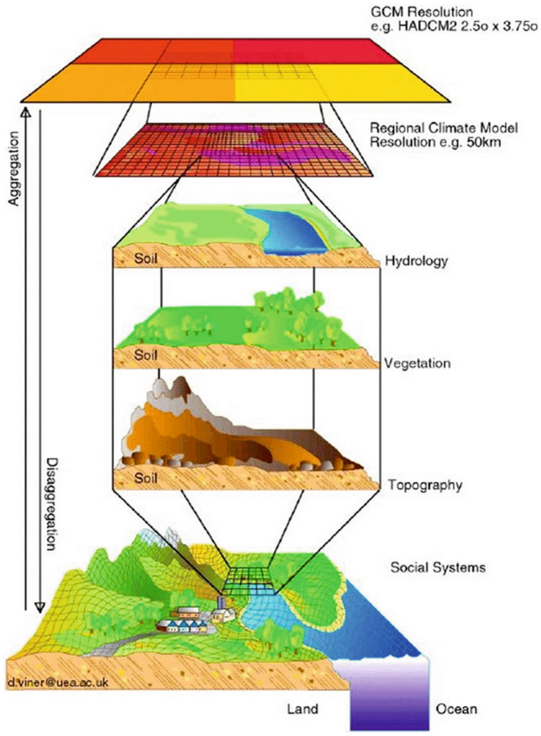

Figure 2.6: Schematic for Downscaling[94]

The variability of winds close to the ground in areas with diverse topography is often significant and localized which the GCMs cannot capture. However, by using downscaling techniques, it's possible to predict these complex wind patterns more efficiently [40]. A multitude of downscaling techniques have been devised to extract local climate change details from the broad-scale outputs of Global Climate Models[45].

Downscaling Techniques can be broadly divided into two categories: Statistical Downscaling and Dynamical Downscaling. The following subsections now discuss these methods in detail.

2.4.1. Dynamical Downscaling

Dynamical downscaling primarily relies on RCMs, which produce higher-resolution output by simulating atmospheric physics over a specific area [4]. RCMs utilize the large-scale atmospheric data provided by Global Climate Models at the boundaries and integrate additional factors such as complex topography, land-sea contrast, surface variations, and detailed physical processes to produce realistic climate data

at a spatial resolution typically ranging from 20 to 50 kilometers [10]. However, since RCMs are nested within GCMs, the accuracy of the downscaled output depends on the quality of the large-scale input from the GCM and any biases it may have [80]. Despite capturing regional-scale features better than coarse-resolution GCMs, RCM outputs still contain systematic errors and often require bias correction and further downscaling to achieve higher resolution [10]. In general, Regional Climate Models (RCMs) excel in spatial downscaling rather than temporal downscaling. They tend to perform better at monthly or coarser timescales due to significant biases in daily scale outputs [34]. Some advantages and disadvantages of dynamical downscaling, as highlighted by Mearns et al [61] are given below:
Advantages

- Offers precise spatial and temporal resolution
- Suitable for regions with important meso-scale features like mountain ranges
- Vital for analyzing regional climate, especially in areas with limited observational data

Disadvantages

- Uncertainty exists in sub-grid process parameterization
- Fails to rectify systematic biases inherited from GCMs
- Demands significant computational resources
- Absence of feedback between RCMs and GCMs may impact GCM output
- Often necessitates the application of statistical bias correction techniques

With the completion of the discussion on dynamical downscaling, the next subsection now shifts to examining another pertinent approach: Statistical downscaling.

2.4.2. Statistical Downscaling

In statistical downscaling, empirical relationships are established between historical or current large-scale atmospheric conditions and local climate variables. These relationships are then utilized to predict future local climate variables using projected atmospheric conditions from GCMs. Unlike RCMs, which are limited to spatial resolutions of 20-50 kilometers, statistical downscaling can generate site-specific climate projections[10]. However, this approach hinges on the assumption that the relationship between large-scale circulation and local climate remains consistent under various forcing conditions of potential future climates[102].
Statistical downscaling methods frequently require bias correction to align GCM output with observed data effectively. This process usually entails harmonizing monthly or seasonal averages from the GCM with observed averages. Popular bias correction techniques involve mapping GCM projections (such as precipitation and temperature) to baseline observations using probability density functions or cumulative distribution functions, including quantile and histogram methods[59, 58].
There is a diverse array of statistical downscaling techniques spanning from basic linear interpolation to more complex methodologies like Canonical Correlation Analysis (CCA), Principal Component Analysis (PCA), Model Output Statistics (MOS), Perfect Prognosis (PP), Multiple Linear Regression, Artificial Neural Network (ANN), Multivariate Autoregressive Model, and Conditional Weather Generator. Linear interpolation stands out as the simplest approach for generating high-resolution climate scenarios by interpolating large-scale flow anomalies into finer scales, which represent the scale of impact modeling. Interpolation methods are commonly employed when quick evaluations of numerous climate change scenarios are necessary[99].
Linear and multivariate regressions are frequently employed in downscaling procedures. In these regression models, the large-scale variables obtained from a GCM run are inputted into the same model to predict surface variables under a modified future climate scenario. Following this, bias correction is applied to both the current climate and GCM climate simulations. The disparity between these two datasets is then added to the observational time series to produce projections under the modified climate conditions[34]. Given below are a few pros and cons of statistical downscaling are given below:
Advantages of statistical downscaling methods include[34]:

- High spatial and temporal resolutions
- Computational efficiency and flexibility

- Rapid application to multiple GCMs
- Explicit estimation of uncertainty associated with downscaling

Statistical downscaling also has some drawbacks[34]:

- Dependency on biased inputs from GCMs
- Assumption of stationarity in empirical relationships for future scenarios
- Fluctuating skill levels across different climatic regions
- Requirement for accurate and lengthy data records for predictors

A summerized comparison can be made now using the above descriptions of both dynamical and statistical downscaling techniques and can be found in the table 2.4 below:

Table 2.4: Comparison between Dynamical and Statistical Downscaling Methods

Criteria	**Dynamical Downscaling**	**Statistical Downscaling**
Computational Demand	Requires significant computational resources.	More computationally efficient and flexible.
Model Basis	Grounded in physical laws, necessitating detailed data on topography and land use.	Empirically derived, utilizing historical data to establish relationships.
Application	Effective for regions with complex geographic features.	Can be rapidly applied to various climate models and scenarios.
Parameterization	Involves uncertainty in sub-grid scale processes.	Assumes consistent relationships over time.
Corrections Needed	Systematic biases from GCMs require correction.	Requires statistical adjustments to align with observational data.
Advantages	Provides detailed simulation of physical processes.	Flexible and quick, enabling explicit uncertainty estimation.
Disadvantages	May fail to correct inherited biases from GCMs.	Skill level varies by region and depends on robust historical records.

Often, a combined approach employing both dynamical and statistical methods called dynamical-statistical downscaling is preferred[10]. This hybrid technique, first utilizes an RCM to downscale the output from a GCM and then subsequently, statistical equations are applied to further refine the downscaled RCM output to achieve a finer resolution. By integrating dynamical downscaling with statistical methods, specific aspects of regional climate modeling are enhanced, providing improved predictors for generating higher-resolution output through statistical downscaling [42]. This method of Statistical-dynamical downscaling, while being more intricate, is computationally lighter than dynamical downscaling.This approach also statistically pre-filters the GCM outputs into a limited number of characteristic states, which are then utilized in RCM simulations[39]. This approach, however, has not been described in detail in this report.

2.5. Data sources

Datasets used in this study have been retrieved from the copernicus [22] and provided by RWE offshore wind. The CDS offers comprehensive information covering historical, current, and projected climate conditions across the globe. It encompasses diverse data categories such as satellite observations, on-site measurements, climate model simulations, and seasonal outlooks[22]. The CORDEX data and

CMIP projections have been retrieved from CDS whereas the statistically downscaled CMIP projections have been provided by RWE offshore wind. This section discusses them in detail.

2.5.1. CMIP6

The CMIP project, under the umbrella of the World Climate Research Programme (WCRP), delivers climate projections crucial for comprehending historical, current, and future climate shifts. Its data infrastructure plays a pivotal role in the assessments conducted by the IPCC and various international and national climate evaluations [96].
This comprehension involves evaluating model performance across historical periods and assessing the factors contributing to the variability in future projections. Furthermore, researchers conduct idealized experiments to enhance their understanding of model responses. Apart from examining long-term responses, experiments are conducted to explore the predictability of the climate system across different time and spatial scales, as well as generating predictions based on observed climate states[97].
The CMIP data consists of historical and climate projection experiments. The historical experiments include the modern climate observations showing GCM performance for past climate from 1850 to 2014. This data can also be used as reference data for comparison with different future scenarios. On the other hand, Climate projection experiments follow the SSPs and RCPs and show how climate is expected to change relation to different scenarios of economic and industrial development [12].

Organization and key Elements of CMIP6

CMIP6 encompasses essential experiments called as the DECK: Diagnostic, Evaluation, and Characterization of Klimaand CMIP historical simulations, serving to maintain coherence and document fundamental model attributes across CMIP phases[14].
The DECK comprises four foundational experiments: the historical Atmospheric Model Intercomparison Project (AMIP) simulation, a pre-industrial control simulation (piControl or esm-piControl), a simulation subjected to an abrupt quadrupling of CO2 (abrupt-4×CO2), and a simulation featuring a 1% annual CO2 increase (1pctCO2). These experiments ensure consistency across CMIP iterations and deepen insights into the climate system's responses to diverse forcings [77].

The CMIP historical simulations (spanning from 1850 to the near present) endeavor to replicate observed climate variations throughout the historical era by incorporating external forcings like greenhouse gas concentrations, solar activity, and volcanic eruptions. These simulations establish shared standards, coordination mechanisms, and comprehensive documentation to streamline model output dissemination and ensemble characterization. Figure 2.7 gives a schematic of CMIP6 for a better understanding; the central circle and the accompanying text outline standardized aspects common to all CMIP DECK experiments and the CMIP6 historical simulation. The middle circle highlights scientific themes unique to CMIP6 addressed by the CMIP6-Endorsed MIPs, with MIP-specific topics depicted in the outer circle. This structure is overlaid on the scientific context for CMIP6, represented by the seven WCRP Grand Science Challenges.[55]

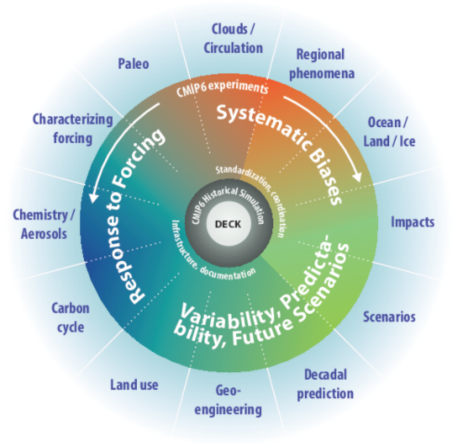

Figure 2.7: CMIP6 experiments schematic

CMIP6's federated structure facilitates a diverse array of experiments customized to address specific scientific inquiries, offering a flexible framework capable of accommodating the dynamic requirements of the climate modeling community. This approach not only supports the distribution of tasks across various modeling groups but also aligns them with their scientific interests and priorities[77].

2.5.2. CORDEX

The Coordinated Regional Climate Downscaling Experiment (CORDEX) is an initiative led by the World Climate Research Program (WCRP). It leverages cutting-edge General Circulation Models (GCMs) from CMIP5 to generate climate projections for diverse global regions. This project employs a dynam-

ical downscaling methodology using a variety of Regional Climate Models (RCMs). By integrating advanced GCMs with RCMs, CORDEX aims to enhance the accuracy of regional climate representations, primarily through increased spatial resolution [35]. CORDEX was developed to assist the international coordination and transfer of knowledge and and therefore to facilitate easier analysis by scientists and end-user communities at the local level[10].
CORDEX has developed a downscaling technique aimed at providing high-resolution climate data for researchers. The datasets used within CORDEX are generated using a dynamical downscaling approach facilitated by Regional Climate Models (RCMs), also known as limited area models (LAMs). These models utilize boundary conditions from Global Circulation Models (GCMs) to produce detailed climate information at a finer scale, typically ranging from 10 to 50 kilometers. The accuracy of simulations relies on both the quality of the RCM and the GCM employed in the process. However, experts suggest that RCMs have a more significant influence on local variables compared to their driving GCMs, although the extent of this influence may vary depending on location and season [35].

CORDEX domains

CORDEX activities are organized into domains representing different regions across the globe. There are currently in total 14 domains of CORDEX as mentioned below[26]:

Africa	Europe (EURO)	South Asia	East Asia
Central Asia	North America	South America	Central America
Arctic	Antarctica	Australasia	Mediterranean(MED)
Middle East North Africa (MENA)	South-East Asia (SEA)		

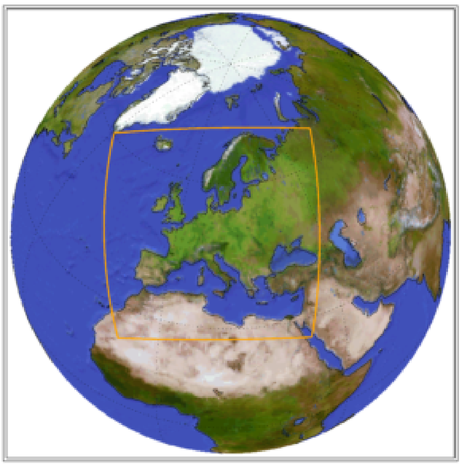

Figure 2.8: EURO-CORDEX Domain[27]

In this study, the EURO-CORDEX domain has been utilized when analysing the locations in Europe. EURO-CORDEX stands out for its superior temporal resolution, reaching up to hourly intervals, and spatial resolution of up to 0.11°x0.11° grid, surpassing other CORDEX domains. The coverage of EURO-CORDEX simulations as shown in figure 2.8 encompasses the European region, providing valuable insights for climate research [78].
Along with exploring the valuable insights offered by the CORDEX datasets and CMIP projections, it's crucial to augment the understanding of climate change with additional sources of data. In this context, RWE offshore Wind GmbH has provided statistically downscaled data, offering a more localized perspective on climate projections. This additional dataset allows for a deeper examination of region-specific climate trends on a higher spatial resolution as compared to CORDEX and CMIP6. The following section delves into the details of this statistically downscaled data.

2.5.3. Statistically downscaled GCMs

The last set of wind speed projection datasets utilized in this study have been provided by RWE Offshore Wind GmbH. These datasets originate from CMIP simulations and have been statistically downscaled to achieve a higher resolution of 3 km at several locations. Further details regarding these datasets are available in the Methodology section of the report (refer to Chapter 3). The downscaling technique employed here is known as Multivariate Quantile Mapping Bias Correction (MBC). Alex J. Cannon in his work *"Multivariate quantile mapping bias correction: an N-dimensional probability density function transform for climate model simulations of multiple variables"* [7] has presented the algorithm to perform the downscaling using this method ([7]). The detailed analysis on this method is out of the scope of this project.

It should be noted that modelled climates represented by these simulations from CMIP6 GCMs, CORDEX and the statistically downscaled CMIP6 GCMS are not synchronized with the real climate, especially at hourly or daily scales, and a comparison day by day would not be accurate. On a small temporal scale, the climate simulation results primarily reflect mathematical randomness rather than the physical processes simulated by the climate models. Thus, the comparison between the dataset of reference and the climate simulations must be carried out by a statistical study spanning a wide period (over 10 years) that includes climate stimuli [35, 78]

The literature review on climate change and downscaling methods wraps up here, providing a foundational understanding for the ensuing analysis of wind resource assessment. By establishing the groundwork through an exploration of climate change dynamics, this review now moves to a detailed examination of the specific parameters utilized in assessing wind resources. These parameters play a pivotal role in determining the complex interplay between climatic variables and wind energy potential, thus informing strategic decision-making processes in renewable energy planning and development. Further details on these can be found in the next section.

2.6. Wind Resource Assessment Parameters

This section outlines the essential tools and parameters used in assessing and managing wind resources for wind farms. It also introduces fundamental definitions necessary for understanding the methodology and interpreting the results discussed in the subsequent chapters.

2.6.1. Power law

The near surface wind projections that are obtained from CMIP6 and CORDEX are projected for a height of 10m which needs to be extrapolated to the hub height of the wind turbine. The power law has been used in many literature for this purpose, even though it does not account for temporal and spatial variations in surface roughness and atmospheric stability conditions,which can affect the wind speed profile [78, 31, 43]. The power law is given as the follows:

$$u(z) = u_{ref} \left(\frac{z}{z_{ref}} \right)^{\alpha} \tag{2.1}$$

here, u_{ref} is the wind speed at height z_{ref} and u(z) is the required wind speed at the desired hub height z. α is the wind shear exponent and is usually set as 1/7 for neutral stability conditions[78, 81]. Because meteorological conditions fluctuate, the power law exponent changes over time. Often, there are no long-term wind speed measurements from various heights available, which would enable the estimation of a time-dependent and spatially explicit power law exponent. That is why, as a result, the mean of the power law exponent or a constant value of 0.14 is commonly assumed [81].

2.6.2. Wind Power

The power output that can be harnessed from wind can be formulated in the following equation:

$$P = \frac{1}{2} \rho A c_p u^3 \tag{2.2}$$

where, P is the power output (in watts)
A = πr^2 is the swept area of the wind turbine blades
r is the rotor radius of the wind turbine (in meters, m)
ρ is the air density (in kilograms per cubic meter, kg/m³)
c_p is the coefficient of performance (dimensionless), representing the efficiency of the turbine in converting wind power to mechanical power.
u is the wind speed (in meters per second, m/s) The Power of wind turbine can also be visualised using the Power curve of that turbine. Figure 2.9 represents the power curve of a 5 MW NREL reference wind turbine [32].

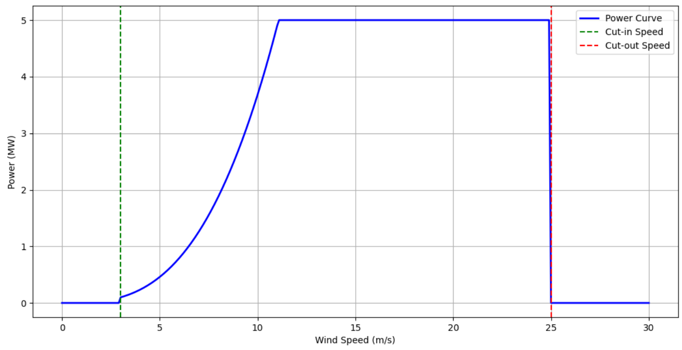

Figure 2.9: Power curve of NREL 5 MW reference wind turbine [32]

From the power curve it can be interpreted that the wind turbine starts producing Power at cut-in speed of 3m/s and reaches the maximum or the rated power at the u-rated which can be using the equation 2.2. The wind turbine shuts down or stops generating power once it reaches the cut out speed, u-cut out at usually 25m/s. The power curve is fundamental when determining the energy yield of the turbine.

2.6.3. Probability distribution function

Probability density functions (PDFs) are typically used to describe wind speed distribution, facilitating the optimal selection of wind turbines for a specific location and estimating the available energy over a required period [60]. The choice of PDF is critical in wind energy analysis as wind energy is directly related to wind speed distribution parameters. An accurately fitting PDF reduces uncertainties in wind energy output estimates [60]. Numerous studies have utilized various PDFs to characterize wind speed data [8]. Commonly used unimodal distributions include Weibull, Rayleigh, inverse Gaussian, gamma, lognormal, normal, inverse Weibull, Pearson type V, kappa, logistic, Gumbel, binomial, and extreme value type I [29, 3, 53, 100]. Weibull and one-parameter Rayleigh have been the most prevalent in the field [60] and the former has been employed in this study.
The weibull pdf f(u) is given by the following equation [84]:

$$f(u) = \left(\frac{k}{a}\right)\left(\frac{u}{a}\right)^{k-1} \exp\left(-\left(\frac{u}{a}\right)^{k}\right) \tag{2.3}$$

where, k is the shape parameter,
a is the scale parameter,
u is the wind speed in meters per second (m/s)

2.6.4. Annual Energy Yield of Wind Turbine

Once the power curve of the wind turbine and the probability distribution function of the wind speed is known, the Annual energy yield (AEP) can be easily computed using the following formula:

$$E_y = 8760 \int_{u_{\text{cut-in}}}^{u_{\text{cut-out}}} P(u) f(u)\, du \tag{2.4}$$

Where, P(U) is the Power generated as wind speed changes (Watt),
f(u) is the PDF of the wind speeds,
u_{cut-in} and $u_{cut-out}$ are the cut in and cut out wind speeds respectively.
Equation 2.4 can also be graphically represented through figure 2.10 given below:

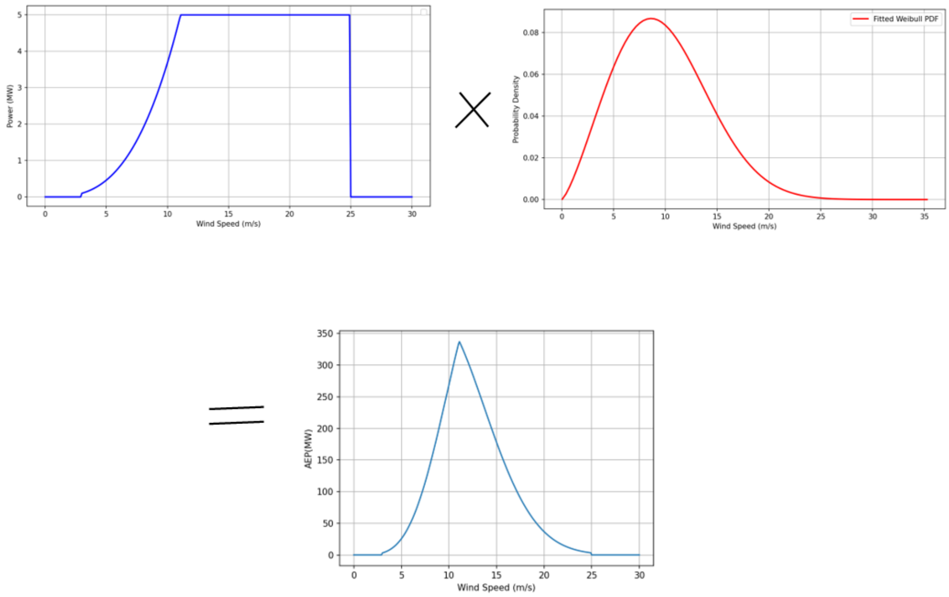

Figure 2.10: Graphical representation of Energy yield equation 2.4

2.6.5. Capacity Factor

The capacity factor measures the efficiency of an energy source (wind turbine in this case) in generating power compared to its maximum potential output. Typically evaluated over a year, it provides valuable insights into the reliability and consistency of the turbine's availability[87]. It reflects not only the total number of hours it operated throughout the year but also the percentage of its maximum production capacity utilized during that time[79]. The capacity factor can be expressed by the equation given below[11]:

$$\text{Capacity Factor} = \frac{\text{Actual Energy Output}}{\text{Maximum Power Rating x operating hours}} \times 100\% \tag{2.5}$$

A higher capacity factor, approaching 100%, indicates a more consistently available energy source throughout the year, highlighting the effectiveness of the turbine's location and the overall dependability of the energy source [87].

2.6.6. Likelihood of Outcome

The IPCC uses a scale with five categories to communicate confidence levels in its findings: starting from the lowest certainty "very low," then rising through "low" and "medium" to the more certain "high" and the highest level "very high" [49]. The IPCC divides the likelihood of outcomes due to climate change into the following categories

1. 99–100% probability: virtually certain
2. 90–100% probability: very likely
3. 66–100% probability: likely
4. $\sim$50% probability: more likely than not
5. 33-66% probability: about as likely as not
6. 0-33% probability: unlikely
7. 0-10% probability: very unlikely
8. 0-5% probability: extremely unlikely

2.6.7. Sensitivity factor

The sensitivity factor used in this work can be defined as the ratio between the relative change in Annual Energy Production (AEP) and the relative change in wind speed compared to historical values. The higher the sensitivity factor, the greater the impact of changes in wind speed on AEP. This indicates that even small variations in wind speed can lead to significant changes in AEP, reflecting the system's sensitivity to wind conditions. The sensitivity factor can be calculated using the following equation:

$$\text{Sensitivity factor} = \frac{\text{change in AEP (\%)}}{\text{change in wind speed (\%)}} \tag{2.6}$$

2.6.8. Haversine Equation

Haversine formula is used to compute the distance between two points on the surface of a sphere using the longitudes and latitudes of those points [98]. In this study, this is used to find the distance between the coordinate points of the GCMs and the reanalysis data.

Given two points on the Earth, $(\text{lat}_1, \text{lon}_1)$ and $(\text{lat}_2, \text{lon}_2)$, the Haversine formula to calculate the distance D between these points is given by:

$$D = 2R \times \left|\arcsin\left(\sqrt{a}\right)\right| \tag{2.7}$$

where

$$a = \sin^2\left(\frac{\Delta\text{lat}}{2}\right) + \cos(\text{lat}) \cdot \cos(\text{lat}) \cdot \sin^2\left(\frac{\Delta\text{lon}}{2}\right)$$

Δlat and Δlon are the differences in latitude and longitude, respectively:

$$\Delta\text{lat}_{\text{rad}} = \text{lat}_2 - \text{lat}_1$$

$$\Delta\text{lon}_{\text{rad}} = \text{lon}_2 - \text{lon}_1$$

lat_1, lon_1, lat_2, and lon_2 are the latitudes and longitudes of the two points converted from degrees to radians and R is the Earth's radius measured approximately 6371 kilometers.

Having explored the key elements of wind resource assessment, the focus now shifts to the fundamental definitions that support these concepts. Section 2.6 will provide essential definitions and metrics that are crucial for a clear understanding of the terms and methodologies used throughout this study.

2.7. Fundamental Definitions

2.7.1. Quantile

An x-quantile (also known as fractile) is the value in a distribution such that x*N observations fall below it, where 0<x<1 and N is the total number of observations. These can also be computed in percent when 0%<x<100% . The x-quantile can also be referred as X-percentile, with X=x*100; for instance a 0.30-quantile could be designated as 30-percentile, as well [83].

2.7.2. Mean Wind Speed

The mean of a dataset is defined as the averaging metric that provides the total average. The mean is calculated by summing up all the values in a dataset, and dividing by the number of observations, N [38]. This can simply be translated to daily, monthly or annual wind speeds where N would be the number of hours or days using the following equation:

$$(\bar{u}) = \frac{\sum_{i=1}^{N}(v_u)}{N} \tag{2.8}$$

where, $\bar{u}$ is the mean of the wind speeds,
N is the total number of hours/days,
u is the wind speed at each time stamp.

2.7.3. Median

The median is the central value in a data set that is arranged by magnitude. It separates the data into two equal halves: one with values greater than or equal to the median, and the other with values less than or equal to it. The primary advantage of the median is its immunity to extreme values (outliers), since it is a positional measure rather than one influenced by the magnitude of the values. This characteristic makes the median a reliable indicator of central tendency [6].

2.7.4. Rolling mean

A rolling mean, also known as a moving average, is a metric used to identify trends over shorter time periods within a dataset. This technique is beneficial for highlighting long-term trends that may be obscured by short-term fluctuations. The rolling average is calculated as the sum of data points over a specified time period divided by the number of time periods [85]. In science and engineering, the mean is typically calculated from an equal number of data points on either side of a central value to ensure that mean variations align with data variations, avoiding time shifts [18]. The central moving mean formula is given by:

$$\bar{X}_t = \frac{1}{2a+1}\sum_{i=-a}^{a} X_{t+i} \tag{2.9}$$

where, $\bar{X}_t$ is the central moving mean at time t,
a is the number of data points on each side of the central value. This determines the window size, which is 2a+1. For example, if a = 5, the window size is 11 (i.e., 5 points before, the central point, and 5 points after) and ,
X_{t+i} are the data points within the window centered at t.

2.7.5. Normalisation

Normalisation a dataset involves adjusting values measured on different scales to a common scale, typically before averaging them. This process creates modified versions of the original statistics by shifting and scaling them. The goal is to enable meaningful comparisons of normalized values across different datasets by eliminating the impact of major influencing factors, such as anomalies in a time series [19].

2.7.6. Error metrics

In this work, the error metrics presented below and the correlation coefficients in the next subsection have been used to make comparison between the historical wind speed projections given by the re-analysis data ERA5 and CMIP6 GCMs and statistically downscaled GCMs.

Mean absolute percent error

The mean absolute percentage error (MAPE) evaluates the accuracy of a prediction model by averaging the absolute percentage errors between predicted and observed values. MAPE can be computed by using the formula [78]:

$$\text{MAPE} = \frac{100}{n}\sum_{i=1}^{n}\frac{|p_i - o_i|}{o_i} \tag{2.10}$$

where, n is the number of data points,
o_i is the observed value, p_i is the predicted value.

Percent Bias (PBIAS)

PBIAS measures whether simulated/predicted values tend to be larger or smaller than observed values on average. The ideal PBIAS value is 0.0, which indicates perfect accuracy. Lower magnitude values suggest more accurate model simulations. Positive PBIAS values indicate the model is overestimating, whereas, the negative values indicate underestimation [72]. The percentage Bias can be calculated using the following formula [78]:

$$\text{Bias} = \frac{1}{n}\sum_{i=1}^{n}(p_i - p_i) \tag{2.11}$$

2.7.7. Correlation coefficients

The Correlation coefficients are used to determine whether their is a good statistical correlation between the two datasets. The correlation degree is influenced by factors like terrain complexity, site location similarity, elevation differences, and primarily, the distance between sites [56]. This study utilizes Pearson's correlation coefficient and the coefficient of determination to analyze the relationship between predicted and observed values.

Pearson's correlation coefficient, r

The Pearson correlation coefficient measures how well data points fit a line of best fit.
r=1 indicates a perfect positive linear relationship,
r=−1 indicates a perfect negative linear relationship,
r=0 indicates no linear relationship.
The value of R can be computed using the following formula

$$r = \frac{\sum_{i=1}^{n}(o_i - \bar{o})(p_i - \bar{p})}{\sqrt{\sum_{i=1}^{n}(o_i - \bar{o})^2 \sum_{i=1}^{n}(p_i - \bar{p})^2}} \tag{2.12}$$

where, n is the number of data points,
o_i is the observed value,
p_i is the predicted value,
$\bar{o}$ is the mean of observed values,
$\bar{p}$ is the mean of predicted values
Even though Pearson's correlation coefficient is useful for identifying relationship between datasets but it does not reflect the magnitude of data, which may give a false sense of accuracy [76].

Coefficient of determination, r^2

The coefficient of determination assesses how well predicted values match observed values, taking both magnitude and fit into account. Unlike the best fit line, it measures the distance between data points and the 1:1 line. An r^2 value of 1 indicates perfect prediction, 0 indicates random prediction, and less than 0 indicates predictions worse than random. The closer the points are to the 1:1 line, the higher the r^2 value [76].
According to literature, the correlation between predicted and actual values is rated as follows based on the correlation coefficient r^2: very poor if r^2 is below 0.6, poor if it is between 0.6 and 0.7, moderate for 0.7 to 0.8, good for 0.8 to 0.9, and very good for 0.9 to 1.0 [2].

Having established the fundamental definitions necessary for wind resource assessment in this section, the following section 2.7 will now review recent literature on the impact of climate change on wind resource assessment. This section explores key studies and findings that illustrate the evolving understanding of how climate change affects wind energy potential.

2.8. Recent literature on climate change impact on wind resource assessment

This section discusses the extensive research done by various scientists and experts in assessing the impact of climate change on wind resource assessment for different locations in the world and their critical findings and suggestions.

Current and future wind energy resources in the North Sea according to CMIP6 [43]

This work investigates the mid-century changes in hub-height wind speed and power density over northern Europe using an ensemble of CMIP6 model outputs under historical and SSP5-8.5 scenarios. Hahmann et. al. found that the annual mean values between the past (1995–2014) and the future (2031–2050) show non-significant differences. However, over 75% of the models predict a decrease in wind resources during summer in the North Sea and an increase during winter in the Baltic Sea.

The accuracy of CMIP6 models in capturing wind resources at levels accessible to current wind turbines has been validated against long-term measurements and reanalysis data. However, using a constant power law to extrapolate wind speeds to turbine height often exaggerates future changes, as it does not account for changes in surface roughness and atmospheric stability.

Changes in wind energy production are expected to range between 5% and 10%, which may seem small but can have significant economic impacts due to higher financing costs and revenue losses for wind farm operators. Importantly, the predicted decrease in summer wind resources could be mitigated by solar power, although the overall effects on power system operations require further study. This work underscores the importance of using a comprehensive set of models and considering simplifications and numerical imprints on model-generated time series in power system studies.

IJmuiden Ver Wind Farm Zone Wind Resource Assessment report, prepared for Rijksdienst voor Ondernemend Nederland (RVO) [78]

This report analyzes the impact of climate change on wind resources at a North Sea site near the IJmuiden Ver measurement point using a EURO-CORDEX multi-model ensemble. They validated the accuracy of seven CORDEX models against historical wind speed data over a 26-year period, finding the models reliable for future projections.

Key findings for this work include:

- The analysis used seven validated climate models to construct three ensembles for short (2022-2045), medium, and long-term (2075-2099) scenarios under RCP4.5 and RCP8.5 pathways.
- Ensemble F projects a 0.55% decrease in mean wind speed and a 1.5% reduction in annual energy yield for 2022-2045 under RCP8.5. Similar trends were observed in a study for the German North Sea.
- By 2075-2099, the mean wind speed and energy yield could decrease by 1% and 3%, respectively, under RCP8.5. The impact is smaller under RCP4.5, with projected decreases of 0.7% in mean wind speed and 1.7% in annual energy produced.
- Two ensembles indicate a significant reduction in summer wind power density and energy yield generation under RCP8.5, reaching up to 20% and 25%, respectively, in the long term.
- An overall decline in energy yield and operation hours is expected due to reduced wind speeds and increased frequency of extreme wind events, particularly under RCP8.5.

The study highlights the need for regional analysis to enhance reliability and acknowledges the lack of bias correction in the long-term climate projections.

Impacts of climate change on energy systems in global and regional scenarios [101]

This study reviewed about 220 papers on the impacts of climate change on energy systems, with a focus on renewable energy sources, including wind power. It was found that the impacts of climate change on wind power potential are mixed, with variations across different regions and studies. In Europe, both increases and decreases in wind power potential have been reported. Specifically, decreases are projected for southern Europe, while slight increases are expected in central and northern Europe. Some regional studies indicated a low probability of changes in wind power for South Africa, whereas other studies reported favorable future conditions for wind power in parts of the United States and Brazil. Additionally, a recent global study indicated an overall increase in wind energy potential in the Southern Hemisphere.

These findings underscore the need for a consistent multi-model assessment framework to accurately evaluate the climate impacts on wind energy and support regional and global energy planning. Comprehensive studies with harmonized methodologies are essential to reduce uncertainties and improve comparability. Policymakers should take these mixed impacts into account in their planning to ensure the sustainability and resilience of wind energy systems.

Climate change impacts on wind energy generation in Ireland [31]

A multi-model ensemble of high-resolution climate models was utilized in this study to address uncertainties in future wind energy projections for Ireland. The results indicate significant variability among the climate models, with a general trend of projected wind energy decrease ranging from 0.4% to 2%, particularly pronounced during the summer months with reductions of up to 6%, while winter months could see slight increases of up to 1.1%. This variability leads to greater intra-annual fluctuations in wind energy production, posing challenges for energy system stability, especially with the increased occurrence of low-power periods during the summer.

The study highlights the frequency and duration of low-power events, particularly offshore, are projected to increase by the end of the century, necessitating the strategic planning of wind farms across diverse wind regimes to optimize regional compatibility and maintain a consistent energy supply. Additionally, the Irish offshore wind energy network, though currently small, could play a crucial role in balancing the energy system, as offshore wind resources are projected to have longer durations of low-power events during the summer.

Overall, the projected decrease in wind energy generation underscores the need for a continuously evolving renewable energy system to ensure a stable and secure electricity supply. The study's findings, particularly on the projected changes for low- and high-power events, emphasize the importance of comprehensive planning and development of both onshore and offshore wind resources to balance the energy supply and mitigate the impacts of climate change on wind energy production.

Climate change impacts on wind power generation for the Italian peninsula [5]

In this study, researchers analyzed the impact of climate change on the availability of future wind resources using an ensemble of 11 Euro-CORDEX regional climate models and the MERIDA meteorological reanalysis at different resolutions. The analysis involved bias correction of wind variables to ensure accurate wind power production estimates, based on the VESTAS V112—3000 kW wind turbine. The study assessed wind producibility for both onshore and offshore areas within 40 km of the Italian coast, across short (2021–2050), medium (2051–2080), and long-term (2071–2100) periods, under ”business as usual” RCP 8.5 and RCP 4.5 scenarios.

They found that Short-term projections show small and unreliable variations in wind producibility with high uncertainty. Whereas, the Medium and long-term projections for the RCP 8.5 scenario indicate significant and statistically significant changes, particularly a decrease in wind producibility in the western offshore areas and the SICI and SARD market areas. Moreover, The eastern plains of the NORD market area show a reliable increase in wind producibility during the summer season. The RCP 4.5 scenario projects decreases in the west coast, SICI, and SARD market areas, especially in autumn, and increases in winter wind producibility in Central Italy's mountainous regions and the NORD market area.

The study concludes that the impact of climate change on wind producibility will remain small and not statistically significant in the short term. However, medium and long-term projections suggest that climate-related changes should be considered in future planning, particularly for new offshore wind farms. Future installations should focus on areas with lower expected decreases in producibility, such as the eastern Italian coast and southeast offshore regions. The study also highlights the importance of considering multi-decadal fluctuations of wind energy linked to internal climate variability, which align with the average life cycle of wind farms. Future research should investigate intra-daily and inter-annual variability impacts and explore how different types of wind turbines might affect wind producibility under climate change scenarios.

Climate change impact on Northwestern African offshore wind energy resources [82]

This study provides a comprehensive analysis of the impact of climate change on wind resources in the Northwestern African offshore region, utilizing high-resolution regional climate models. By employing two REMO-OASIS-MPIOM (ROM) simulations in both uncoupled and coupled modes, alongside a CORDEX-Africa multi-model ensemble, the study investigates the climate change signal in offshore wind resources.

The analysis reveals that the Azores high-pressure system, combined with the thermal low over North Africa, generates persistent alongshore winds, particularly along western North Africa. These winds create significant annual and seasonal energy density patterns, with the highest wind energy resources found downstream of Cape Ghir and between Cape Bojador and Cape Blanc. Projections indicate that while the overall wind energy patterns remain stable, there are notable changes in available wind resources. For instance, annual wind energy is projected to decrease in the southern offshore areas, especially under the RCP8.5 scenario. Conversely, increases in wind energy density are expected in the coastal regions of Morocco and offshore Western Sahara during specific seasons.

The findings suggest that more detailed assessments of wind energy generation in the Northwestern African offshore region, considering specific turbines and sub-daily output scales, are necessary. Additionally, further research on wind model level interpolation and logarithmic extrapolation for energy density is recommended to enhance the accuracy of wind energy assessments.

The background chapter ends here. It highlighted the critical components and techniques in wind resource assessment, emphasizing the importance of accurate climate models and downscaling methods in predicting wind energy potential under changing climate conditions. Building on this foundation, the following methodology section will outline the specific aims of this study, the selected sites for analysis, and the detailed procedures for data collection and preparation, ensuring a thorough examination of wind power generation potential.

3 Methodology

This chapter details the methodologies employed in this study to address the research questions outlined in Section 3.1. Building on the foundational concepts discussed in Chapter 2, this chapter outlines the sites assessed in this work in section 3.2, the processes of data collection and preparation (Section 3.3), the design of experiments including the different models used in Section 3.4, and the methods and techniques employed for data analysis (Section 3.5) that lead to the results presented in the next chapter.

3.1. Research Questions

The interplay between climate change and wind energy highlights the importance of accurately assessing future wind resources. The various data types and sources, along with climate change scenarios, underscore the complexity of predicting wind speed variations. Additionally, the techniques of downscaling and the parameters used in wind resource assessment raise questions about the reliability and implications of different modeling approaches. The assessment of wind speed variations is critical for understanding future climate impacts on wind energy production and to ensure efficient planning and optimization of wind farms.
This study focuses on the methodologies used to project wind speed variations and evaluates their implications on energy yield and financial outcomes. Specifically, this research aims to address the following questions:

1. How do the downscaling methods impact the assessment of future variations in mean wind speed in specific regions under different climate change scenarios ? What implications does it have for the energy yield, capacity factor and revenue?
2. How do the downscaled and the non-downscaled GCMs perform in projecting historical wind speed variation in comparison to reanalysis data?

3.2. Sites in Analysis

A total of 7 sites in Europe and 2 sites in North America have been chosen for the analysis of wind resource in this study. The location coordinates have been anonymized due to a non-disclosure agreement with the data owner. The sites have been labelled with acronyms indicating the country or general location in figure 3.1 below. Table 3.1 presents an overview of the locations and the respective terrain type.

Table 3.1: List of sites used in the project

Site name	location	Terrain type
NS1	North Sea	Offshore

NS2	North sea	Offshore
FR	France	Inland, complex
IT	Italy	Inland, complex
UK1	United Kingdom	Inland, complex
UK2	United Kingdom	Offshore
UK3	United Kingdom	Inland, simple
NA1	North America	Onshore
NA2	North America	Offshore

(a) Sites in North America

(b) Sites in Europe

Figure 3.1: Maps of USA and Europe showing the sites analysed in this report

3.3. Data Collection and Preparation

This section outlines describes the data utilized in this study. It is divided into three subsections, each discussing data collection practices for different components: Climate Models, Reanalysis Data, and the Reference Wind Turbine utilized in this report.

3.3.1. Climate models

Three types of datasets have been used in this study namely: dynamically downscaled CMIP5 GCMs from the CORDEX experiment, non-downscaled CMIP6 GCMs and statistically downscaled CMIP5/6 (depending upon availability) GCMs provided by RWE. The Daily CORDEX projections have been retrieved from the Climate data store for the time period of 2006 to 2099. The CMIP6 data is available in two forms: historical (from 1850 to 2014) and experimental (from 2015-2100) as mentioned in section 2.5.1. Daily near surface wind speed projections have been retrieved separately for these time periods and combined into one file selecting the common CMIP6 models in both for all the sites. These projections have been used as raw data or data with lower spatial resolution and no downscaling for comparison with rest of the datasets. The statistically downscaled daily CMIP6 projections by RWE are available from year 2000 to 2099. However, since the CORDEX climate change scenario datasets are only available from 2006 that is why the assessment have been carried out using the wind speeds from year 2006 to 2023 as reference historical period.
The operational period has been chosen to be from year 2030 to 2060. For the further assessment three more time periods in the future have been chosen namely: Near, mid and far future. Table 3.2 below provided an overview of the year and the respective labeled period:

Table 3.2: Time Periods chosen to analyse wind speed variation

year	period
2006-2023	Historical
2030-2060	Operational
2031-2050	Near-Future
2051-2070	Mid-Future
2071-2090	Far-Future

Moreover, the near surface wind speed obtained from CMIP6 models and CORDEX has been projected for a height of 10m. In order to proceed with the assessment, it is necessary to translate it to the hub height of the wind turbine. Therefore, using the power law mentioned in equation 2.1 the wind speeds have been extrapolated to the hub height of 100m with α= 1/7. The statistically downscaled data provided by RWE has already been translated to 100m so no adjustment has been made to it.

3.3.2. Reanalysis data

ERA5 hourly data for u and v component of wind has been retrieved for a historical period of 1994 to 2023 at heights 10m and 100m above the surface of the Earth from climate data store [24]. The 'u' component represents the eastward component of the wind, that is the horizontal speed of air moving in the east. Whereas, the 'v' component of the wind is the northward component of wind or the vertical speed of air moving towards the north [24]. To make use of this reanalysis data, the magnitude of vector sum of the u and v components of wind is computed using the following formula:

$$u_{era5} = \sqrt{u^2 + v^2} \tag{3.1}$$

The reanalysis data is gridded at regular lat-lon grid of 0.25 degrees and a sub-region is extracted for the desired location by providing the limits for longitudes and latitudes. This involves defining the boundaries to the north, east, west, and south by selecting grid points that are closest to the provided reference coordinates provided by RWE, ensuring that these points are spaced 0.25 degrees apart. This approach effectively boxes the reference coordinates within the chosen sub-region. Consequently, a netCDF file is generated, which includes the u and v components of wind at the four boundary coordinates of the sub-region. From these, the coordinate nearest to the reference point is selected for subsequent comparisons with climate model outputs. The distance between the two coordinates has been computed using the haversine formula mentioned in equation 2.7.

3.3.3. 5MW NREL reference wind turbine

A 5MW NREL reference wind turbine has been used in this study to perform the energy yield calculations. The gross properties of the wind turbine are stated in the table 3.3 below:

Table 3.3: NREL 5MW wind turbine specifications[32]

Rating	5 MW
Rotor Orientation, Configuration	Upwind, 3 Blades
Control	Variable Speed, Collective Pitch
Drivetrain	High Speed, Multiple-Stage Gearbox
Rotor, Hub Diameter	126 m, 3 m

Hub Height	90 m
Cut-In, Rated, Cut-Out Wind Speed	3 m/s, 11.4 m/s, 25 m/s
Cut-In, Rated Rotor Speed	6.9 rpm, 12.1 rpm
Peak power coefficient, c_p	0.482
Rated Tip Speed	80 m/s
Overhang, Shaft Tilt, Precone	5 m, 5°, 2.5°
Rotor Mass	110,000 kg
Nacelle Mass	240,000 kg
Tower Mass	347,460 kg
Coordinate Location of Overall CM	(-0.2 m, 0.0 m, 64.0 m)

3.4. Design of Experiment

This section details the climate change scenarios, number of models for the different datasets that have been used in this study.
Firstly, figure 3.2 shows the three different data sets with their corresponding climate change scenario and resolutions. The main focused climate change scenario in this study is RCP4.5 or the SSP2-4.5 since it is the most probable baseline scenario with carbon emissions falling after year 2050[49]. However, a comparison has been made for the RWE statistically downscaled data between RCP4.5 and RCP8.5 to analyse what implications would this "worst case" scenario, with continuous rise in carbon emissions, has on the mean wind speed variation.

Dataset	CMIP6	Statistically downscaled CMIP5/6	Dynamically downscaled CMIP5 by CORDEX
Resolution	100-200 km	3 km	12.5 km
Climate change scenario covered	SSP2-4.5	• RCP4.5/SSP2-4.5 • RCP8.5/SSP5-8.5	RCP4.5

Figure 3.2: Datasets used in this work

The CMIP6 climate models have the lowest resolution data ranging from 100-200km. On the other hand, the statistically (RWE) and dynamically downscaled CMIP models have a resolution of 3 km and 12.5 km respectively. Figure 3.3 given below presents the number of models used in each dataset for each site. Colour coding has been done to show the CMIP model used. CMIP 5 models use the climate change scenario RCP4.5 whereas the CMIP6 models incorporate the SSP2-4.5 scenario. Both the scenarios are primarily the same in terms of Radiative forcing. The SSP scenarios also further include the underlying socio-economic parameters as mentioned in chapter 2.
The CORDEX data has not been assessed for the NA sites due to lack of data.

More information on the choice of models is presented in the subsection 3.4.1 below.

Climate change scenario:	RCP4.5/ SSP2-4.5			RCP8.5/ SSP5-8.5
Site	Statistically downscaled CMIP	Cordex	CMIP6	Statistically downscaled CMIP
NS1	19	11	20	21
NS2	20	11	19	20
FR	19	11	20	20
IT	19	11	20	19
UK1	20	11	20	20
UK3	20	11	20	21
UK2	20	11	20	21
NA1	19	n/a	19	21
NA2	19	n/a	20	21

CMIP6 CMIP 5

Figure 3.3: Number of models utilised for each dataset and site under different climate change scenarios

3.4.1. Model ensembles

From the literature, it has been understood that there are different sets of models that provide climate projections based on laws of physics. For simplicity CMIP6 models, statistically downscaled CMIP6 models provided by RWE and CORDEX models that consist of CMIP6 downscaled models using RCMs have been called dataset 1, 2 and 3 respectively from now on in this section.
It is worthwhile to note that these models for each case are not used individually but in an ensemble. This implies that a multi-model approach has been used in order to strengthen the reliance of outcomes. Multi-model approach has been proved to be good when dealing with climate modeling limits due to various reasons. A few of them have been stated below:

- Each climate model represents an incomplete picture of reality as it is not possible that all spatial and temporal scales are captured because of the computational resources. Climate processes occur on large time and spatial scales that can range from centuries to hourly and 10KM to 1000Km to below 1KM respectively [35, 28].
- Certain climate processes and interactions, such as turbulent exchanges in stable conditions and the life cycles of aerosols, have not been completely understood yet. [78]
- Each climate model operates on certain assumptions that can shape the outcomes, highlighting the importance of comparing and integrating various models when analyzing climate change.
- RCP scenarios, which force the climate simulations also rely on future assumptions and account for the natural variability within the climate system.

Therefore, using just one model might conceal compensating errors, but employing multiple models can mitigate this issue. A multi-model strategy helps cancel out potential errors and diminishes the impact of natural climate variability, offering a clearer insight into climate change effects [35, 28, 66].
All the available models for CMIP6 have been utilised in order to strengthen the confidence on the results. A detailed description of these models for each dataset is given below:

CMIP6 model ensemble

The CMIP6 models have been used to get near surface wind speed projections which are serving as raw data or the data with no downscaling in this investigation. Table 3.4 presents the models along with their resolution and developer institution and countries.

Table 3.4: CMIP6 models used in this report for raw data projections

CMIP6 Model	Institution	Country	Resolution (KM)	Citation
ACCESS-CM2	CSIRO-ARCCSS CSIRO and Austr. Res. Council Centre of Excellence for Climate System Science	Australia	140	Dix et al. (2019a)
BCC-CSM2-MR	BCC Beijing climate centre, china	China	100	Xin et al. (2018)
CESM2	NCAR National Center for Atmospheric Research (USA)	USA	100	Danabasoglu (2019f)
CMCC-CM2-SR5	CMCC Centro Euro-Mediterraneo sui Cambiamenti Climatici (Italy)	Italy	100	Gopinathan et al. (2019a)
CMCC-ESM2	CMCC Centro Euro-Mediterraneo sui Cambiamenti Climatici (Italy)	Italy	100	Lovato and Peano (2020a)
GFDL-ESM4	Geophysical Fluid Dynamics Laboratory (USA)	USA	100	Krasting et al. (2018b)
HadGEM3-GC31-LL	MOHC Met Office Hadley Centre (UK)	UK	140	Ridley et al. (2018a)
IITM-ESM	Centre for climate change Research,Indian Institute of Tropical Meteorology India	India	170	Gopinathan et al.(2019a)
INM-CM4-8	INM Institute of Numerical Mathematics (Russia)	Russia	150	Volodin et al. (2019a)
INM-CM5-0	INM Institute of Numerical Mathematics (Russia)	Russia	150	Volodin et al. (2019d)
IPSL-CM6A-LR	Institut Pierre Simon Laplace (France)	France	160	Boucher et al. (2018c)
KACE-1-0-G	National Institute of Meteorological sciences, Korea meteorological administration, Republic of Korea	Republic of Korea	140	Byun et al. (2019b)
KIOST-ESM	Korea Institute of Ocean Science & Technology	Republic of Korea	190	Kim et al. (2019a)
MIROC-ES2L	Japan Agency for Marine-Earth Science and Technology, Atmosphere and Ocean Research Institute and National Institute for Environmental Studies	Japan	250	Hajima et al. (2019a)
MIROC6	Japan Agency for Marine-Earth Science and Technology	Japan	250	Tatebe and Watanabe (2018)
MPI-ESM1-2-LR	MPI-M Max Planck Institute for Meteorology	Germany	170	Wieners et al. (2019b)
MRI-ESM2-0	MRI Meteorological Research Institute	Japan	100	Yukimoto et al. (2019e)
NorESM2-LM	NCC Norwegian Climate Centre	Norway	190	Seland et al. (2019a)

NorESM2-MM	NCC Norwegian Climate Centre	Norway	100	Bentsen et al. (2019b)
UKESM1-0-LL	MOHC Met Office Hadley Centre	UK	140	Tang et al. (2019)

The number of models used per site in this report varies according to the availability of data (see figure 3.3). For example, in the analysis of site HKW all CMIP6 models mentioned in the table above have been utilized except the ACCESS-CM2 and MIROC-ES2L. And in site analysis of Oklahoma onshore wind farm, the model: IITM-ESM is absent.

CORDEX model ensemble

CORDEX downscales CMIP5 models using the RCMs. In the table 3.5 given below, the CMIP5 models have been presented with the corresposing RCMs that they have been downscaled using.

Table 3.5: CMIP6 and corresponding RCM models used in CORDEX downscaling

CMIP model	CMIP Institute	CMIP Country	RCM	RCM Institute	RCM country
EC-EARTH	EC: Earth Consortium	Europe	CCLM4_8_17	CCLM: Climate Limited Area Modelling Community	Europe
EC-EARTH	EC: Earth Consortium	Europe	REMO2015	GERICS and MPI: Climate Service Center and Max Planck Institute	Germany
EC-EARTH	EC-Earth Consortium	Europe	RACMO22e	KNMI: Royal Netherlands Meteorological Institute	Netherlands
IPSL-CM5A-MR	IPSL: Institut Pierre Simon Laplace	France	WRF381p	CRC: Center for Research on Preservation	France
IPSL-CM5A-MR	IPSL: Institut Pierre Simon Laplace	France	RCA4	SMHI: Swedish Meteorological and Hydrological Institute	Sweden
HadGEM2-ES	MOHC: Met Office Hadley Centre	UK	HIRHAM5	DHI: Danish Meteorological Institute	Denmark
HadGEM2-ES	MOHC: Met Office Hadley Centre	UK	REMO2015	GERICS and MPI-CSC: Climate Service Center and Max Planck Institute	Germany
HadGEM2-ES	MOHC: Met Office Hadley Centre	UK	RCA4	SMHI: Swedish Meteorological and Hydrological Institute	Sweden
MPI-ESM-LR	MPI: Max Planck institute for Meteorology	Germany	RCA4	SMHI: Swedish Meteorological and Hydrological Institute	Sweden
NorESM1-M	NCC: Norwegian Climate Centre	Norway	REMO2015	GERICS and MPI-CSC: Climate Service Center and Max Planck Institute	Germany
NorESM1-M	NCC: Norwegian Climate Centre	Norway	RCA4	SMHI: Swedish Meteorological and Hydrological Institute	Sweden

RWE Statistically downscaled CMIP model ensemble

The CMIP6 and CMIP 5 GCMs have been statistically downscaled using the MBC method and bias corrected with ERA 5 at resolution of 3 km. The phase of CMIP used varies for sites depending on the availability. Complete list of the models used is presented in Appendix A.1.1.

3.5. Data Analysis

This sections presents the methods followed in this study to evaluate the mean wind speed variation, its impact on annual energy yield and revenue and to compare the GCMs with reanalysis data.
For evaluation the mean wind speed variation, all nine sites have been utilized to assess the performance and behavior of different datasets and models in projecting wind speed. This comprehensive analysis allowed for a broader understanding of the variability and reliability of wind speed projections across diverse geographical locations.

For the estimation of AEP and comparison of GCMs projections with ERA5 historical data, a selective approach has been employed, focusing on four specific sites. This selection was driven by the need to provide a detailed and representative analysis of both onshore and offshore wind energy potential. The chosen sites include two onshore locations with varying terrain complexities—FR (a site with moderate terrain complexity) and IT (a site characterized by highly complex mountainous terrain) and additionally, two offshore sites, NS1 and NS2.

3.5.1. Annual wind speed variation

Daily wind speed projections from all the datasets have been to converted to annual mean wind speeds simply by taking the per year mean for all the models for each site. The variation in wind speed has been calculated by normalising the yearly wind speeds with the historic wind speed period of 2006 to 2023. The detailed steps of the procedure are mentioned below:

1. The long term historical mean wind speed has been calculated by taking the mean of all the annual wind speeds from year 2006 to 2023 for the ensemble of models.
2. All annual mean wind speeds are then divided by this reference mean historical wind speed from the corresponding model and simply multiplied by 100 to get the percent variation. This provides the variation shown by each model for the future or operational period with respect to the historical period.
3. A rolling mean with a window of 10 years has been calculated for the entire time series for each model. This is done by taking an average from 5 years before the year x to five years after year x where x ranges from year 2006 to 2090. However, since there is no possibility of going five years before for the years 2006 to 2010, a looking forward window of 10 years is used where the average is calculated for the x+10 years.
4. In the next step, the median of the rolling averages of all the models is obtained. This helps observe the trend of wind speed variation over the years. The median is preferred since it is not affected by the extreme outliers or non-symmetric distributions. However, to make this plot more meaningful, rolling mean of the normalised wind speeds is taken.
5. Long term statistics of the wind speed variation are also computed in the following way: the median of the normalised long-term mean wind speeds given by all models (from step 2) is obtained for the operational period of 2030 to 2060 simply by averaging out the normalised annual mean wind speed for this period and taking then median value of the models.
6. Similarly he median of the historical long-term mean wind speeds given by all models is also obtained in order to perform comparison analysis. This is done by taking the time slice of normalised mean wind speed from 2006 to 2023 and taking median just as done in step 4. Since the historical mean wind speeds have been normalised by themselves the long term historical mean wind speed variation is simply 1 or 100%. This is used as a reference line to compare the change projected for the long term operational period.
7. However, this long term median only tells the variation in mean wind speed that the 50% of the models are predicting. So to rely completely on these statistics does not strengthen the

confidence on the assessment. Therefore, $\pm$ 33% quantiles are also calculated as per the IPCC Risk threshold guidelines. These quantiles are calculated using the long term mean wind speed projection given by each model and taking the 50+33= 83% quantile or 83rd percentile and the 50-33=17% quantile or 17th percentile in other words.

8. The quantiles basically tell the wind speed variation predicted by 17% and 83% of the models. When considering a risk to wind resource assessment, the 83% quantile is taken into account. This means that if 83% of the models show a decline or increase in the wind speed variation in the operational period as compared to the historic reference period, then a risk to wind resource is taken into account.

This procedure has been carried out for all the datasets and different scenarios for operational period, near, mid and far future using the programming language python in Visual Code Studio.

3.5.2. Annual Energy Yield

The annual energy yield calculations have been performed for four European sites (NS1, NS2, FR, IT) using the ERA5 reanalysis data and the 5MW NREL reference wind turbine for the operational period. Step by step procedure is as follows:

1. The first step involves obtaining the Power curve for the 5 MW NREL wind turbine. Based on the wind turbine specifications (table 3.3) and using the wind power formula the following power curve is obtained:

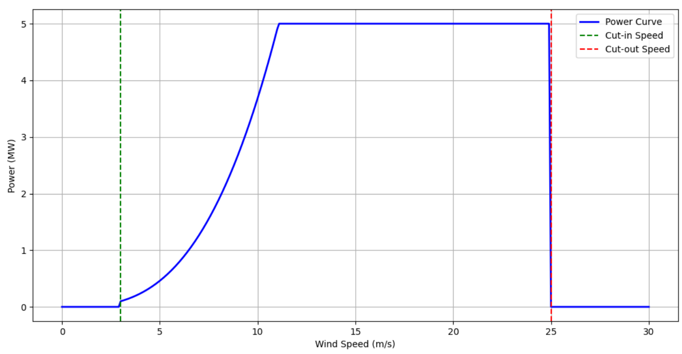

Figure 3.4: Power curve of 5MW NREL reference wind turbine[32]

2. The next step is to plot the historic weibull curve. ERA5 Hourly wind speed projections , u_{era5}, at 100m from year 2004 to 2023, as mentioned in section 3.3.2 are translated to the hub height of 90m using the power law and plotted into a histogram. The histogram is fitted using a weibull distribution and the weibull parameters: shape (k) and scale (a) factors are obtained.
3. Using the Shape and scale factors the probability distribution function for each site is calculated with dU= 0.1m/s with equation 2.3.
4. Ultimately the $AEP_{historic}$ is calculated using the equation 2.4.
5. To observe the change in AEP due to change in wind speeds, a decrement of 1%,3%,5% and 10% is applied to the u_{era5} by simply multiplying the wind projections by 0.99, 0.97, 0.95 and 0.90 respectively. These specific percentages are chosen to systematically assess the sensitivity of AEP to variations in wind speed. By evaluating a range of small to moderate decreases, the study aims to understand how fluctuations in wind speed affect energy yield at specific sites. Moreover, it is assumed that the distribution does not change over time.
6. Step 2 is repeated again with the new decreased wind speed and weibull curve is plotted. An expected outcome is change in the scale factor as the wind speeds decrease now as shown in figure 3.5.

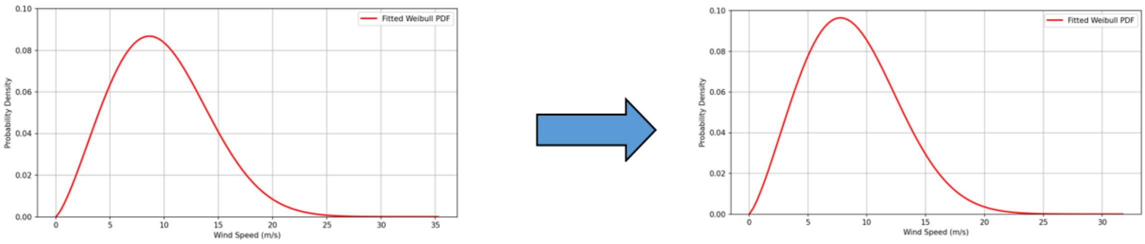

Figure 3.5: Shift in the Weibull curve upon decreasing the wind speed by a constant factor

7. Using the new weibull curve, the shape and scale factors are re-calculated and and step 3 and 4 are repeated, yielding new values of AEP.
8. Relative percentage variation of the new AEP with respect to the historic AEP is calculated.
9. Sensitivity factor is measured as well for all the sites.

3.5.3. Capacity factor

The capacity factor of the wind turbine is calculated using the equation 2.5 mentioned in chapter 2 and the relative change is capacity factor with respect to historic period is calculated.

3.5.4. Impact on Revenue of electricity

Literature says that in short term electricity market, when there is a shortage in the electricity generation, the price of electricity increase as the supply decreases while the demand stays constant or even increases. When there is an increase in the generation, the prices usually tend to go down [86, 95]. As a result, utilities may need to buy extra energy from more expensive backup sources, which results in higher costs being passed on to consumers. Furthermore, the limited availability of electricity increases competition for the existing supply, driving prices even higher.
The impact of wind speed variation affects the AEP which subsequently alters the price [17].

For long term future, it is more complex to predict how the electricity market would react to the changes. To proceed with this analysis, a 10 year average of power purchase agreement prices or the whole sale prices of electricity for the locations have been retrieved [33] and the total revenue has been calculated simply by multiplying the Eur/MWh electricity price with the energy produced in the future. A 50MW wind farm consisting of 10 5MW NREL reference wind turbines has been assumed for this evaluation and the total AEP of the farm is calculated using the AEP calculated in 3.5.2.
This method provides a quantitative evaluation of how variations in AEP induced due changes in wind speed influence electricity prices. However, this is simply an approximation and there are several factors that can influence the costs [17, 89]:

- Factors like electricity market structures, taxes, Supply chain issues, transmission and distribution systems etc. have a strong influence on the prices[89, 17].
- Availability of alternative sources of generation (eg. hydro,solar,etc.).
- Interventions by regulators or market operators can mitigate price spikes.
- Seasonal variations and time of the day affects the generation which can influence the prices.
- There is a possibility of consumers responding to the spike in prices by reducing their consumption which can stabilize or reduce the prices again.

Real-world models are more complex and require detailed analysis at each step considering factors like supply and demand curves, regulatory policies based on the region or country. For estimations with higher accuracy a detailed analysis on economics of energy markets of the regions is necessary which is out of the scope of this project.

3.5.5. GCMs comparison with Reanalysis data

This section outlines the methodology used to compare wind speed projections from the two datasets: GCMs from CMIP6 and statistically downscaled CMIP GCMs, both under the RCP4.5/SSP2-4.5 scenario. These projections are evaluated against the ERA5 reanalysis data for the four sites in Europe as mentioned in previous sections at a height of 10m.

The approach for this analysis is adapted from the methodology employed by the Rijksdienst voor Ondernemend Nederland (RVO) in their wind resource assessment report for the IJmuiden Ver wind farm zone in the North Sea [78]. Historical experiments are chosen for the comparison to avoid getting the influence of climate change scenarios. Table gives an overview of the datasets used:

Table 3.6: Datasets used for comparison with reanalysis data

Dataset	Time period
CMIP6	1994-2014
Statistically downscaled CMIP GCMs	2006-2020

Both the datasets are compared with the daily ERA5 projections obtained by taking the daily mean of hourly u_{era5} calculated using equation 3.1 for their corresponding historical period.
To initiate the comparison, for each model in the datasets, a new representative year of 358 days is built where wind speed at each date is the long term average of wind speed at that date occurring in the entire historical time series. For instance, daily mean wind speed projection on 1st January of this representative year is the mean of all the daily mean wind speeds that occur on 1st January from year 1994 to 2014 (in case of ERA5). This approach has been adapted because, as mentioned in chapter 2, the absolute values from the simulations by the GCMs are not synchronised with real time and day by day comparison of these would not be accurate. Therefore, the GCMs should only be used for long term statistics spanning over 10 years [78, 35]. For simplicity and consistency the 358 days representative year is constructed with 30 days in months from March to January and 28 days in February aligning with the use of 30 days in a month by GCMs.

After getting this representative year for the datasets, the comparison has been conducted by measuring the following error metrics: Bias (%), Mean absolute percent error (%) and correlation coefficients: Pearson's correlation coefficient (R) and Coefficient of Determination (R^2).
Further analysis of the results involves measuring the distances between the coordinates of the GCMs and the ERA5 dataset using the haversine formula once again (see equation 2.7), examining the terrain of the locations, and estimating how the MAPE varies with distance and terrain type.

The chapter on methodology employed in this study concludes here. The comprehensive approach outlined herein forms the foundation for the subsequent analysis. In the following chapter, the results derived from these methodologies will be presented and discussed in detail. The analysis will include a thorough examination of the data, interpretation of findings, and evaluation of the implications that would lead the reader to the answers of the research questions.

4

Results and Discussion

This chapter presents the key findings of this work answering the research questions mentioned in the methodology. The first section details the outputs from the mean wind speed variation analysis performed for 9 sites and a special analysis on CORDEX models followed by a discussion on annual energy yield and sensitivity and capacity factor. Later in the chapter revenue from thr AEP is presented. The chapter ends with a detailed discussion on comparison of reanalysis data with CMIP6 non-downscaled and statistically downscaled CMIP5/6 GCMs.

4.1. Mean wind speed variation

This section presents the mean wind speed variation obtained for each site from CMIP6, Statistically downscaled CMIP and CORDEX CMIP5 projections.
The time series plots (normalised wind speed vs year) are computed using the methodology given in 3.5.1 in the previous chapter. The error bar graphs compare all the datasets in one graph for operational period and near, mid and far future. Similar to the time series plot, the error bars indicate the range from the 17% to the 83% quantiles. The filled circles indicate the 50% quantiles. The numerical values used to build the plots are tabulated in Appendix XX. PUT APPNEDIX Summary tables for this section, providing an overview of the sites and datasets where a decline in wind resource poses a risk can be found at end of this section . A risk is reported when at least 83% of the GCMs show a decline in the wind speed variation as compared to the historic wind speed projections. Similarly, an opportunity is reported when at least 83% of the models predict an increase in the long-term mean wind speed. For the evaluated locations When the 17% to 83% quantile range is not showing either an increase or decrease of the mean wind speed, no risk is reported, as reliable conclusions cannot be drawn due to the poor agreement across the models. The detailed results and discussion of wind speed variation for each site and each dataset is now presented in the upcoming subsections.

4.1.1. NS1

Figure 4.1 displays the normalized mean wind speed from the historical period through the operational period for the four datasets of NS1. The plots can be interpreted as follows: the Operational mean-83% quantile represents the 83% quantile of the long term mean normalised wind speeds predicted by various models. Similarly, The Operational mean-17% quantile represents the 17% quantile of the long term mean normalised wind speeds predicted by the models and Operational mean-median is the 50% quantile or the median. The 10 year rolling mean- median is the median of rolling mean calculated for normalised annual mean wind speed projections by all the models. The boundaries of the light blue shaded region represent the 83% quantile and the 17% quantile of the 10-year rolling mean of the normalised annual mean wind speeds. And lastly, the grey dotted line represents the reference historic period.

Under climate change scenario SSP2-4.5, the CMIP6 (figure 4.1a) and statistically downscaled CMIP5 projections (figure 4.1c) indicate that the 83% quantile is above the historic reference period at 101.2 %

and 101.433 % respectively. This implies that the long term mean normalised wind speed projections from 83% of the models fall below these percentages signifying that the projections are too scattered to determine any significant decline in wind resources, suggesting no reported risk from these two datasets. At the same time, the 17% quantile is beneath the historic reference, so that the opportunity of an increase in wind speed cannot be predicted either.

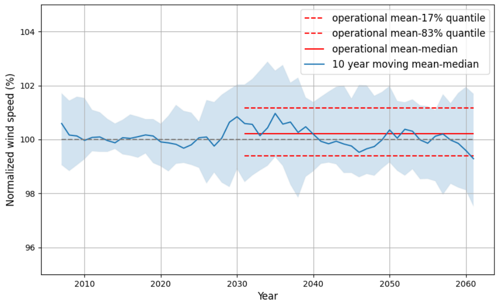

(a) Wind speed projections by 20 CMIP6 GCMs under SSP2-4.5

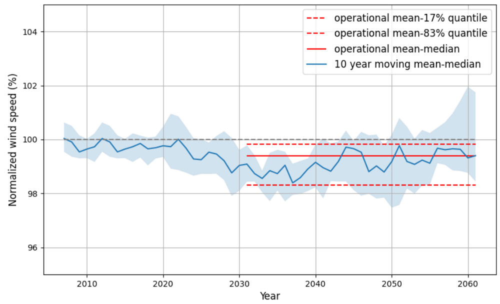

(b) Wind speed projections by 11 CORDEX models under RCP 4.5

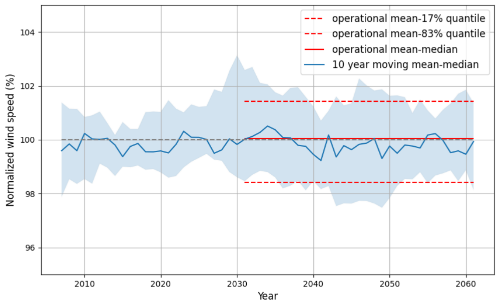

(c) Statistically downscaled wind speed projections by 19 CMIP5 GCMs under RCP 4.5

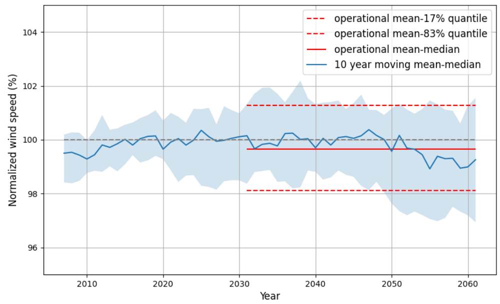

(d) Statistically downscaled wind speed projections by 21 CMIP5 GCMs under RCP 8.5

Figure 4.1: Normalised mean wind speed from the year 2006 to 2060 at Site: NS1

For the CORDEX dataset under RCP4.5 (figure 4.1b), the 83rd percentile falls below the historic reference period at 99.8%, indicating a decline in long-term mean normalised wind speed projections by 83% of the models. According to IPCC guidelines for the likelihood of outcomes, this decline signifies a reported risk.

The 10-year rolling mean- median, along with their respective confidence intervals, illustrate the trend in wind speed variations over time. The spread of the confidence intervals is a measure of the uncertainty in the projections. A narrow confidence interval in the historical period represents low uncertainty. Since the datasets are bias corrected using the ERA5 reanalysis data, they are more aligned causing lower uncertainty.

- For *CMIP6 projections*, as the projections extend further into the future, uncertainties accumulate, leading to broader confidence intervals. Since the CMIP6 models operate at a coarser resolution, they capture large-scale processes well but may miss finer regional details, leading to higher uncertainty. Moreover, the presence of a diverse ensemble of models from various institutions, increasing variability and uncertainty. Furthermore, along the future, the transitioning effects to SSP2-4.5 become more prominent also adding to the increases uncertainty.

- For *Statistically downscaled CMIP5 projections* the uncertainty is initially similar to the raw CMIP6 models due to reliance on the same historical data. Moreover, as the statistical downscaling relies on GCM outputs, and any uncertainties in these models propagate through the downscaling process. While statistical downscaling improves spatial resolution, it may not always accurately capture all local processes, leading to retained or increased uncertainty. Lastly, presence of a diverse ensemble of models , yet again, increases the variability and broadens the confidence intervals.

- Unlike the CMIP6 and statistically downscaled CMIP5 projections, the *CORDEX dataset* exhibits a declining trend in wind speeds between years 2022 and 2042, followed by a slight increase towards the end of the period. The dynamical downscaling used in CORDEX incorporates high-resolution regional data from RCMs, , which allow for a more accurate evaluation of small-scale characteristics, increasing the impact of local conditions on the model predictions.

Figure 4.1d illustrates the statistically downscaled CMIP5 projections under the RCP8.5 scenario. Similar to the CMIP6 and statistically downscaled CMIP5 projections under RCP4.5, no risk is reported for this site, with the 83rd percentile at 101.28%. The rolling mean-median projections indicate minimal variation over the years, and although wind speeds decline towards the end of the period, the long-term 83rd percentile remains above the historic reference period, indicating no significant risk.

Future periods have been classified as near, mid, and far future as mentioned in chapter3, and normalised wind speed projections for these periods are presented through the error bar graph in figure 4.2 for the RCP 4.5/SSP2-4.5 scenario. Additionally, a comparison between the RCP 4.5 and RCP 8.5 scenarios has been made for the statistically downscaled CMIP projections, as shown in Figure 4.3. This dataset was selected due to its high resolution of 3 km.

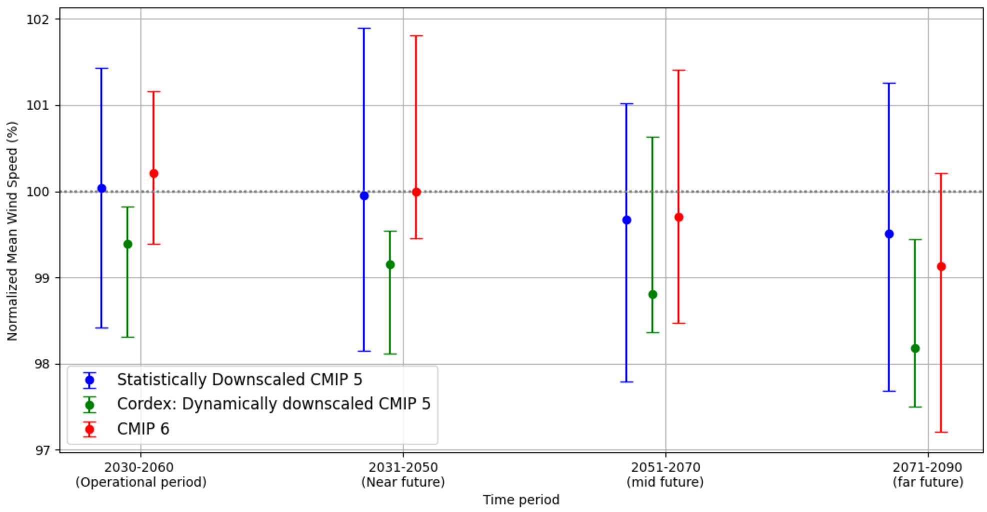

Figure 4.2: Normalised wind speed projections for different future time periods under RCP 4.5/SSP2-4.5 at site: NS1. Confidence intervals show the 83% and 17% quantiles, point in between shows the median of the models

From figure 4.2, no risk is reported by statistically downscaled CMIP5 and the raw CMIP6 projections for all time periods. The statistically downscaled projections exhibit a higher spread of confidence intervals compared to the CMIP6 projections during the operational period and near future. However, this spread becomes almost the same towards the mid and far future. Additonally, the CORDEX dataset indicates a decline in wind speed in both the near and far future periods.

Figure 4.3 below presents the comparison between RCP 4.5 and RCP 8.5 scenarios for the statistically downscaled CMIP projections. Both the scenarios indicate no risk across the time periods. The difference in magnitude of 83% quantile between the two scenarios shows the variation in the spread of model projections rather than the extent of wind speed increase.

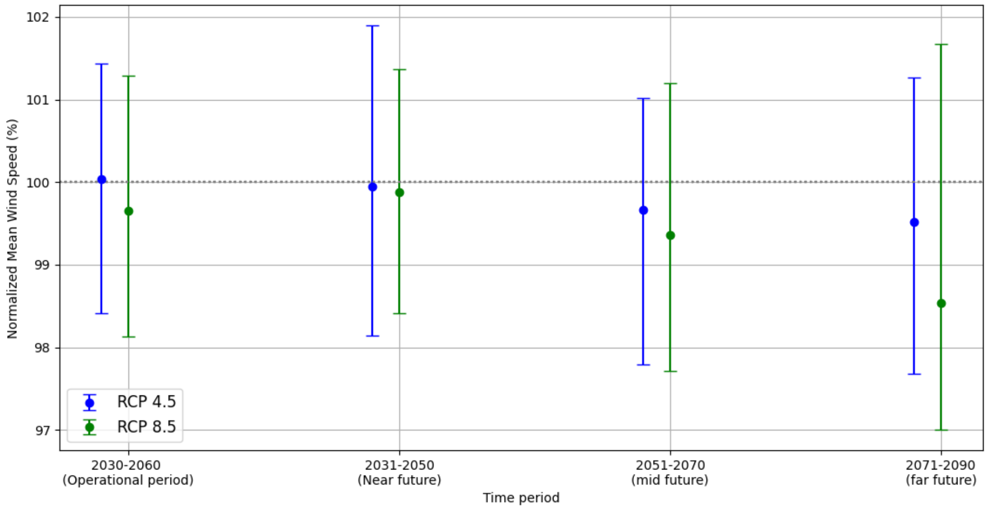

Figure 4.3: Comparison between normalised wind speed projections under climate change scenarios RCP 4.5 and RCP 8.5 for different future time periods at site: NS1. Confidence intervals show the 83% and 17% quantiles, point in between shows the median of the models

4.1.2. NS2

Figure 4.4 displays the normalized mean wind speed from the historical period through the operational period for the four datasets at site NS2. Under climate change scenario SSP2-4.5, the CMIP6 (figure 4.4a) and statistically downscaled CMIP6 projections (figure 4.4c) indicate that the 83% quantile is above the historic reference period at 100.57% and 100.92% respectively. Since the projections are too scattered to determine any significant decline in wind resources, no risk is reported these two datasets.
For these two datasets, the 10-year rolling mean- median, along with their respective confidence intervals, indicate a declining trend in wind speed variations over time with CMIP6 models showing higher decline that the statistically downscaled CMIP6. A heightened uncertainty can be seen again for the future periods.

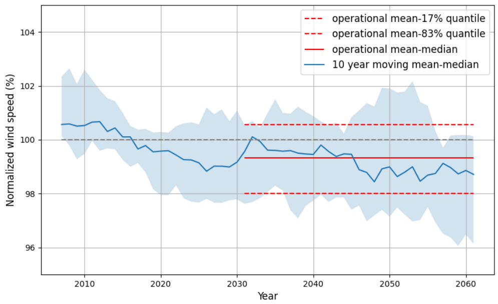

(a) Wind speed projections by 19 CMIP6 GCMs under SSP2-4.5

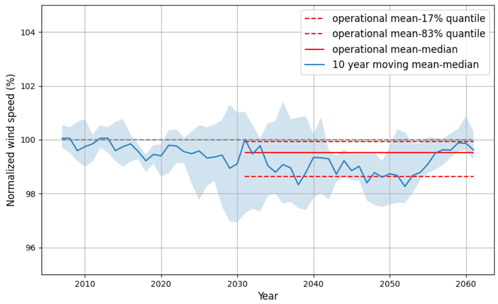

(b) Wind speed projections by 11 CORDEX models under RCP 4.5

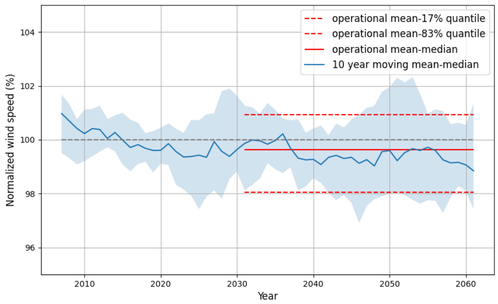

(c) Statistically downscaled wind speed projections by 20 CMIP6 GCMs under SSP2-4.5

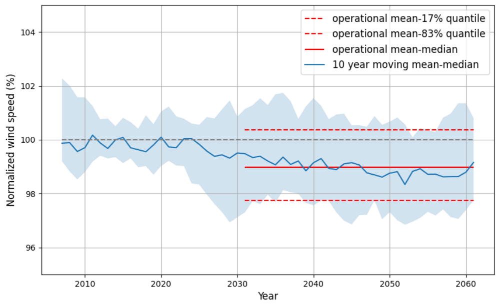

(d) Statistically downscaled wind speed projections by 20 CMIP6 GCMs under SSP5-8.5

Figure 4.4: Normalised mean wind speed from the year 2006 to 2060 at Site: NS2

For the CORDEX dataset under RCP4.5 (figure 4.4b), the 83rd percentile falls below the historic reference period at 99.94%, indicating a slight decline in long-term mean normalised wind speed projections by 83% of the models. Therefore it has been reported as a risk. Similar to the the CMIP6 and statistically downscaled CMIP5 projections, the CORDEX dataset also exhibits a declining trend in wind speeds,however, an increase is seen at the end of the operation period around year 2052. The confidence interval however, is higher in the middle of the operational period. This can be attributed to the finer regional details in the climate picked by the high resolution RCMs used in the process of dynamical downscaling.

Figure 4.1d illustrates the statistically downscaled CMIP6 projections under the SSP5-8.5 scenario. Similar to the CMIP6 and statistically downscaled CMIP6 projections under SSP2-4.5, no risk is reported for this site, with the 83rd percentile at 100.38%. The rolling mean-median projections indicate a decline in wind speed as they move along the period.

Figure 4.5 shows the normalised wind speed in further divided future time periods under SSP2-4.5/RCP4.5.

In the near future, all the datasets show the 83% quantile above the historic reference so no risk can be predicted. Moreover, statistically downscaled CMIP6 and the raw CMIP6 projections also do not show any risk in mid and far futur. However, 83% of the CORDEX models do show a decline in the wind speed, indicating a risk.

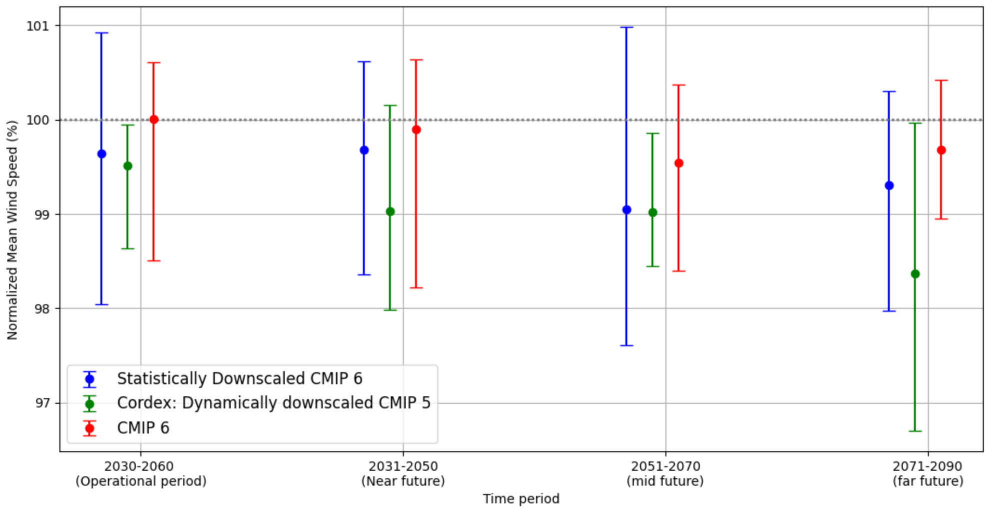

Figure 4.5: Normalised wind speed projections for different future time periods under RCP 4.5/SSP2-4.5 at site: NS2. Confidence intervals show the 83% and 17% quantiles, point in between shows the median of the models

Figure 4.7 below presents the comparison between SSP2-4.5 and SSP5-8.5 scenarios for the statistically downscaled CMIP projections. Under SSP2-4.5 no risk is reported for all the time periods. However, under SSP5-8.5 in the mid-fututre the 83% quantile is below the historic reference, indicating a risk.

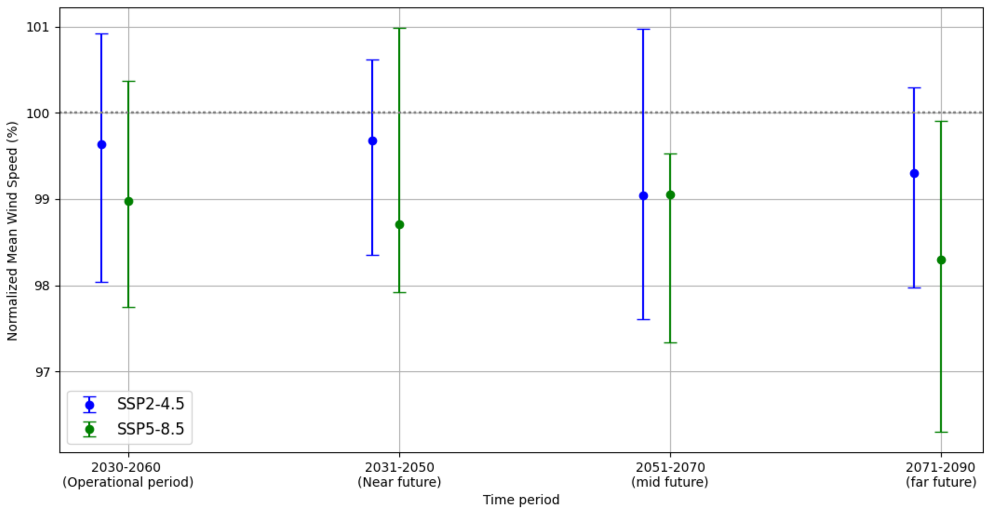

Figure 4.6: Comparison between normalised wind speed projections under climate change scenarios SSP2-4.5 and SSP5-8.5 for different future time periods at site: NS2. Confidence intervals show the 83% and 17% quantiles, point in between shows the median of the models

4.1.3. FR

Figure 4.7 displays the normalized mean wind speed from the historical period through the operational period for the four datasets at site FR. Under climate change scenario SSP2-4.5, the CMIP6 (figure 4.7a) and statistically downscaled CMIP6 projections (figure 4.7c) indicate that the 83% quantile is above the historic reference period at 101.05% and 100.70% respectively. Therefore, as per the explanation provided in 4.1.1, no risk is reported these two datasets.
For the CMIP6 projections, the 10-year rolling mean- median, shows a declining trend in wind speed variations over time. The statistically downscaled CMIP6 projections, on the other hand, decline around year 2038. A higher uncertainty is present in the CMIP6 projections as compared to its statistically downscaled version.

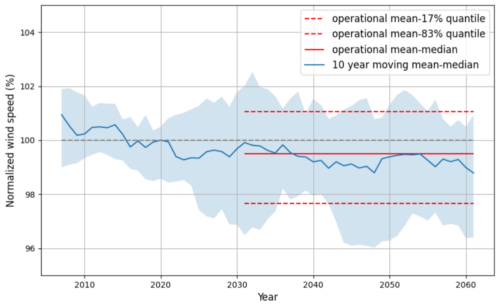

(a) Wind speed projections by 20 CMIP6 GCMs under SSP2-4.5

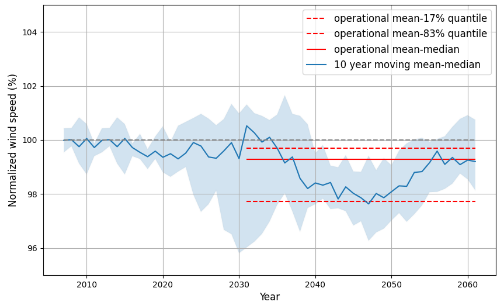

(b) Wind speed projections by 11 CORDEX models under RCP 4.5

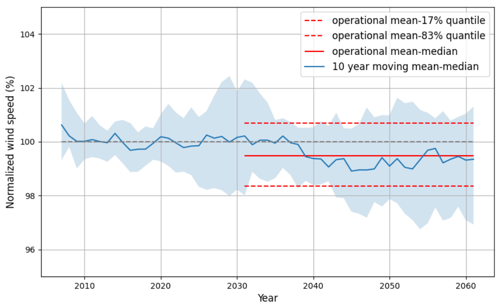

(c) Statistically downscaled wind speed projections by 19 CMIP6 GCMs under SSP2-4.5

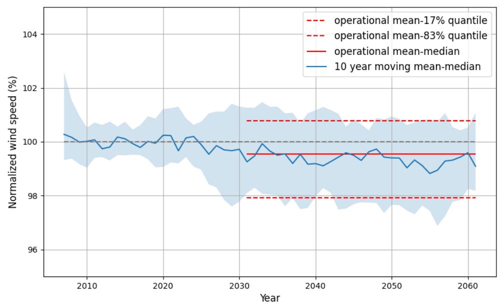

(d) Statistically downscaled wind speed projections by 20 CMIP6 GCMs under SSP5-8.5

Figure 4.7: Normalised mean wind speed from the year 2006 to 2060 at Site: FR

For the CORDEX dataset (figure 4.7b), the 83rd percentile falls below the historic reference period at 99.70%, indicating a decline in long-term mean normalised wind speed projections by 83% of the models. Therefore it has been reported as a risk. The rolling mean shows a steep decline in wind speed around year 2033 until 2048 when it starts to rise again. The confidence interval however, is very broad in the middle of the operational period indicating high uncertainty and then narrows down after 2040. This can be attributed to the finer regional details in the climate picked by the high resolution RCMs in the middle years used in the process of dynamical downscaling. These details can introduce short-term variability that models may capture differently, leading to a temporary increase in uncertainty.

Figure 4.7d illustrates the statistically downscaled CMIP6 projections under the SSP5-8.5 scenario. Similar to the CMIP6 and statistically downscaled CMIP6 projections under SSP2-4.5, no risk is reported for this site, with the 83rd percentile at 100.77%. The rolling mean-median projections indicate a slight decline in wind speed as they move along the period.

Figure 4.8 shows the normalised wind speed in further divided future time periods under SSP2-4.5. No risk is reported by statistically downscaled CMIP6 and the raw CMIP6 projections for all time periods. The CORDEX dataset indicates a decline in wind speed in both the near and mid future periods but not in the far-future.

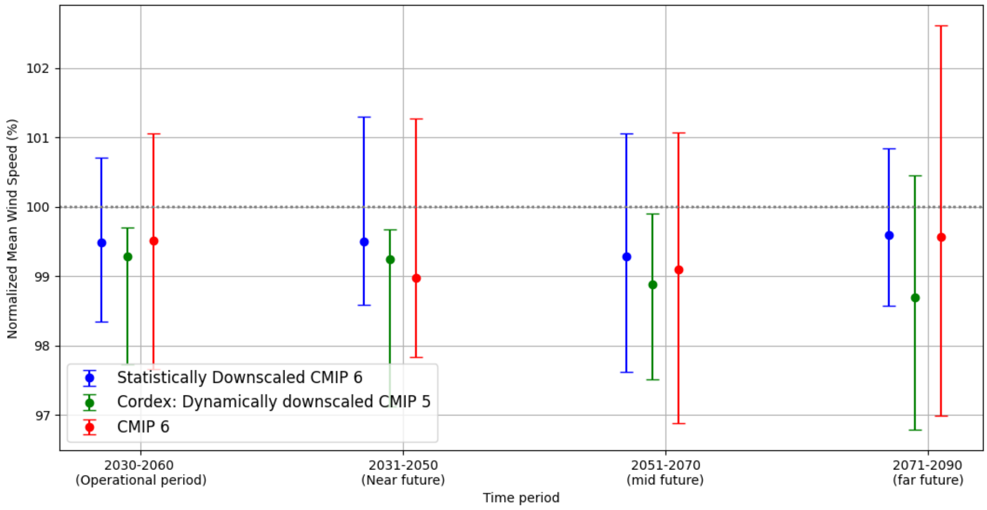

Figure 4.8: Normalised wind speed projections for different future time periods under RCP 4.5/SSP2-4.5 at site: FR. Confidence intervals show the 83% and 17% quantiles, point in between shows the median of the models

Figure 4.9 below presents the comparison between SSP2-4.5 and SSP5-8.5 scenarios for the statistically downscaled CMIP projections. Both the scenarios indicate no risk across the time periods

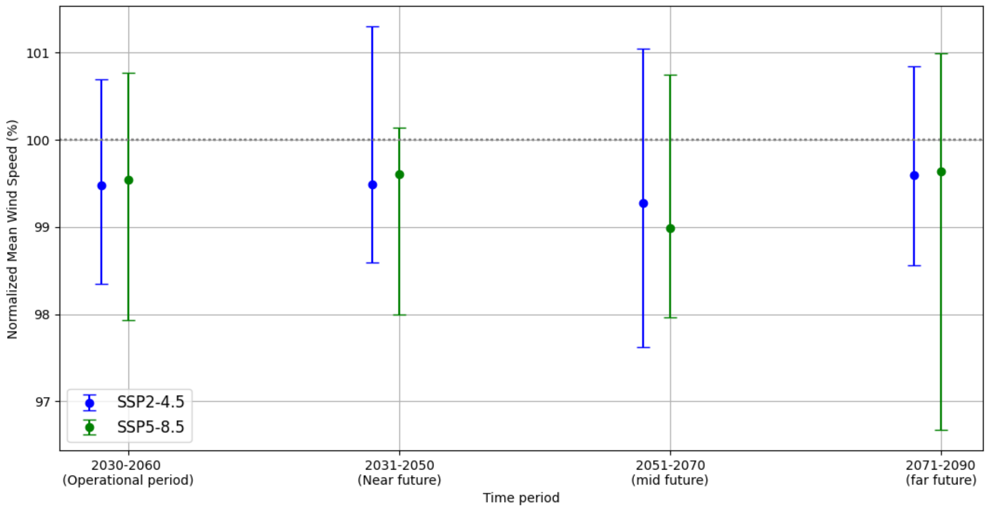

Figure 4.9: Comparison between normalised wind speed projections under climate change scenarios SSP2-4.5 and SSP5-8.5 for different future time periods at site: FR. Confidence intervals show the 83% and 17% quantiles, point in between shows the median of the models

4.1.4. IT

Figure 4.10 displays the normalized mean wind speed from the historical period through the operational period for the four datasets at site IT. under the climate scenarios using a radiative forcing of 4.5 W/m^2, SSP2-4.5 and RCP4.5 all the datasets: the CMIP6 (figure 4.7a), CORDEX (figure 4.10b) and statistically downscaled CMIP6 projections (figure 4.7c) indicate that the 83% quantile is below the historic reference period at 98.72%, 98.41% and 99.46 % respectively. Therefore, the risk of a reduction in the wind resource is reported by all the datasets.
For the CMIP6 and statistically downscaled CMIP6 projections, the 10-year rolling mean exhibits a steep declining trend in wind speed variations over time. In contrast, the CORDEX projections show a decline around 2030, followed by a slight increase after 2041. However, these projections still remain below the wind speeds observed during the historical period.

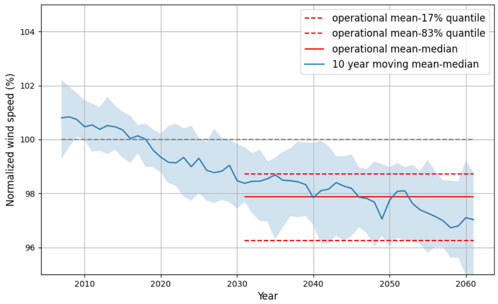

(a) Wind speed projections by 20 CMIP6 GCMs under SSP2-4.5

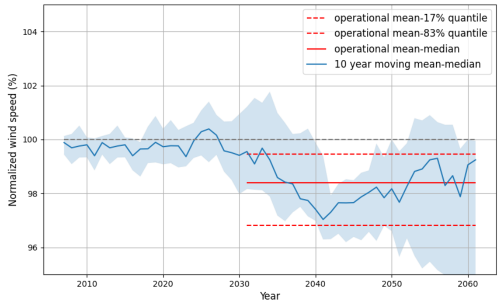

(b) Wind speed projections by 11 CORDEX models under RCP 4.5

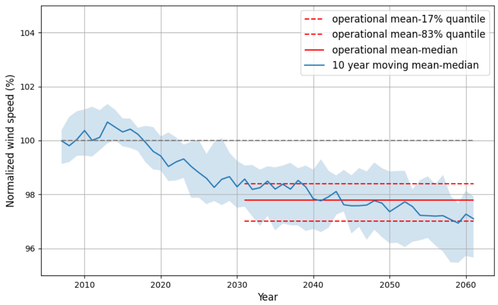

(c) Statistically downscaled wind speed projections by 19 CMIP6 GCMs under SSP2-4.5

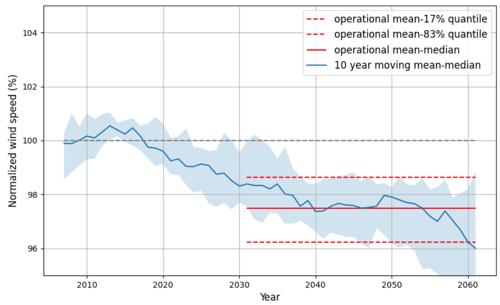

(d) Statistically downscaled wind speed projections by 19 CMIP6 GCMs under SSP5-8.5

Figure 4.10: Normalised mean wind speed from the year 2006 to 2060 at Site: IT

Figure 4.10d illustrates the statistically downscaled CMIP6 projections under the SSP5-8.5 scenario. Similar to the projections under SSP2-4.5, this scenario also reports a risk for this site under SSP5-8.5, with the 83rd percentile at 98.63%. The rolling mean also indicates a steep decline in the wind speed projections over time.

Figure 4.11 shows the normalised wind speed in further divided future time periods under SSP2-4.5. A risk is reported by statistically downscaled CMIP6 and the raw CMIP6 projections for all time periods. The CORDEX dataset indicates a decline in wind speed in both the near and mid future periods and shows very high scatter also for the mid future. In in the far-future no risk is reported which can explained as due to larger uncertainty for the far future combined with the lower number of available models from CORDEX.

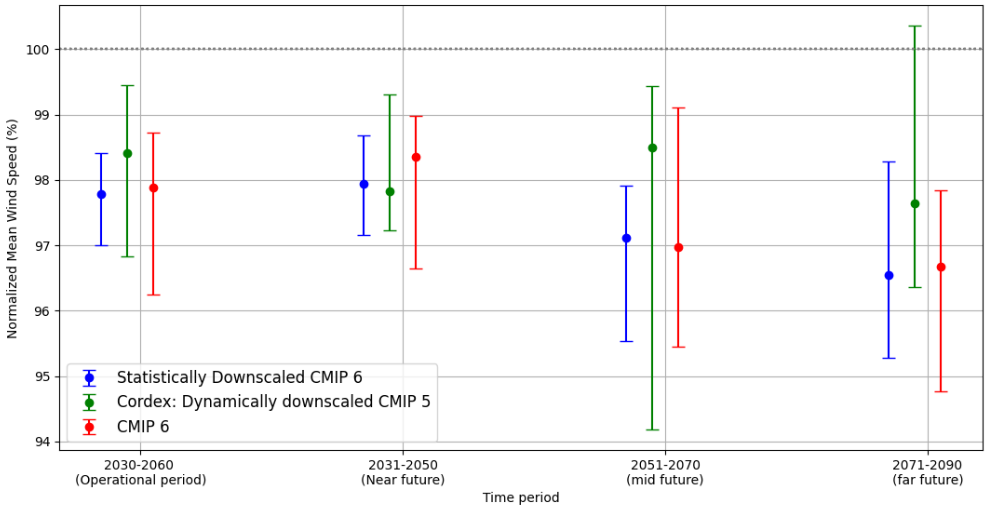

Figure 4.11: Normalised wind speed projections for different future time periods under RCP 4.5/SSP2-4.5 at site: IT. Confidence intervals show the 83% and 17% quantiles, point in between shows the median of the models

Figure 4.12 below presents the comparison between SSP2-4.5 and SSP5-8.5 scenarios for the statistically downscaled CMIP projections. Both the scenarios show a decline in wind speed projections therefore indicating risk across the time periods.

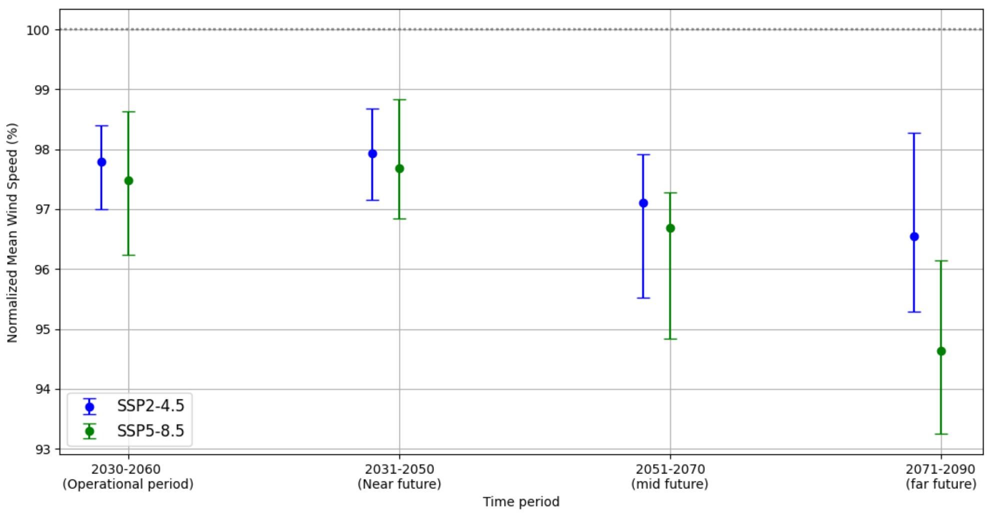

Figure 4.12: Comparison between normalised wind speed projections under climate change scenarios SSP2-4.5 and SSP5-8.5 for different future time periods at site: IT. Confidence intervals show the 83% and 17% quantiles, point in between shows the median of the models

4.1.5. UK1

Figure 4.13 displays the normalized mean wind speed from the historical period through the operational period for the four datasets at site IT. Under climate change scenario SSP2-4.5, all the datasets: the CMIP6 (figure 4.13a), CORDEX (figure 4.13b) and statistically downscaled CMIP6 projections (figure 4.13c) indicate that the 83% quantile is above the historic reference period at 100.53%, 101.38% and 100.64%respectively. Therefore, no risk to wind resource is reported from all the datasets.
For the CMIP6 and statistically downscaled CMIP6 projections, the 10-year rolling mean shows a decline in wind speed variations over time. In contrast, the CORDEX projections show a an increase from around year 2041.

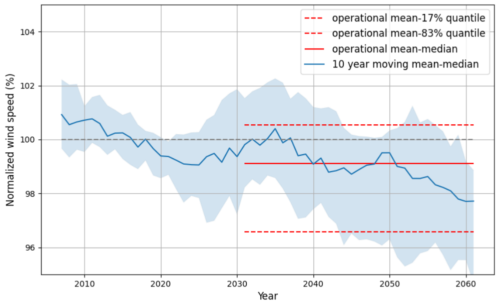

(a) Wind speed projections by 20 CMIP6 GCMs under SSP2-4.5

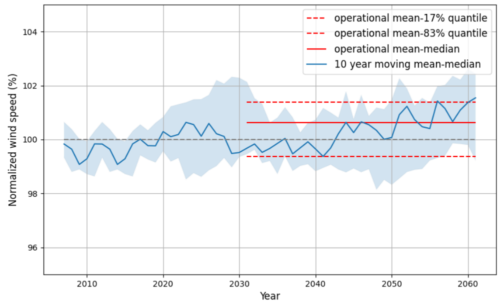

(b) Wind speed projections by 11 CORDEX models under RCP 4.5

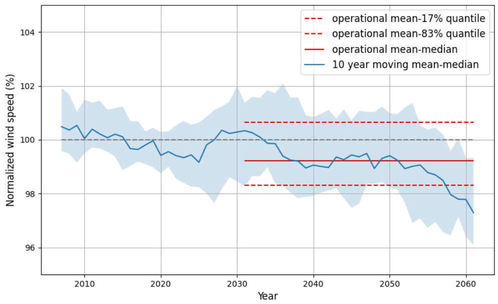

(c) Statistically downscaled wind speed projections by 20 CMIP6 GCMs under SSP2-4.5

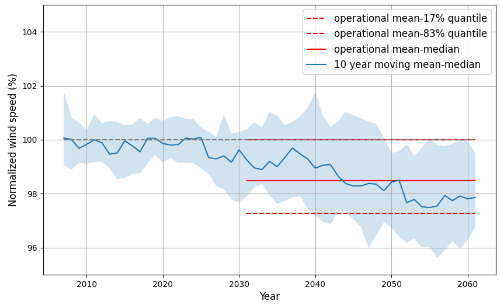

(d) Statistically downscaled wind speed projections by 20 CMIP6 GCMs under SSP5-8.5

Figure 4.13: Normalised mean wind speed from the year 2006 to 2060 at Site: UK1

Figure 4.13d presents the statistically downscaled CMIP6 projections under the SSP5-8.5 scenario. Similar to the projections under SSP2-4.5, this scenario also reports no risk for this site under SSP5-8.5, with the 83rd percentile at 100.004%. The rolling mean however, indicates a decline in the wind speed projections over time.

Figure 4.14 shows the normalised wind speed in further divided future time periods under SSP2-4.5. In the near and the far future, all datasets indicate no risk. In contrast, in the mid-future scenario, the CMIP6 and statistically downscaled CMIP6 projections indicate a risk whereas CORDEX projections do not.

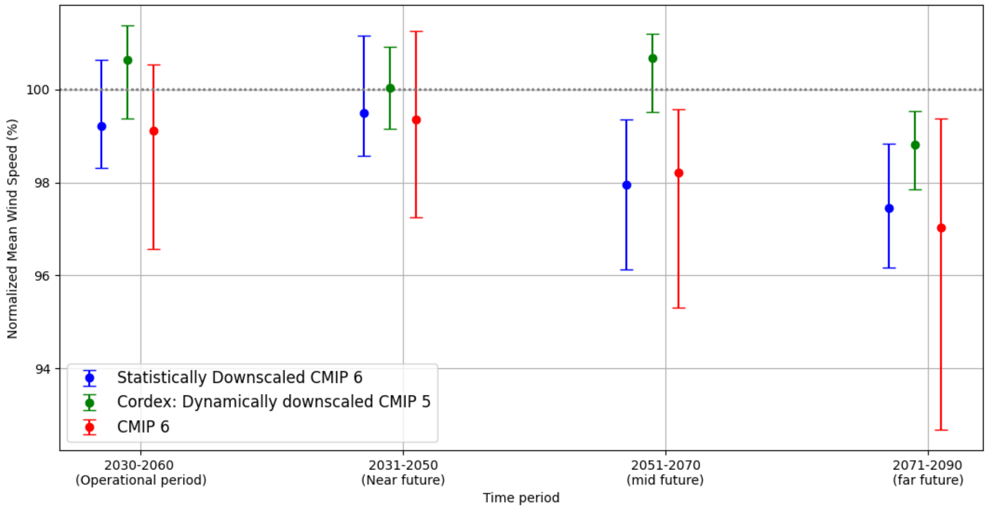

Figure 4.14: Normalised wind speed projections for different future time periods under RCP 4.5/SSP2-4.5 at site: UK1. Confidence intervals show the 83% and 17% quantiles, point in between shows the median of the models

Figure 4.15 below presents the comparison between SSP2-4.5 and SSP5-8.5 scenarios for the statistically downscaled CMIP6 projections. Both the scenarios show a decline in wind speed projections in mid and far future therefore indicating risk across these time periods. No risk reported in near future.

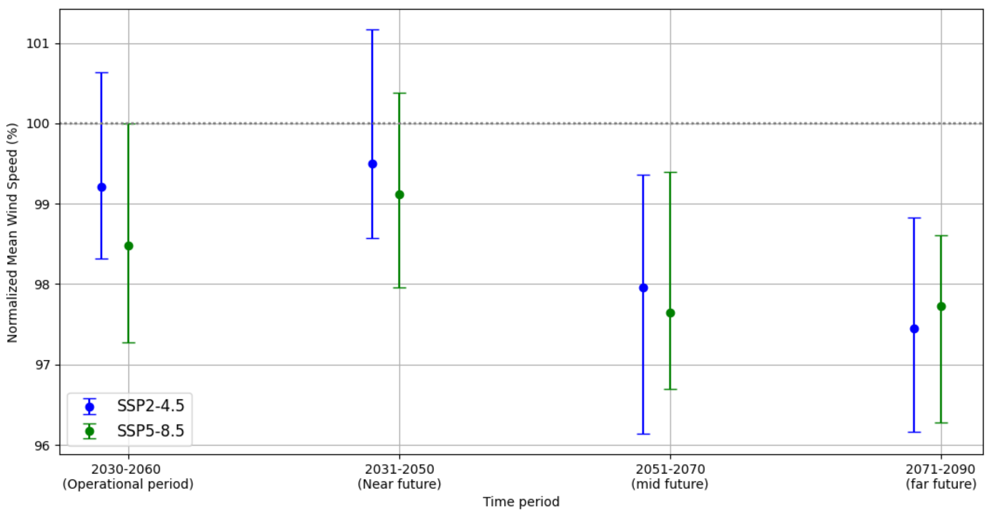

Figure 4.15: Comparison between normalised wind speed projections under climate change scenarios SSP2-4.5 and SSP5-8.5 for different future time periods at site: UK1. Confidence intervals show the 83% and 17% quantiles, point in between shows the median of the models

4.1.6. UK2

Figure 4.16 displays the normalized mean wind speed from the historical period through the operational period for the four datasets at site UK2. Under climate change scenario RCP 4.5, all the datasets: the CMIP6 (figure 4.16a), CORDEX (figure 4.16b) and statistically downscaled CMIP5 projections (figure 4.16c) indicate that the 83% quantile is above the historic reference period at 100.34%, 100.46% and 100.38% respectively. Therefore, no risk to wind resource is reported from all the datasets.
For the CMIP6 and statistically downscaled CMIP5 projections, the 10-year rolling mean shows a decline in wind speed variations over time. A higher decline is projected by CMIP6 GCMs as compared to downscaled CMIP5 GCMs. For CORDEX projections, initially, the wind speed remains stable with narrow confidence intervals. Around 2030, a significant decline in mean wind speed is observed, with increased uncertainty. From 2040 onwards, wind speeds begin to stabilize but remain below historical levels, with confidence intervals narrowing, indicating reduced uncertainty. By the end of the timeline, a slight increase is seen, but wind speeds do not fully return to historical levels,

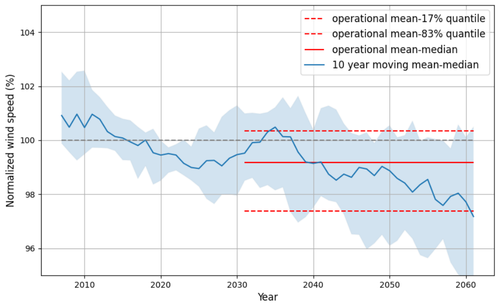

(a) Wind speed projections by 20 CMIP6 GCMs under SSP2-4.5

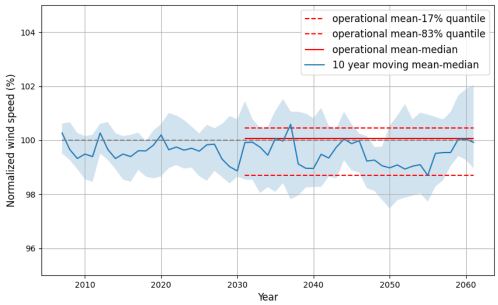

(b) Wind speed projections by 11 CORDEX models under RCP 4.5

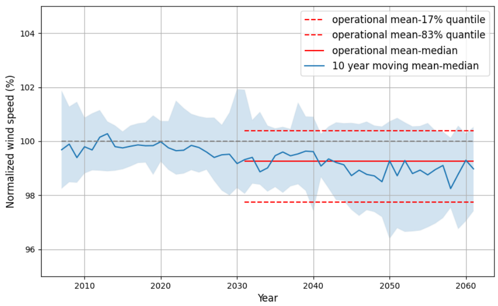

(c) Statistically downscaled wind speed projections by 20 CMIP5 GCMs under RCP 4.5

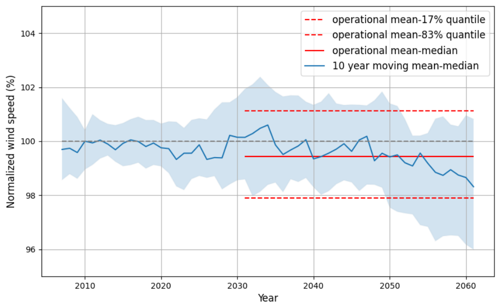

(d) Statistically downscaled wind speed projections by 21 CMIP5 GCMs under RCP 8.5

Figure 4.16: Normalised mean wind speed from the year 2006 to 2060 at Site: UK2

Figure 4.16d presents the statistically downscaled CMIP5 projections under the RCP 8.5 scenario. Similar to the projections under RCP 4.5, this scenario also reports no risk for this site, with the 83rd percentile at 101.12%. The rolling mean shows a decline in the wind speed projections by the end of the operational period from around year 2040. A higher uncertainty is induced around 2025 as one move towards the future.

Figure 4.17 shows the normalised wind speed in further divided future time periods under RCP 4.5. In the near future scenario, all datasets indicate no risk. Moving further towards the mid-future, CMIP6 and statistically downscaled CMIP5 projections indicate a decline in the wind speed, whereas, from CORDEX projections no risk can be observed. Lastly, in the far-future scenario, the CMIP6 and CORDEX projections indicate a risk whereas tatistically downscaled CMIP5 projections do not.

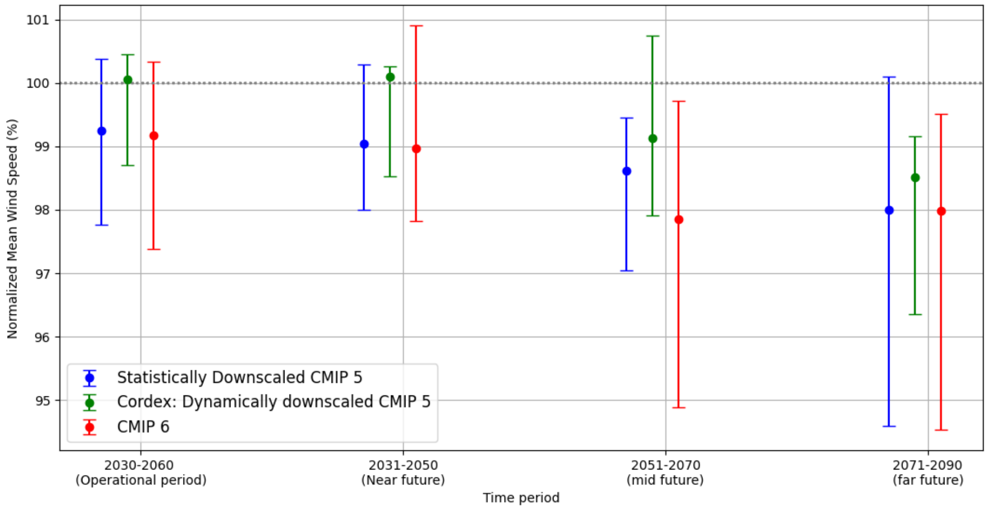

Figure 4.17: Normalised wind speed projections for different future time periods under RCP 4.5/SSP2-4.5 at site: UK2. Confidence intervals show the 83% and 17% quantiles, point in between shows the median of the models

Figure 4.18 below presents the comparison between RCP 4.5 and RCP 8.5 scenarios for the statistically downscaled CMIP5 projections. Both the scenarios show no risk to the wind resource in near and far future. However in mid-future, under RCP 4.5, the wind speed projections are lower than the historic projections, thereby indicating a risk.

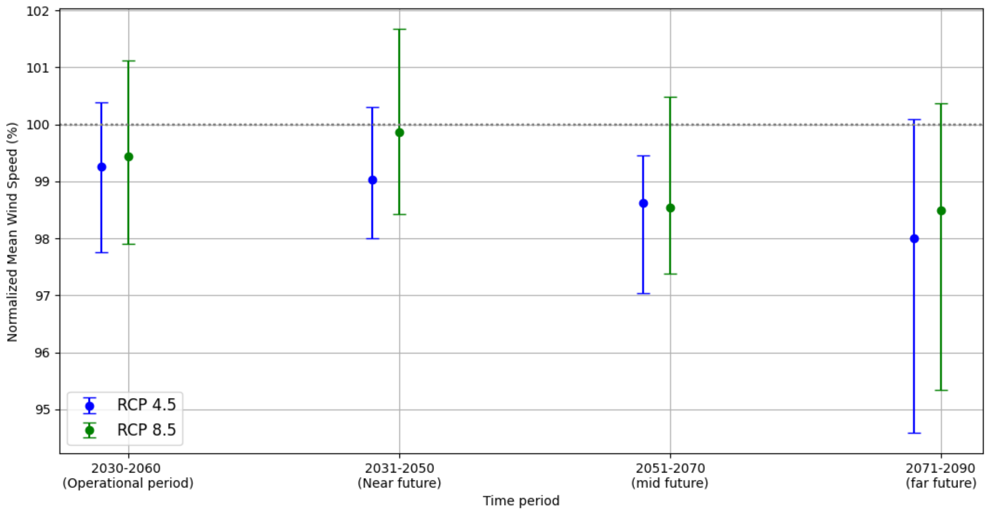

Figure 4.18: Comparison between normalised wind speed projections under climate change scenarios RCP 4.5 and RCP 8.5 for different future time periods at site: UK2. Confidence intervals show the 83% and 17% quantiles, point in between shows the median of the models

4.1.7. UK3

Figure 4.19 displays the normalized mean wind speed from the historical period through the operational period for the four datasets at site UK3. Under climate change scenario RCP 4.5, the datasets: the CMIP6 (figure 4.19a)and statistically downscaled CMIP5 projections (figure 4.19c) report a risk with the 83% quantile being below the historic reference period at 98.94% for both. In contrast, 83% quantile of the CORDEX projections is above the historic projections, indicating no risk can be predicted (4.19b). For the CMIP6 and statistically downscaled CMIP5 projections, the 10-year rolling mean exhibits a declining trend in wind speed variations over time with uncertainty rising on moving towards the future years. The CORDEX projections show a considerable width of the uncertainty band in the middle years indicating notable variability, reflecting possible changes in wind patterns or other influencing factors. However, the trend is consistent enough to suggest that significant deviations from the current wind speeds are not expected, apart from occasional peaks and troughs within the broader stable trend.

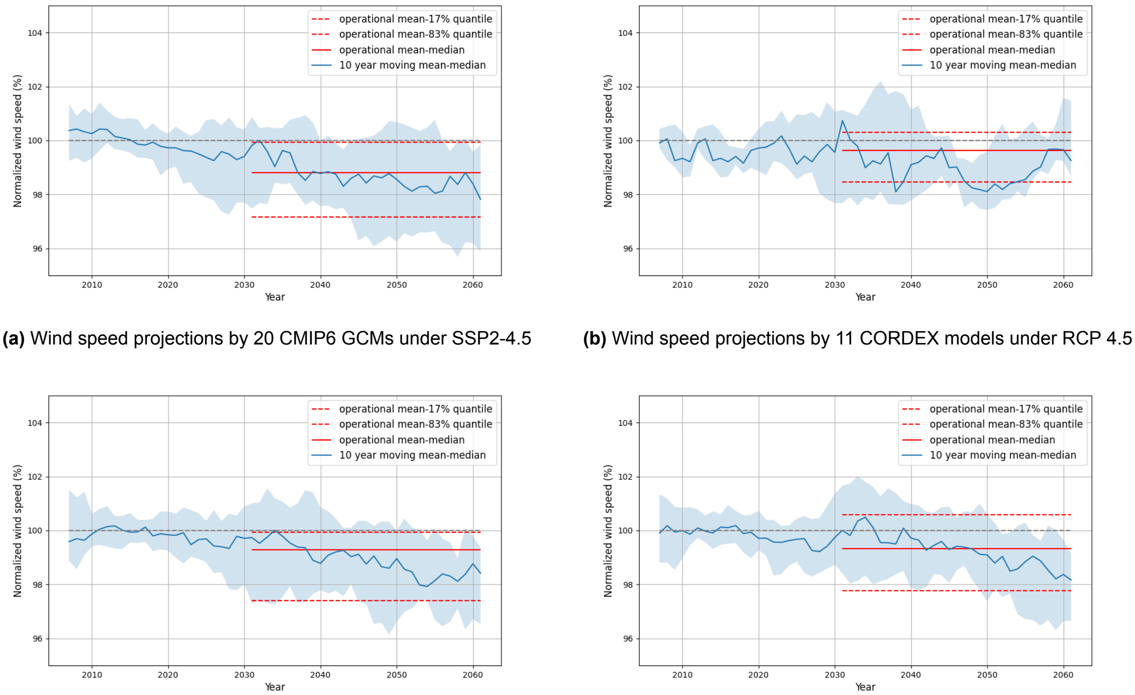

(a) Wind speed projections by 20 CMIP6 GCMs under SSP2-4.5

(b) Wind speed projections by 11 CORDEX models under RCP 4.5

(c) Statistically downscaled wind speed projections by 20 CMIP5 GCMs under RCP 4.5

(d) Statistically downscaled wind speed projections by 21 CMIP5 GCMs under RCP 8.5

Figure 4.19: Normalised mean wind speed from the year 2006 to 2060 at Site: UK3

Figure 4.19d presents the statistically downscaled CMIP5 projections under the RCP 8.5 scenario. Unlike to the projections under RCP-4.5, this scenario reports no risk for this site, with the 83rd percentile at 100.58%. The rolling mean shows a decline in the wind speed projections by the middle of the operational period from around year 2035. A higher uncertainty is also visible from around 2025 as one move towards the future.

Figure 4.20 shows the normalised wind speed in further divided future time periods under RCP 4.5. In the near future, all datasets indicate no risk. Moving further towards the mid-future, from CMIP6 and statistically downscaled CMIP5 projections, no risk can be reported. Whereas, the CORDEX projections indicate a decline in the wind speed. Lastly, in the far-future scenario, the CMIP6 and CORDEX projections indicate a risk whereas statistically downscaled CMIP5 projections do not.

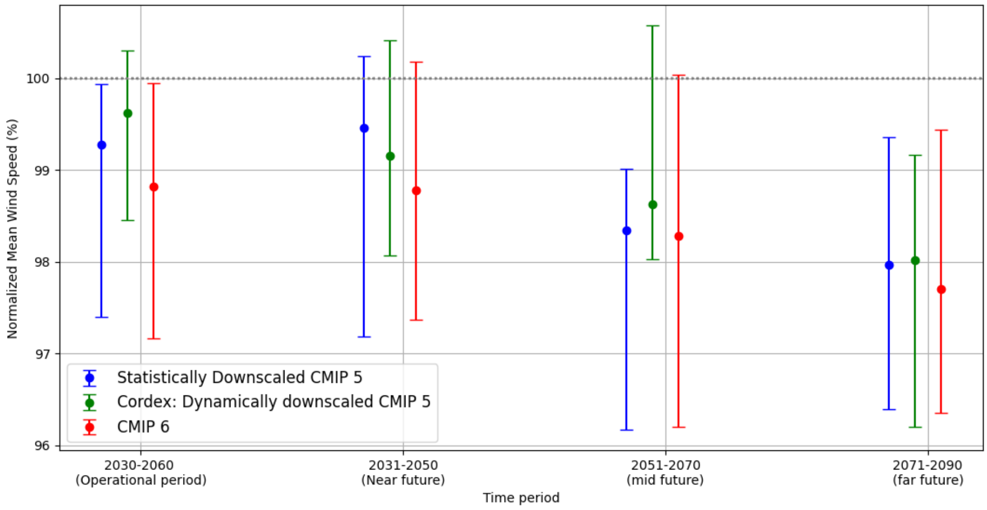

Figure 4.20: Normalised wind speed projections for different future time periods under RCP 4.5/SSP2-4.5 at site: NS2. Confidence intervals show the 83% and 17% quantiles, point in between shows the median of the models

Figure 4.21 below presents the comparison between RCP 4.5 and RCP 8.5 scenarios for the statistically downscaled CMIP5 projections. Both the scenarios show no risk to the wind resource in the near future. However in mid and far future, the wind speed projections are lower than the historic projections, thereby indicating a risk under both RCP 4.5 and RCP 8.5 scenarios.

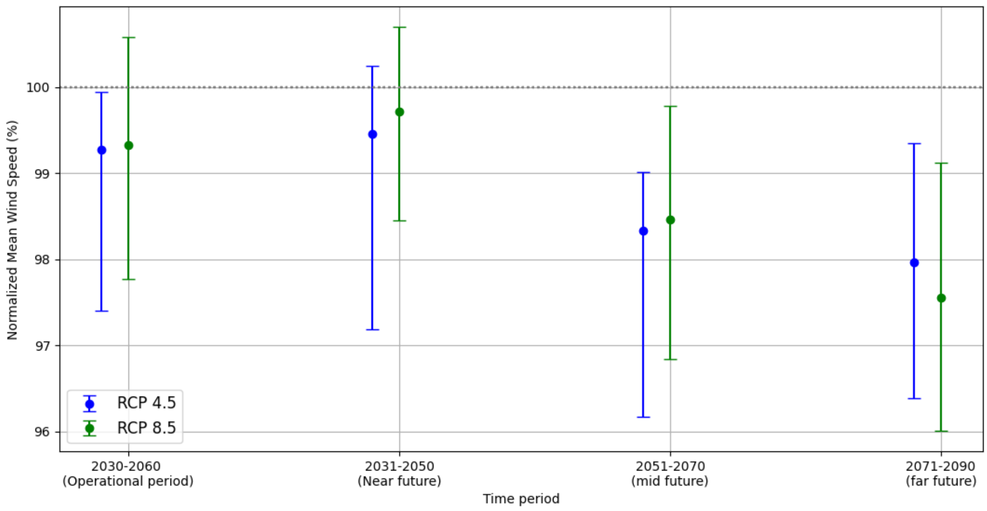

Figure 4.21: Comparison between normalised wind speed projections under climate change scenarios RCP 4.5 and RCP 8.5 for different future time periods at site: NS2. Confidence intervals show the 83% and 17% quantiles, point in between shows the median of the models

4.1.8. NA1

Figure 4.22 displays the normalized mean wind speed from the historical period through the operational period for the three datasets at site NA1. Under climate change scenario RCP 4.5, for the datasets: the CMIP6 (figure 4.19a) and statistically downscaled CMIP5 projections (figure 4.19c) 83% quantile is above historic reference projections, at 102.17% and 101.39% respectively. So no risk can be reported from these datasets. For CMIP6 projections, the 10-year rolling mean-median stays stable over time with uncertainty increasing significantly after 2040, reflecting greater variability and less confidence in long-term projections. For statistically downscaled CMIP5 projections as well, wind speeds are mostly stable, with slight fluctuating 100% over the projection period. The 10-year moving mean-median line shows minor variations but no significant long-term trend. The uncertainty, represented by the shaded area, is moderate, indicating consistent projections with some variability. This suggests a stable outlook for wind speeds under this scenario, with a moderate level of confidence.

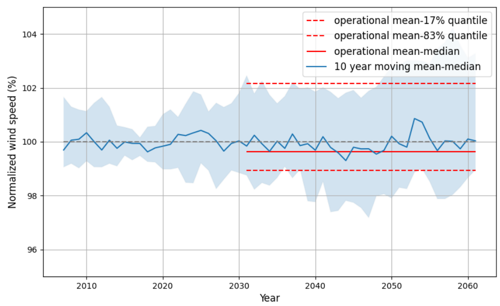

(a) Wind speed projections by 19 CMIP6 GCMs under SSP2-4.5

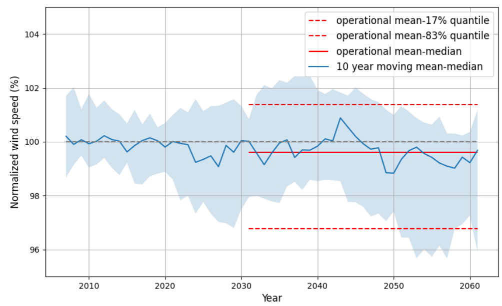

(b) Statistically downscaled wind speed projections by 19 CMIP5 GCMs under RCP 4.5

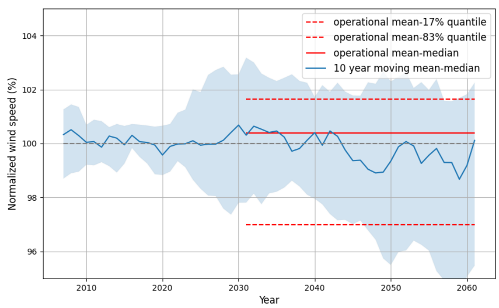

(c) Statistically downscaled wind speed projections by 21 CMIP5 GCMs under RCP 8.5

Figure 4.22: Normalised mean wind speed from the year 2006 to 2060 at Site: NA1

Under RCP 8.5, the downscaled CMIP5 projections also do not report any risk (figure 4.22c). The Wind speeds show more fluctuation compared to the other projections but remain around the 100% mark overall. The 10-year moving mean-median line shows periods of increase and decrease, indicating variability in short-term trends. The shaded area, representing uncertainty, is wider than in Figure 4.51, especially towards the end of the period, indicating higher variability and less confidence in these projections. This suggests that while wind speeds are generally stable, there is more uncertainty compared to other scenarios.

Figure 4.23 shows the normalised wind speed in further divided future time periods under RCP 4.5. For both the datasets, the 83% quantile is above the historic wind speed projection in all the future scenarios therefore, no risk can be predicted from these datasets.

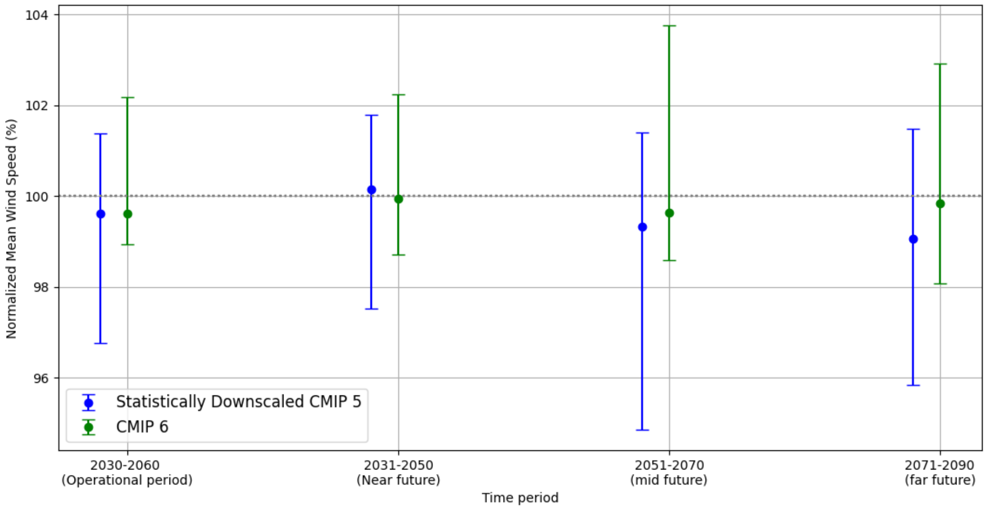

Figure 4.23: Normalised wind speed projections for different future time periods under RCP 4.5/SSP2-4.5 at site: NA1. Confidence intervals show the 83% and 17% quantiles, point in between shows the median of the models

Figure 4.24 below presents the comparison between RCP 4.5 and RCP 8.5 scenarios for the statistically downscaled CMIP5 projections. Again, under both the climate change scenarios, the 83% quantile is above the historic wind speed projection in all the future scenarios therefore, no risk can be predicted from these datasets.

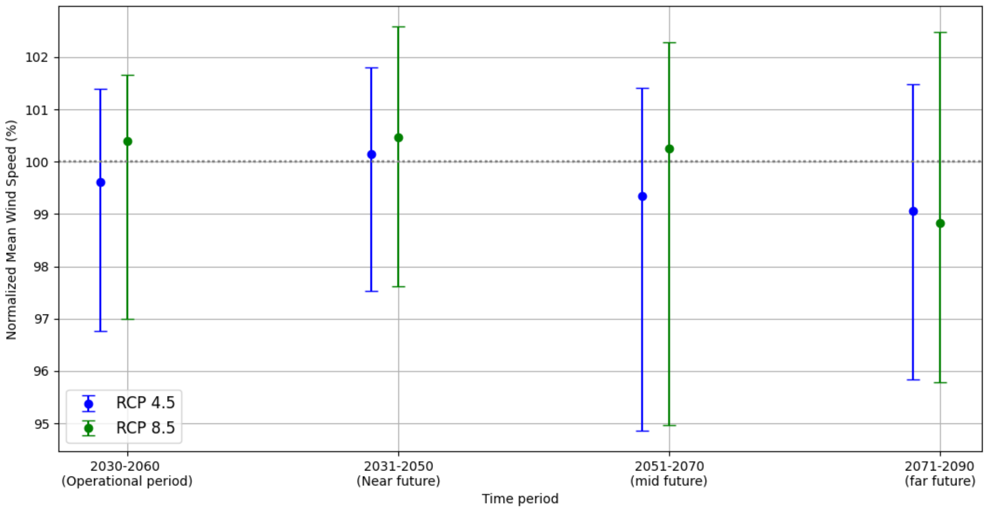

Figure 4.24: Comparison between normalised wind speed projections under climate change scenarios RCP 4.5 and RCP 8.5 for different future time periods at site: NA1. Confidence intervals show the 83% and 17% quantiles, point in between shows the median of the models

4.1.9. NA2

Figure 4.25 displays the normalized mean wind speed from the historical period through the operational period for the three datasets at site NA2. Under climate change scenario RCP 4.5, for the datasets: the CMIP6 (figure 4.19a) and statistically downscaled CMIP5 projections (figure 4.19c) 83% quantile is above historic reference projections, at 100.17% and 99.92% respectively. So a decline in wind speed is reported from the statistically downscaled CMIP5 GCMs.

For CMIP6 projections, the 10-year rolling mean declines around year 2025 till 2033 after which it stabilizes to stay below the historic projections. The uncertainty increases significantly after 2045, suggesting greater variability and less confidence in the projections over the long term. The Statistically downscaled CMIP5 projections also show a decline from year 2020 and it goes on until the end of the operational period. The uncertainty, in this case, is moderate, reflecting consistent projections with some variability, suggesting a stable outlook for wind speeds under this scenario with a moderate level of confidence. It's worth commenting that the statistically downscaled data shows a risk with 83% quantile just below 100 while the CMIP6 do not report a risk with 83% quantile just above 100%. Therefore, it could be stated that this site "is on the edge" and more accurate investigations should be conducted to evaluate whether there is a risk of decline in the wind resource or not.

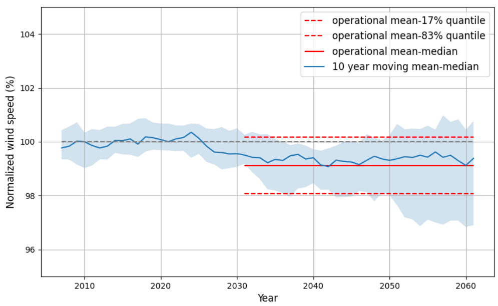

(a) Wind speed projections by 20 CMIP6 GCMs under SSP2-4.5

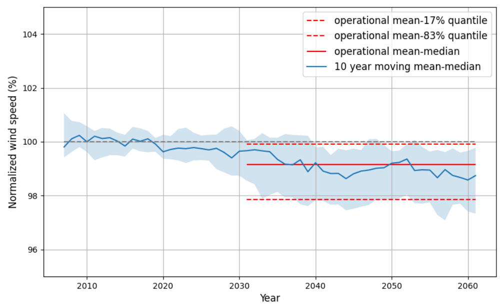

(b) Statistically downscaled wind speed projections by 19 CMIP5 GCMs under RCP 4.5

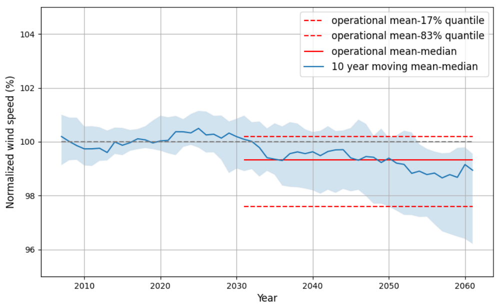

(c) Statistically downscaled wind speed projections by 21 CMIP5 GCMs under RCP 8.5

Figure 4.25: Normalised mean wind speed from the year 2006 to 2060 at Site: NA2

Under RCP 8.5, from the downscaled CMIP5 projections no risk can be reported as the 83% quantile is above the historical projections (100.19%, figure 4.25c). Wind speeds show more fluctuation compared to other projections but remain around the 100% mark overall until 2030, after which a decline becomes visible. The uncertainty in the dataset is wider than in the corresponding RCP 4.5 cases, especially towards the end of the period, indicating higher variability and less confidence in these projections. This suggests that while wind speeds are generally stable, there is more uncertainty compared to the RCP 4.5 scenario.

Figure 4.26 shows the normalized wind speed projections for different future time periods under RCP 4.5. Both datasets indicate a risk in the near and far future, as wind speed projections are lower than historical levels. However, in the mid-future, the statistically downscaled CMIP5 projections again suggest a risk. In contrast, the CMIP6 projections for the mid-future exhibit a wider spread among the models, making it a case where "no risk can be predicted" due to the increased variability and uncertainty in the projections. Again, these results from the future scenarios analysis show that this site is "on the edge"

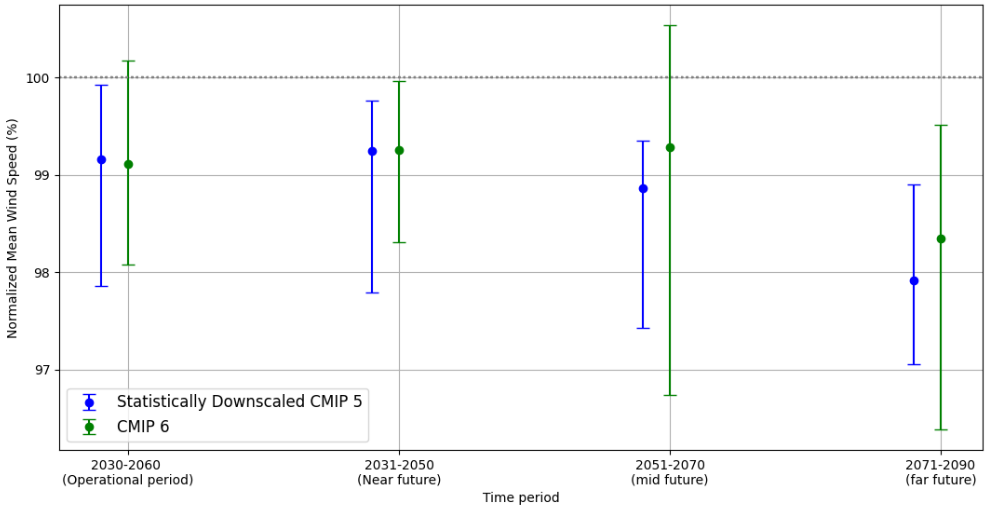

Figure 4.26: Normalised wind speed projections for different future time periods under RCP 4.5/SSP2-4.5 at site: NA2. Confidence intervals show the 83% and 17% quantiles, point in between shows the median of the models

Figure 4.27 below illustrates the differences between RCP 4.5 and RCP 8.5 scenarios for the statistically downscaled CMIP5 projections. In the near future, under RCP 4.5, 83% of the models indicate a decline in wind speed. Additionally, under both climate change scenarios (RCP 4.5 and RCP 8.5) for the mid and far future, the 83rd percentile of projections falls below historical wind speed levels. This consistent trend suggests a significant risk of reduced wind speeds over time.

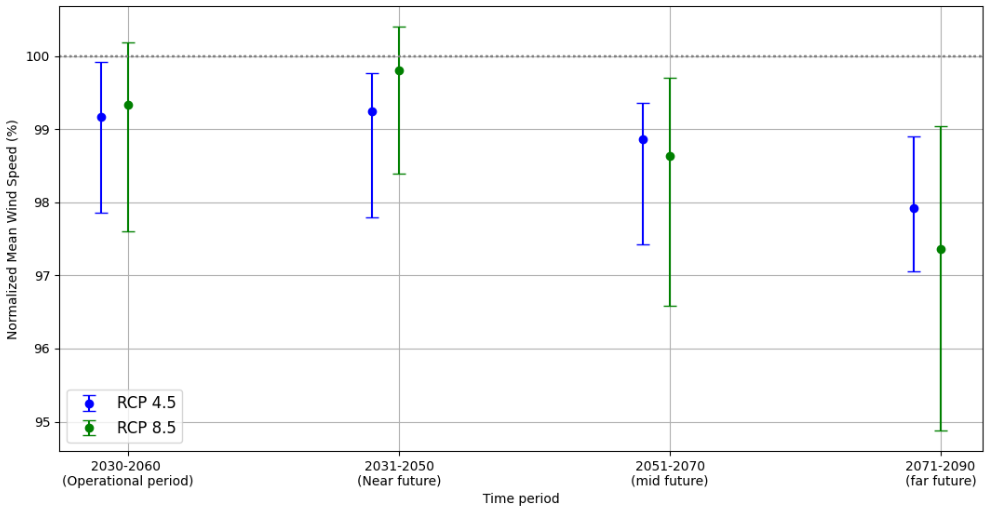

Figure 4.27: Comparison between normalised wind speed projections under climate change scenarios RCP 4.5 and RCP 8.5 for different future time periods at site: NA2. Confidence intervals show the 83% and 17% quantiles, point in between shows the median of the models

4.1.10. Results Summary

Table 4.1 presents the overview of risk assessment of sites using different datasets during operational period (2030-2060) under RCP4.5/SSP2-4.5

Table 4.1: Risk assessment based on 83% quantile for different sites under various climate models

CMIP5 CMIP6	83% Quantile		
site	**CMIP6 (SSP2-4.5)**	**CMIP downscaled (RCP4.5/SSP2-4.5)**	**CORDEX (RCP4.5)**
NS1	No risk	No risk	99.825
NS2	No risk	No risk	99.944
FR	No risk	No risk	99.702
IT	98.723	98.405	99.456
UK1	No risk	No risk	No risk
UK2	No risk	No risk	No risk
UK3	99.943	99.940	No risk
NA1	No risk	No risk	n/a
NA2	No risk	99.921	n/a

Based on the table 4.1, the following conclusions can be drawn:

- The CMIP6 and statistically downscaled CMIP GCMs show an agreement in the results with each other for 88.89% of the sites, i.e., 8 out of 9 sites. Both datasets report a risk in IT and UK3. Whereas, there is no agreement for the site NA2 as the downscaled CMIP GCMs report a risk of wind speed decline as opposed to CMIP6 GCMs,for no risk can be predicted due to the large scatter of the models.

- On the other hand, CORDEX models show an agreement with both CMIP6 and downscaled CMIP GCMs for 3 out of 7 sites (42.86%). The dataset predicts a decline in wind speed for the sites NS1, NS2, FR and IT while the other two datasets report no risk for the first three sites. The three datasets agree with each other at sites UK1 and UK2 where no decline can be predicted and at site IT where all datasets report a risk of wind speed decline.

Table 4.2 presents a comparison made between the climate change scenarios RCP4.5/SSP2-4.5 and RCP8.5/SSP5-8.5 for the risk assessment of sites using statistically downscaled CMIP GCMs during operational period (2030-2060).
It is observed that under RCP4.5/SSP2-4.5, the statistically downscaled CMIP GCMs predict a risk at 3 out of 9 sites (IT,UK3 and NA2) and under RCP8.5/SSP5-8.5, only at site IT there is a wind speed decline reported.

Table 4.2: Comparison between climate change scenarios RCP4.5/SSP2-4.5 and RCP8.5/SSP5-8.5 for the risk assessment using statistically downscaled CMIP GCMs during operational period (2030-2060). A risk is reported when 83% of the GCMs show a decline in the long term wind speed variation with respect to the historic projections.

CMIP5 **CMIP6**	**83% Quantile**	
site	**CMIP downscaled RCP4.5/SSP2-4.5**	**CMIP downscaled RCP8.5/SSP5-8.5**
NS1	no risk	no risk
NS2	no risk	no risk
FR	no risk	no risk
IT	98.405	98.628
UK1	no risk	no risk
UK2	no risk	no risk
UK3	99.940	no risk
NA1	no risk	no risk
NA2	99.921	no risk

The future years have been divided into near future from year 2031-2050, mid future from 2051 to 2070 and far future from 2071-2090 as mentioned in chapter 3. Figure 4.3 presents the overview of risk assessment of sites using different datasets during these periods under RCP4.5/SSP2-4.5. The mark 'x' represents a reported risk and d1, d2, d3 represent the datasets: CMIP6 ensemble, Statistically downscaled CMIP emsemble and CORDEX model ensemble respectively.

Table 4.3: Risk assessment for different future periods and datasets

Future-Period	near future (2031-2050)			mid-future (2051-2070)			far-future (2071-2090)		
site | dataset	d1	d2	d3	d1	d2	d3	d1	d2	d3
			x						x
NS2						x			x
FR			x			x			
IT	x	x	x	x	x	x	x	x	
UK1				x	x		x	x	x
UK2				x	x		x		x
UK3					x		x	x	x
NA1									
NA2	x	x			x		x	x	

Under the climate change scenario RCP4.5/SSP2-4.5, the following conclusions can be drawn:

- In the near future (2031-2050), which is part of the operational period, the CMIP6 GCMs and statistically downscaled CMIP GCMs are in complete agreement, predicting a decline in wind speeds for IT and NA2, with no risk for the other sites. CORDEX models concur with these datasets for 71.14% of the sites (5 out of 7), indicating a decline in wind speed at NS1, FR, and IT.

- In the mid-future (2051-2070), CMIP6 and statistically downscaled CMIP GCMs agree on 7 out of 9 sites (77.78%), predicting a decline in wind speed at IT, UK1, and UK2. Additionally, the downscaled GCMs also show a risk at UK3 and NA2. CORDEX models align with CMIP6 and statistically downscaled CMIP GCMs at 42.86% and 28.57% of the sites, respectively, predicting wind speed declines at NS2, FR, and IT.
- For the years 2071-2090 (far future), there is strong agreement between CMIP6 and statistically downscaled CMIP GCMs at 8 out of 9 sites. Both models indicate a risk of declining wind speeds at IT, UK1, UK3, and NA2, with CMIP6 also predicting risk at UK2. Comparing CMIP6 with CORDEX, 4 out of 7 sites show similar results, with CORDEX models reporting risk at NS1, NS2, UK1, UK2, and UK3. However, when comparing CORDEX with statistically downscaled CMIP GCMs, there is agreement at only 2 out of 7 sites.

At the sites that present risks only for mid or far future, the climate change is going to affect the wind resource only the very long term and that is not therefore relevant for wind projects currently under development. Additionally, having risk only in the short and mid future, but not in the long, could be due to an increase of the uncertainty in the distant future.

Figure 4.4 presents a comparison made between the climate change scenarios RCP4.5/SSP2-4.5 and RCP8.5/SSP5-8.5 for the risk assessment of sites using statistically downscaled CMIP GCMs in the near,mid and far future. The mark 'x' again represents a reported risk and d2a and d2b, represent the climate change scenarios RCP4.5/SSP2-4.5 and RCP8.5/SSP5-8.5 respectively.

Table 4.4: Comparison between climate change scenarios RCP4.5/SSP2-4.5 and RCP8.5/SSP5-8.5 for the risk assessment using statistically downscaled CMIP GCMs in near, mid and far future. The mark 'x' represents a reported risk, d2a: RCP4.5/SSP2-4.5 and d2b: RCP8.5/SSP5-8.5.

Future-Period	Near future			Mid-future			Far-future		
	(2031-2050)			(2051-2070)			(2071-2090)		
site | dataset	d1	d2	d3	d1	d2	d3	d1	d2	d3
			x						x
NS2						x			x
FR			x			x			
IT	x	x	x	x	x	x	x	x	
UK1				x	x		x	x	x
UK2				x	x		x		x
UK3					x		x	x	x
NA1			n/a			n/a			n/a
NA2	x	x	n/a		x	n/a	x	x	n/a

From table 4.4, the following information has been derived:

- In the near future, under both the scenarios, risk of wind speed decline is predicted at site IT. Additionally, under RCP4.5, there is risk prediction at NA2.
- In the mid-future, under both scenarios, sites IT,UK1, UK3 and NA2 are under risk of wind speed decline. Moreover, under RCP4.5, UK2 is also subjected to risk and under RCP8.5/SSP5-8.5, risk is predicted for NS2 and NA2 as well.
- In the far future, sites IT, UK1, UK3 and NA2 are predicted to be under risk of wind speed decline under both the scenarios. Furthermore, under SSP5-8.5 NS2 is also subjected to the risk.

From the wind speed analysis results discussed above, it was observed that CORDEX models tend to disagree in many cases with the CMIP6 and statistically downscaled CMIP GCMs. For example, during the operational period, an agreement is noted only for 3 out of the 7 sites, i.e., 42.86% of the sites. Therefore, the wind speed projections from CORDEX models were further analysed.

4.1.11. CORDEX models analysis

The long term mean wind speeds for the operational period obtained from all the CORDEX models were plotted individually against the time. Figure 4.28 presents these wind speeds for plotted for the seven sites. Individual plots for these can be found in appendix B.

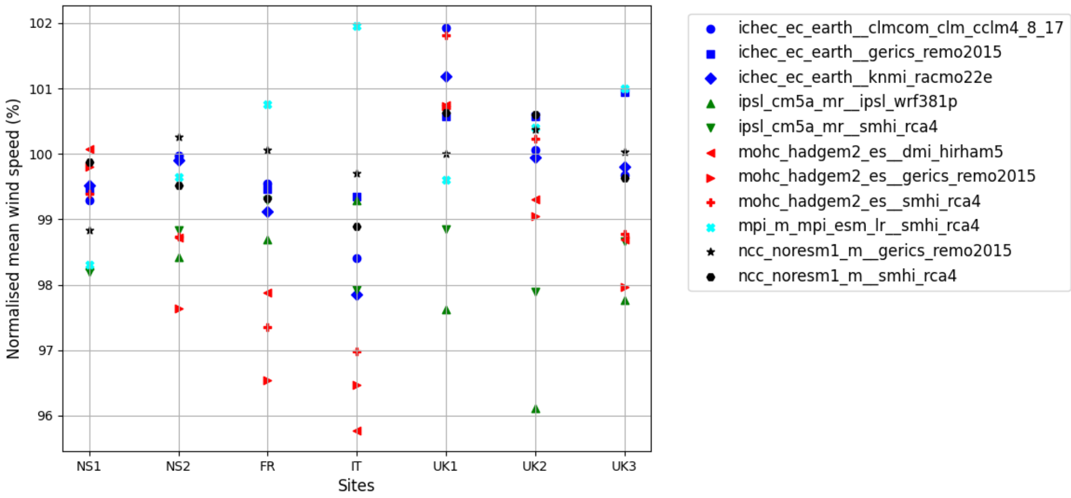

Figure 4.28: Long term mean wind speed during operational years by 11 CORDEX models under RCP4.5. Wind speeds with same colour represent same GCM used by different RCMs

In figure 4.28, the wind speeds plotted with same colours represent the common GCM that has been used as the boundary condition for the RCM plotted by different shapes. This color coding allows for easy identification of trends in the models. Grouping between the GCM-RCM coupled-models having common GCMs is visible. For example, the ichec-ec-earth CMIP5 model by Earth Consortium is has been paired with 3 different RCMs: CCLM-8-17, REMO2015 and RACMO22e. Despite of having different RCMs, mean wind speed projections by the coupled-models is visible to be heavily influenced by the common GCM having values 99.97%, 99.93% and 99.90% respectively at site NS2. This influence can be seen in all the sites present in figure 4.28 as well as the other models that use the same GCMs. In this research, a total of eleven CORDEX models have been used in which one there are only five GCMs being paired with different RCMs. Therefore, in order to have confidence in the wind speed projections by CORDEX models, the author recommends to have as many GCMs as possible, since different RCMs coupled with the same GCMs give similar results.

This sections ends here. The next section moves to the results obtained for the annual energy yield and capacity factor in the operational period for the four sites: NS1, NS2, FR, IT in Europe. It also discusses the sensitivity factors and factors influencing them.

4.2. Annual Energy yield and Capacity factor

According to the methodology described in the section 3.5.2 of chapter 2, the Annual energy yield by a 5MW NREL reference wind turbine at two offshore sites: NS1 and NS2 and two onshore sites: IT and FR has been calculated for the operational period based on different percentages of wind speed decline (-1%, -3%, -5%, -10%) and the absolute values are presented in table 4.5.

Table 4.5: AEP based on variation in wind speed (GWh)

Site | Percent change	Historic	-1%	-3%	-5%	-10%
NS1	25.58	25.29	24.69	24.07	22.40
NS2	23.64	23.36	22.76	22.14	20.51
FR	13.89	13.60	12.99	12.38	10.87
IT	6.40	6.24	5.91	5.59	4.82

Using the historic AEP and the new predicted AEP from table 4.5, the relative percent change in AEP is calculated and is tabulated in 4.6.

Table 4.6: Relative change in AEP based on variation in wind speed

Site | Percent change	-1%	-3%	-5%	-10%
NS1	-1.14	-3.48	-5.92	-12.45
NS2	-1.23	-3.75	-6.36	-13.27
FR	-2.18	-6.56	-10.93	-21.79
IT	-2.58	-7.66	-12.66	-24.70

The table 4.6 indicates that as wind speed decreases, there is a corresponding negative impact on AEP at all sites. The impact is more pronounced with greater declines in wind speed. For instance, a 10% decrease in wind speed results in the most significant AEP reduction, with IT experiencing the highest relative decline, followed by FR, NS2, and NS1. This highlights the sensitivity of wind energy production to changes in wind speed and therefore, the sensitivity factor under these wind conditions is calculated using the formula 2.6.

Table 4.7: Sensitivity Factor based on decrease in wind speed variation

Site | Percent change	-1%	-3%	-5%	-10%
NS1	1.14	1.16	1.18	1.25
NS2	1.23	1.25	1.27	1.33
FR	2.18	2.19	2.19	2.18
IT	2.58	2.55	2.53	2.47

Table 4.9 shows that sensitivity factors are consistent across different levels of wind speed decline for each site. Sites like FR and IT have higher sensitivity factors, indicating that their AEP is more significantly affected by wind speed reductions compared to NS1 and NS2. This can be attributed to NS1 and NS2 being offshore sites as the wind speed distribution for these sites has a higher probability of high wind speeds. Whereas, for onshore sites like IT and FR, the occurrence of lower wind speeds is more. This can be seen in figure 4.29 which shows the probability distribution function for sites NS1 and IT for historical and operational periods (refer to appendix B.2 for PDFs of NS2 and FR). Assuming a constant shape factor, for a decrease of 10% in the wind speed in operational period, the scale factor also decreases by 10% in this case for both the sites. This implies that the probability of high wind speed increases at offshore site NS1 and at onshore site IT, the probability of low wind speeds

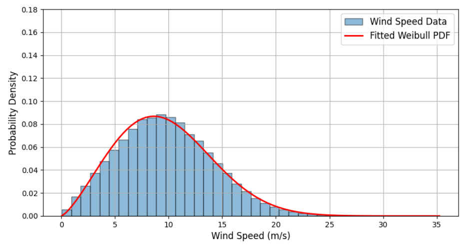

(a) PDF for wind speeds at site NS1

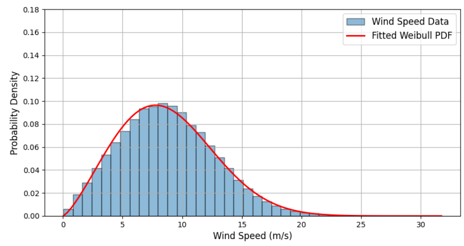

(b) PDF for 10% lower wind speeds at site NS1

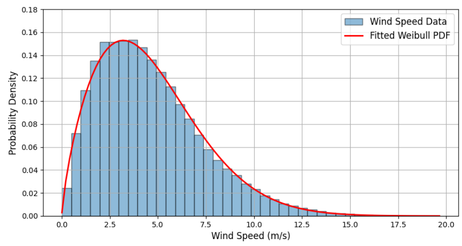

(c) PDF for wind speeds at site IT

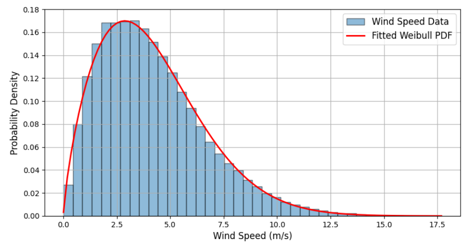

(d) PDF for 10% wind speeds at site IT

Figure 4.29: PDF for wind speeds at site NS1 and IT before and after 10% decline

increases resulting in a higher higher sensitivity factor at onshore site. The above done analysis can be done for to the actual wind speed projections given by the GCMs. From the summary tables 4.1 and 4.2, it is seen that at site IT, each dataset has predicted a risk in wind speed decline. Therefore, for the Italian site the AEP and sesnitivity factor are calculated based on wind speed projections by different datasets in table 4.8:

Table 4.8: Summary of relative changes in wind speed variation, AEP, and sensitivity factor by different datasets under different scenarios for site in Italy

Parameter	Statistically down-scaled CMIP6 (SSP2-4.5)	CMIP6 (SSP2-4.5)	CORDEX CMIP5 (RCP4.5)	Statistically down-scaled CMIP6 (SSP5-8.5)
Relative change in wind speed (%)	-1.59	-1.28	-0.54	-1.37
AEP (GWh/year)	6.14	6.19	6.31	6.18
Relative change in AEP (%)	-4.10	-3.29	-1.40	-3.53
Sensitivity factor	2.57	2.57	2.58	2.57

The relative change in AEP shows a significant decline in the statistically downscaled CMIP6 (SSP2-4.5) scenario at -4.10%, followed by the CMIP6 (SSP2-4.5) at -3.29%, the statistically downscaled CMIP6 (SSP5-8.5) at -3.53%, and the CORDEX CMIP5 (RCP4.5) at -1.40%. The sensitivity factors are quite similar across all scenarios, ranging from 2.57 to 2.58, indicating a consistent sensitivity of AEP to changes in wind speed.
The last topic of this section is the capacity factor. Using the equation 2.5, the capacity factor for 5MW NREL reference wind turbine is calculated for different percentages of wind speed decline and is given in the table below:

Table 4.9: Capacity Factor based on decrease in wind speed variation

Site | Percent change in wind speed	Historic	-1%	-3%	-5%	-10%
NS1	0.58	0.58	0.56	0.55	0.51
NS2	0.54	0.53	0.52	0.51	0.47
FR	0.32	0.31	0.30	0.28	0.25
IT	0.15	0.14	0.13	0.13	0.11

For NS1, the capacity factor remains stable at 0.58 for a 1% decline but drops to 0.51 with a 10% decline. NS2 follows a similar trend, decreasing from 0.54 under historic conditions to 0.47 with a 10% decline. FR's capacity factor reduces from 0.32 to 0.25, and IT from 0.15 to 0.11 as wind speeds decline by 10%.
Since capacity factor is a function of AEP, the relative percentage change in capacity factor is same as the relative percentage change in AEP, as mentioned in table 4.10 below:

Table 4.10: Relative change in Capacity factor based on variation in wind speed

Site | Percent change	-1%	-3%	-5%	-10%
NS1	-1.14	-3.48	-5.92	-12.45
NS2	-1.23	-3.75	-6.36	-13.27
FR	-2.18	-6.56	-10.93	-21.79
IT	-2.58	-7.66	-12.66	-24.70

Onshore sites FR and IT have larger decrease in capacity factors as compared to the offshore sites NS1 and NS2. These results highlight the significant impact of even modest reductions in wind speed on the capacity factor, which directly affects the efficiency and output of wind energy production. The substantial declines in capacity factor across all sites underscore the vulnerability of wind energy resources to variations in wind speed. Accurate projections and mitigation strategies are crucial to maintain energy production levels in the face of potential climate-induced changes in wind patterns. This analysis emphasizes the need for robust modeling and comprehensive planning to ensure the resilience of wind energy infrastructure.
The capacity factor for site IT has been computed using on AEP based on wind speed decline predicted by different datasets and is presented below:

Table 4.11: Summary of relative changes in wind speed variation, AEP, and capacity factor under different scenarios for site in Italy

Parameter	Statistically downscaled CMIP6 (SSP2-4.5)	CMIP6 (SSP2-4.5)	CORDEX CMIP5 (RCP4.5)	Statistically downscaled CMIP6 (SSP5-8.5)
Relative change in wind speed(%)	-1.59	-1.28	-0.54	-1.37
AEP (GWh/year)	6.14	6.19	6.31	6.18
Capacity factor (%)	0.140	0.141	0.144	0.141

Based on the changes in wind speed predicted by different datasets at site Italy, the capacity factor seems to be consistent for all the datasets under both the climate change scenarios. The table highlights that while there are variations in wind speed projections, the impact on capacity factor remains

relatively minimal.
The next section now evaluates the revenue that would be obtained as per the wind speed decline in the operational period.

4.3. Revenue

In order to evaluate the revenue, a 50MW wind farm with 10 5MW NREL reference wind turbine is assumed to be built at the locations. A 10 year mean of wholesale electricity price for each country is obtained [33] and using the predicted AEP (table 4.5) and this price, the revenue is estimated and is presented in table 4.12.

Table 4.12: Revenue (million Eur/year) based on decline in wind speed

Site	mean electricity price (Eur/MWh)	decline in wind speed (%)			
		1	3	5	10
		Revenue (million Eur/year)			
NS1	64.44	16.30	15.91	15.51	14.43
NS2	75.11	17.54	17.09	16.63	15.40
FR	79.89	10.86	10.38	9.89	8.68
IT	95.13	5.93	5.62	5.32	4.59

NS2 consistently generates the highest revenue under all wind speed decline scenarios, which can be attributed to its high mean electricity price and favorable wind conditions that result in higher AEP. NS1 follows closely in revenue generation but with a slightly lower mean electricity price than NS2.
FR and IT show lower revenues compared to NS1 and NS2. This is particularly evident in IT, which despite having the highest mean electricity price, generates the lowest revenue due to lower AEP as a consequence of lower wind speeds.
Based on wind speed decline and AEP reported by all the datasets in table 4.8, the revenue generated has been also estimated in the following table:

Table 4.13: Revenue (million Eur/year) generated at site IT based on decline in wind speed predicted by different datasets

Parameter	Statistically downscaled CMIP6 (SSP2-4.5)	CMIP6 (SSP2-4.5)	CORDEX CMIP5 (RCP4.5)	Statistically downscaled CMIP6 (SSP5-8.5)
Relative change in wind speed(%)	-1.59	-1.28	-0.54	-1.37
$AEP_{windfarm}$ (GWh/year)	61.4	61.9	63.1	61.8
Revenue (Million Eur/year)	5.84	5.89	6.01	5.88

The revenue generated at site IT, as shown in Table 4.13, is ranging from 5.84 million Eur/year to 6.01 million Eur/year. There can be significant impact on the revenue based on the dataset that is used. Therefore, it is necessary to have reliable GCMs when assessing the wind resource.

The next section moves to the comparison of historical data from ERA5 reanalysis data with the datasets used in this research.

4.4. Climate Models comparison with ERA5

This section presents the comparison of historical wind speed projections at 10m between a. the ERA5 and CMIP 6 GCMs (1994-2014), b. ERA5 and statistically downscaled CMIP GCMs (2006-2020) under SSP2-4.5/RCP4.5 using the methodology mentioned in section 3.5.5 of chapter 3. It should be noted that this analysis is not a check for accuracy of the GCMs and just the comparison between the datasets. As mentioned in the chapter 2, the climate models are not synchronized with the real climate and climate simulations are carried out by a statistical study spanning a wide period to study the relative change predicted compared to the historical predictions. Therefore, comparison of absolute values from GCMs with the reanalysis data to perform accuracy or reliability check is not recommended.

4.4.1. ERA5 and CMIP6 GCMs

Percent Bias and mean absolute percentage error are calculated with ERA5 as observed and CMIP 6 projections as predicted data. The figure 4.30 highlights significant variability in wind speed projections from different CMIP6 models across various sites in comparison to ERA5. Percent bias and MAPE metrics indicate that some models consistently underestimate or overestimate wind speeds, with IT showing the highest errors.

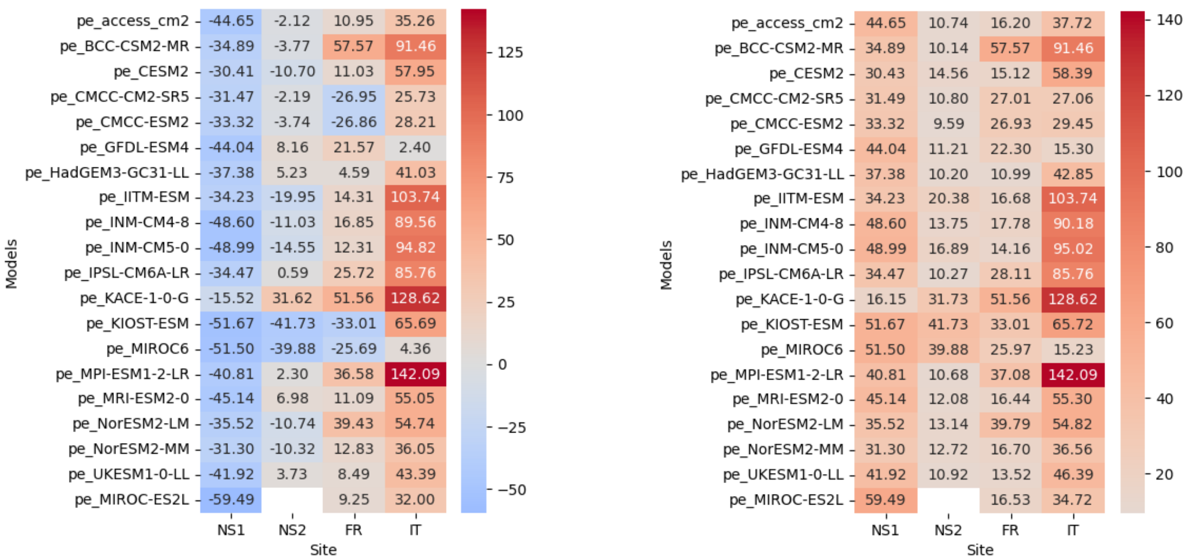

(a) Percent Bias (%) **(b)** Mean absolute percent error(%)

Figure 4.30: Error metrics calculated between historical ERA5 reanalysis data and historical wind speed projections from CMIP6 GGCMs for NS1, NS2, FR and IT

From figure 4.30a showing percet bias, the following is observed:

- NS1: The models show a negative bias, indicating an underestimation of wind speeds in comparison to ERA5. The bias ranges significantly, with pe-MIROC-ES2L having the highest negative bias (-59.49%) and pe-KACE-1-0-G showing the least (-15.52%).
- NS2: Bias is less extreme than NS1 but still predominantly negative, indicating underestimation. 36.8% of the models however, show a positive bias showing overestimation as well.
- FR: The GCMs show varied bias with 16 out of 20 models showing an overestimation and 4 showing large underestimation in comparison to ERA5.
- IT: Models display a significant overestimation as high as 142.09% and as low as 2.40%.

For further clarity, MAPE is plotted in figure 4.30b and the following key points for each site are observed:

- NS1: Most models exhibit moderate to high error rates, with MAPE values ranging from approximately 10% to nearly 60%. Notable high error rates are observed in models such as pe-MIROC-ES2L (59.49%) and pe-KIOST-ESM (51.67%).
- NS2: The error rates for this site are generally lower, with most models showing MAPE values between 10% and 20%. Models like pe-MIROC6 (39.88%) and pe-KIOST-ESM (41.73%) stand out with higher errors.
- FR: Similar to NS2, the error rates are moderate, with pe-CESM2 (15.12%) and pe-HadGEM3-GC31-LL (10.99%) showing relatively low MAPE values. However, pe-IPSL-CM6A-LR (28.11%) and pe-KACE-1-0-G (51.56%) exhibit higher errors.
- IT: This site has the highest error rates, with several models exceeding 100% MAPE, indicating poor accuracy in projections. Models such as pe-MPI-ESM1-2-LR (142.09%) and pe-KACE-1-0-G (128.62%) show the highest errors, indicating substantial overestimation.

Before analysing the possible causes for large bias and mape, Pearson's correlation coefficient and coefficient of correlation are also plotted and presented below:

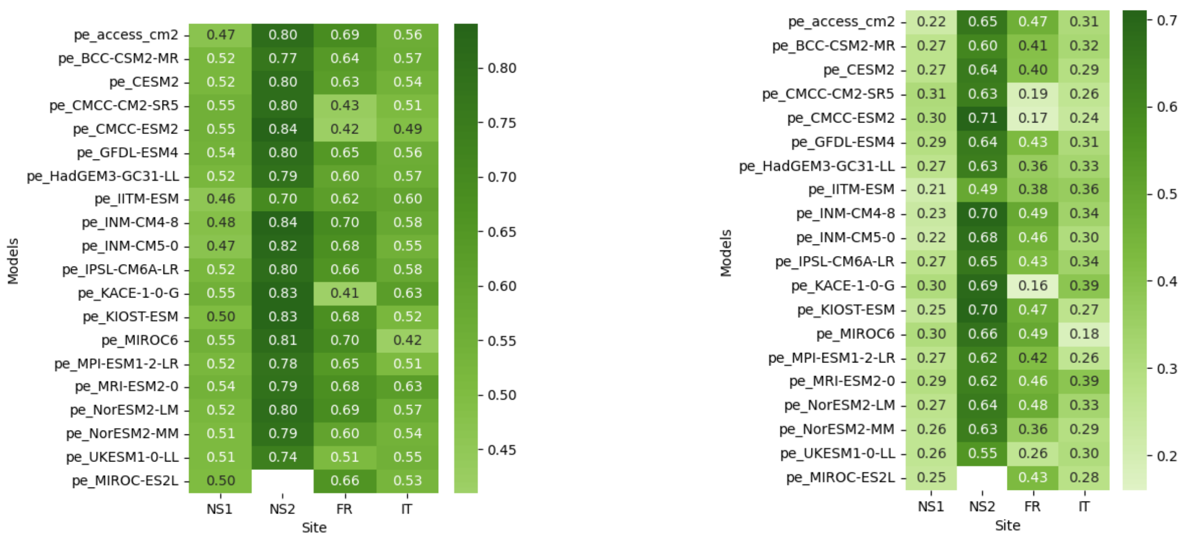

(a) Pearson's correlation coefficient, r

(b) Coefficient of determination, r^2

Figure 4.31: Correlation metrics calculated between historical ERA5 reanalysis data and historical wind speed projections from CMIP6 GGCMs for NS1, NS2, FR and IT

Figures 4.31a and 4.31b present correlation metrics calculated between historical ERA5 reanalysis data and historical wind speed projections from CMIP6 GCMs for four sites: NS1, NS2, FR, and IT. Pearson's correlation coefficient (r) measures the linear relationship between the projected and actual wind speeds. Values close to 1 or -1 indicate a strong linear relationship, while values close to 0 indicate a weak linear relationship. From the plots of Pearson's correlation coefficient, r, the following key points are observed for each site:

- NS1: Most models show moderate positive correlations, with values ranging from 0.47 to 0.55.
- NS2: High positive correlations are observed, with values between 0.69 and 0.85, indicating strong linear relationships.
- FR: Moderate to high positive correlations are seen, with values between 0.50 and 0.74.
- IT: Correlation values are lower, ranging from 0.28 to 0.53, suggesting weaker linear relationships.

The coefficient of determination (r^2) measures how well the regression predictions approximate the real data points. Higher values indicate better model performance. From the figure 4.31b, the following key points are observed for each site:

- NS1: r^2 values range from 0.22 to 0.30, indicating low to moderate explanatory power of the models.
- NS2: Higher r^2 values are observed, ranging from 0.47 to 0.72, suggesting better model performance.
- FR: r^2 values range from 0.25 to 0.55, indicating moderate explanatory power.
- IT: Lower r^2 values are seen, ranging from 0.28 to 0.43, indicating weaker model performance.

The comparison of CMIP6 GCM models against ERA5 in projecting historical wind speeds varies significantly across different sites. The models, at site NS2, show strong linear relationships and high explanatory power. However, these metrics are moderate at sites NS1 and FR, and relatively poor at site IT.
To investigate the possible causes for these results, the distance between the grid points of the GCMs models and ERA5 is calculated and plotted against the MAPE and fitted using a linear fit in the figure 4.32. The data points for the plot are present in appendix B.3.

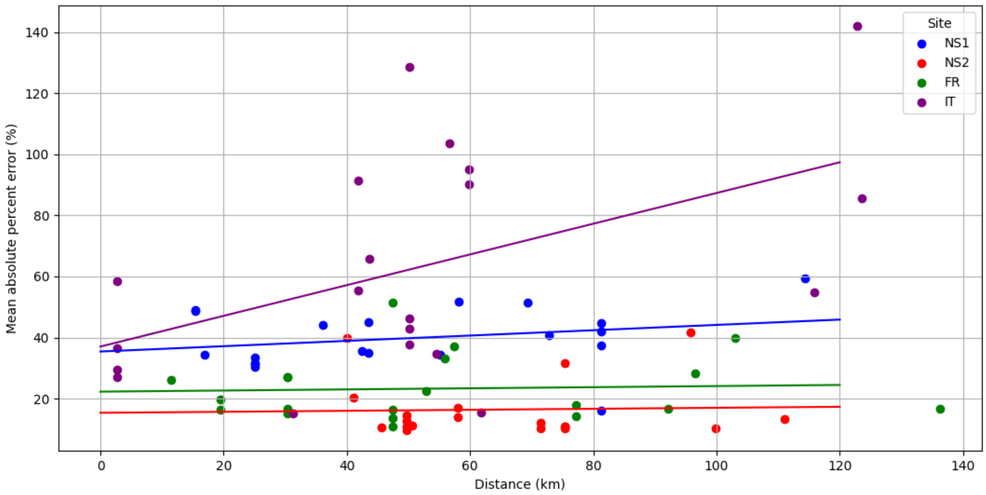

Figure 4.32: Scatter plot of distance vs MAPE calculated for CMIP6 wind speed projections at sites FR, NS1, NS2 and IT.

Even though the linear fit suggests a potential relationship between the distance and MAPE, the scatter of MAPE values is too high to confirm this relationship reliably. The calculated r^2 values of the correlation between the MAPE and the distance shown by the regression lines of figure each site are as follows: NS1: 0.06, NS2: 0.001, FR: 0.001, IT: 0.25. These values indicate a very poor correlation between distance and MAPE, with r^2 values close to zero for most sites. Specifically:
NS1 (0.06): Indicates a very weak correlation, suggesting that distance explains only 6% of the variance in MAPE.
NS2 (0.00): Shows no correlation, indicating that distance has no explanatory power for MAPE variance.
FR (0.00): Similar to NS2, there is no correlation between distance and MAPE.
IT (0.25): While slightly higher, it still indicates a poor correlation, with distance explaining only 25% of the variance in MAPE.
These results suggest that there is no meaningful relationship between distance and MAPE across the sites. The high scatter in MAPE values further reinforces the conclusion that distance is not a reliable predictor of MAPE. Therefore, despite the linear fit, the data does not support establishing a relationship between distance and MAPE and distance cannot be reliably used to predict the reason for large MAPE and extreme bias for the given sites.

Given the high MAPE and poor correlation observed in the previous analysis, the next logical step is to investigate the terrain characteristics of the sites. Due to confidentiality reasons, the terrain images for the sites cannot be shared. However, upon examination, several important observations were made.

The site with the highest MAPE, IT, is characterized by a very complex terrain. This complexity poses a significant challenge for GCMs, which are unable to capture the small-scale details, resulting in poor correlation and overestimated bias. Similarly, site FR has a complex terrain, although it is not as complex as IT. This also contributes to significant bias and correlation issues, albeit to a lesser extent.

In contrast, NS1 and NS2 are offshore sites where one would expect less extreme bias. However, the investigation revealed that many GCMs have their grid points located inland. This inland positioning influences the wind speed projections, as the GCMs' wind data are affected by land characteristics rather than offshore conditions. This inland bias leads to discrepancies in the data for these sites.

Additionally, it is crucial to consider the difference in resolution between the datasets. The ERA5 reanalysis data has a resolution of 25 km, whereas the GCMs used in this analysis have resolutions as low as 100-200 km. The disparity in resolution means that GCMs may not capture small-scale climatic features and local weather patterns as well as the topographic details. In the following subsection now the ERA5 has been compared with the downscaled CMIP GCMs that have a higher resolution than ERA5.

4.4.2. ERA5 and Statistically downscaled CMIP GCMs

This section compares the historical wind speed data from year 2006-2020 obtained from ERA5 reanaylsis and Statistically downscaled GCMs. 4.33 shows the error metrics Percent Bias and MAPE for sites NS1, NS2, FR and IT. For the latter three sites CMIP6 is used and for NS1 CMIP5 and therefore the GCMs used are different. Even though the heatmap colour is same for all the sites, the intensity is different so attention should be paid to the scale.

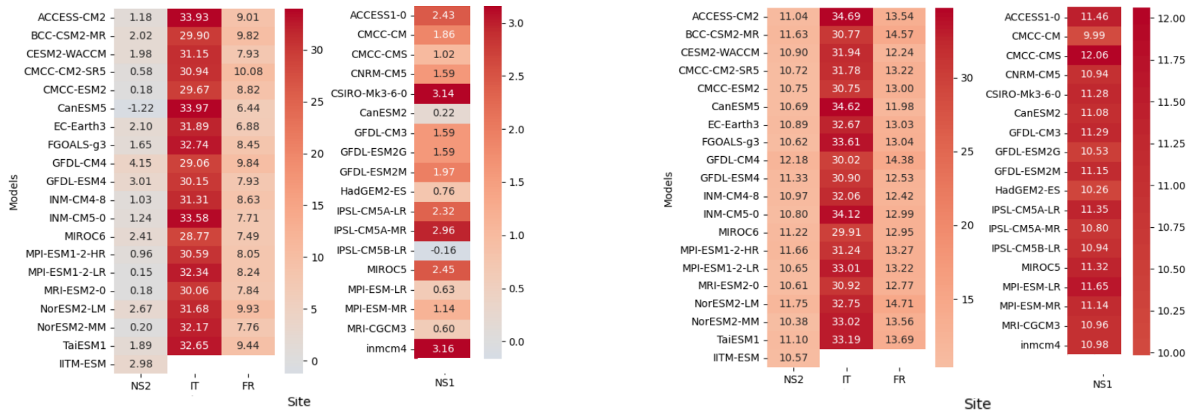

(a) PBias (%) **(b)** MAPE (%)

Figure 4.33: Error metrics calculated between historical ERA5 reanalysis data and historical wind speed projections from statistically downscaled CMIP GGCMs for NS1, NS2, FR and IT

From figure 4.33a the following key-points can be noted:

- NS2: Models exhibit a range of biases, from negative biases (e.g., CanESM5 with -1.22) to positive biases (e.g., IITM-ESM with 2.98). The majority of models show positive biases, indicating an overestimation of wind speeds.
- IT: Higher biases are observed, with values ranging from -0.18 to 30.06. The highest biases are seen in MRI-ESM2-0 (30.06), BCC-CSM2-MR (29.90), and CMCC-CM2-SR5 (30.94), indicating significant overestimations.
- FR: Biases range from 6.44 to 10.08. Most models show moderate positive biases, suggesting

overestimation but to a lesser extent than IT.

- NS1: The biases range from -0.16 to 2.43. Models show a mix of positive and negative biases, indicating both overestimation and underestimation of wind speeds.

Figure 4.33b highlights the following points:

- NS2: MAPE values range from 10.38% to 11.97%, indicating relatively low error rates. Most models show MAPE values around 11%.
- IT: IT exhibits the highest MAPE values among all sites, with values ranging from 29.67% to 34.69%. This indicates significant errors in wind speed projections for this site, likely due to its complex mountainous terrain.
- FR: MAPE values for FR are moderate, ranging from 12.33% to 14.57%. The errors are higher than NS2 but much lower compared to IT.
- NS1: MAPE values are relatively uniform and low, ranging from 10.94% to 12.06%.

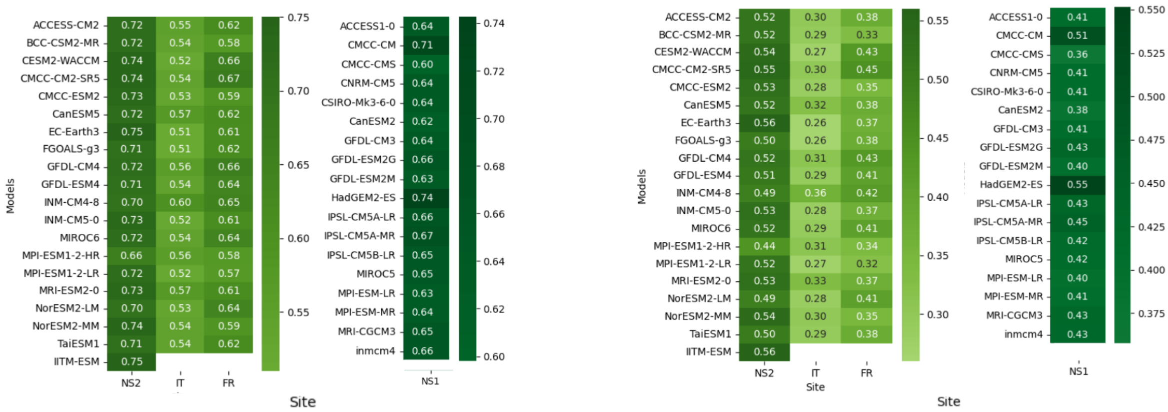

(a) Pearson's correlation coefficient, r

(b) Coefficient of determination, r^2

Figure 4.34: Correlation metrics calculated between historical ERA5 reanalysis data and historical wind speed projections from statistically downscaled CMIP GGCMs for NS1, NS2, FR and IT

Figure4.34a presents the Pearson's correlation coefficient, r across four sites. At site NS2, r values range from 0.71 to 0.75, indicating strong positive correlations between downscaled GCMs and ERA5. In contrast, site IT exhibits lower r values, ranging from 0.50 to 0.56, reflecting moderate correlations. Site FR shows moderate to strong correlations, with r values between 0.59 and 0.67 and for site NS1, r values range from 0.60 to 0.74, showing strong positive correlations.
Figure 4.34b presents the coefficient of determination, r^2. For site NS2, r^2 values range from 0.44 to 0.56. At site IT, r^2 values are even lower, ranging from 0.26 to 0.33. For site FR, r^2 values range from 0.34 to 0.45 and at site NS1, r^2 values range from 0.36 to 0.55. These values are considered very poor and signify that the regression does not explain any of the variability of the wind speed data around its mean.
As discussed in the previous subsection as well, the terrain of the sites is playing a crucial role which can be verified by the plots. IT being an onshore site with very complex terrain shows the highest MAPE followed by FR and lower errors are reported for offshore sites. This can also be attributed to the high risk of wind speed decline predicted at IT.
The GCMs have same grid point at each site and the distance between that and ERA5 grid point is given in the table below:

Table 4.14: Distances from Reference Point for Different Sites

Site	Distance from reference point (km)
NS1	8.94
NS2	12.79
FR	11.60
IT	5.00

From the table 4.14, yet again, for this datasets as well it can be seen that since distances from the point of reference are not too large, therefore distance is not playing a role in the large error metrics. Overall, the analysis reveals significant variability in models across different sites, this highlights the importance of considering site-specific factors, the inherent complexities of the terrain and resolution of models when evaluating model performance. Moreover, the data assimilation processes, and the capture of internal climate variability is different for both the datasets. GCMs are play a crucial role in understanding broad climate trends and making future projections, their direct comparison with reanalysis data for historical periods requires careful consideration.

This chapter on results and discussion ends here. The subsequent chapter will present the conclusions derived from this work, summarizing the key findings and their implications. Additionally, it will discuss the broader impact of the research and recommendations for future work.

5 Conclusion

This study aimed to assess wind speed projections at nine different locations using three climate model ensembles: non-downscaled CMIP6 GCMs, statistically downscaled CMIP5/6 GCMs, and dynamically downscaled CMIP5 GCMs. Projections for the operational period and near, mid, and far future were analyzed to evaluate the risk of wind speed decline and its impact on parameters like AEP, capacity factor, sensitivity factor, and revenue for the operational period. Additionally, historical wind speed projections from CMIP6 GCMs and statistically downscaled CMIP5/6 GCMs were compared with ERA5 reanalysis data. By identifying the limitations and strengths of various modeling approaches, the study provides valuable insights for optimizing wind resource assessments and energy planning. The findings contribute to improving the reliability and efficiency of wind energy systems. Based on the research conducted, the following conclusions and their contributions to the wind energy system have been drawn:

- The statistically downscaled CMIP5/6 GCMs and the non-downscaled CMIP6 GCMs agree with each other when predicting the risk in wind speed decline. For example, in the operational period at 8 out of 9 sites, the results for the two datasets were similar. In the one case where they do not agree, statistically downscaled GCMs had the 83% quantile value of 99.94%, which is ”on the edge” of being a risk.
  Therefore, it can be concluded that the non-downscaled CMIP6 GCMs can be used without downscaling since the same trend is observed in both datasets. This has practical implications for simplifying climate impact studies and reducing computational costs. If non-downscaled GCMs can provide sufficiently accurate projections, they can streamline the integration process by offering a quicker and more cost-effective method for assessing wind resources.
- The CORDEX models showed a different trend as compared to the CMIP6 GCMs and statistically downscaled CMIP GCMs at 4 out of 7 sites. The wind speed projections by GCM-RCM couples used in the dynamically downscaled dataset CORDEX were highly influenced by the GCMs and therefore are not reliable. There should be as many GCMs as possible to couple with the RCMs in order to obtain diverse and more reliable results. This implies that relying on a limited set of GCMs could lead to skewed projections, which might affect the planning and optimization of wind energy systems. Ensuring a broad representation of GCMs in downscaled models can enhance the reliability of wind resource assessments, leading to better-informed decisions in energy planning and infrastructure development.
- AEP of a wind farm depends significantly on the wind resource of the site. A high sensitivity factor is observed at onshore sites where the wind speed is low and the terrain is complex, and a lower sensitivity factor is obtained at offshore sites with high wind speeds and smooth terrain. This finding emphasizes the need for site-specific assessments that account for local topography. Detailed terrain analysis should be prioritized by planners and engineers to optimize wind farm placement and design, thereby maximizing AEP and ensuring more reliable energy outputs.
- GCMs, when compared to reanalysis data, are highly biased by the complexity of terrain. Onshore

sites with complex terrain yield high errors and low correlation, with higher errors at more complex terrain. Offshore sites show better correlation and lower errors.

- GCMs play a crucial role in understanding broad climate trends and making future projections. However, directly comparing GCM outputs with reanalysis data is not advisable due to differences in resolution, data assimilation techniques, and representation of local terrain and climatic phenomena. Even the statistically downscaled GCMs, which have a higher resolution, are designed to improve local-scale accuracy by leveraging historical data but may not capture large-scale atmospheric dynamics as effectively. Therefore, it is essential to understand the limitations and apply appropriate methodologies for such comparisons to avoid misleading conclusions and ensure the reliability of the analysis.

The author recommends the following topics for future research:

- For future research, the effect of variability in the resolution of input data for downscaling methods on wind speed projections can be studied. Subsequently, the influence on critical aspects of wind energy applications can be analyzed. This would involve downscaling the GCM projections and comparing the results with the already downscaled GCMs.
- The author also recommends using CORDEX datasets with a variety of GCMs, when available, to obtain a diverse range of GCM-RCM couples for research. A similar analysis as done in this work should be performed to observe the behavior of the models in projecting wind speed in comparison to other datasets like CMIP6 GCMs.
- Since the downscaling technologies of dynamically downscaled GCMs are different from those for statistically downscaled GCMs, a similar comparison analysis as done in this work can be carried out between the CORDEX models and the reanalysis data. This will help study how the models respond in projecting historical wind speeds in comparison to the reanalysis data.

References

[1] American Meteorological Society. *Regional climate model*. Glossary of the American Meteorological Society. URL: https://glossary.ametsoc.org/wiki/Regional_climate_model.

[2] S. K. Angenent. *Investigating the Accuracy of the Measure-Correlate-Predict Procedure: Analyzing the Effect of Using Different Configurations and Data Types*. Dec. 2023. URL: http://repository.tudelft.nl/.

[3] K.M. Bataineh and D. Dalalah. "Assessment of wind energy potential for selected areas in Jordan". In: *Renewable Energy* 59 (2013), pp. 75–81. DOI: 10.1016/j.renene.2013.03.034. URL: http://doi.org/10.1016/j.renene.2013.03.034.

[4] Nishi Bhuvandas et al. "Review-of-Downscaling-Methods-in-Climate-Change-and-Their-Role-in-Hydrological-Studies". In: (Apr. 2016).

[5] Riccardo Bonanno, Francesca Viterbo, and Riva Giuseppe Maurizio. "Climate change impacts on wind power generation for the Italian peninsula". In: *Regional Environmental Change* (2022). Published online: 16 December 2022. DOI: 10.1007/s10113-022-02007-w. URL: https://doi.org/10.1007/s10113-022-02007-w.

[6] BYJU's. *Measures of Central Tendency: Median*. Accessed: 2024-05-15. 2024. URL: https://byjus.com/commerce/measures-of-central-tendency-median/#:~:text=A%20median%20is%20a%20positional,or%20equal%20to%20the%20median..

[7] Alex J. Cannon. "Multivariate quantile mapping bias correction: an N-dimensional probability density function transform for climate model simulations of multiple variables". In: *Climate Dynamics* 50 (2018), pp. 31–49. DOI: 10.1007/s00382-017-3580-6. URL: https://doi.org/10.1007/s00382-017-3580-6.

[8] J.A. Carta, P. Ramírez, and S. Velázquez. "A review of wind speed probability distributions used in wind energy analysis. Case studies in the Canary Islands". In: *Renewable and Sustainable Energy Reviews* 13.5 (2009), pp. 933–955. DOI: 10.1016/j.rser.2008.05.005. URL: https://doi.org/10.1016/j.rser.2008.05.005.

[9] D. Carvalho et al. "Potential impacts of climate change on European wind energy resource under the CMIP5 future climate projections". In: *Renew Energy* 101 (2017), pp. 29–40. DOI: 10.1016/j.renene.2016.08.036.

[10] CIESIN. *Downscaling*. Tech. rep. CIESIN, Unknown. URL: http://www.ciesin.org/documents/Downscaling_CLEARED_000.pdf.

[11] Circuit Globe. *Capacity Factor*. Online. Year. URL: https://circuitglobe.com/capacity-factor.html.

[12] *Climate Data Store - CMIP6 Projections*. https://cds.climate.copernicus.eu/cdsapp#!/dataset/projections-cmip6?tab=overview.

[13] Climate Impacts Group, University of Washington. *Regional Climate Models*. URL: https://cig.uw.edu/wp-content/uploads/sites/2/2020/12/wacciach2rcm643.pdf.

[14] *Climate Scenarios - Canada*. https://climate-scenarios.canada.ca/?page=cmip6-overview-notes.

[15] ClimateData.ca. *Understanding Shared Socio-Economic Pathways (SSPs)*. ClimateData.ca. URL: https://climatedata.ca/resource/understanding-shared-socio-economic-pathways-ssps/.

[16] ClimateData.ca. *Understanding Shared Socio-economic Pathways (SSPs)*. https://climatedata.ca/resource/understanding-shared-socio-economic-pathways-ssps/. 2014.

[17] Constellation. *How the Market Affects Pricing*. Accessed: 2024-05-21. 2024. URL: https://www.constellation.com/energy-101/energy-choice/how-the-market-affects-pricing.html.

[18] Wikipedia Contributors. *Moving average*. Accessed: 2024-05-15. URL: https://en.wikipedia.org/wiki/Moving_average.

[19] Wikipedia contributors. *Normalization (statistics)*. Accessed: 2024-05-21. 2024. URL: https://en.wikipedia.org/w/index.php?title=Normalization_(statistics)&oldid=1203519063.

[20] Copernicus Atmosphere Monitoring Service. *Climate Forcing*. Copernicus Atmosphere Monitoring Service. URL: https://atmosphere.copernicus.eu/climate-forcing.

[21] Copernicus Climate Change Service. *Reanalysis Q&As*. Accessed: 2024-05-22. 2022. URL: https://climate.copernicus.eu/reanalysis-qas.

[22] Copernicus Climate Change Service. *The Climate Data Store (CDS)*. https://climate.copernicus.eu/the-climate-data-store.

[23] Copernicus Climate Change Service (C3S). *Climate Reanalysis*. Copernicus Climate Change Service (C3S). URL: https://climate.copernicus.eu/climate-reanalysis.

[24] Copernicus Climate Change Service (C3S). *ERA5: Single Levels*. Copernicus Climate Change Service (C3S). URL: https://cds.climate.copernicus.eu/cdsapp#!/dataset/reanalysis-era5-single-levels?tab=overview.

[25] Copernicus Climate Change Service (C3S). *What is Copernicus Climate Change Services' ERA5 reanalysis dataset and what can it do for you?* Copernicus Climate Change Service (C3S). URL: https://climate.copernicus.eu/what-copernicus-climate-change-services-era5-reanalysis-dataset-and-what-can-it-do-you#:~:text=ERA5%20provides%20its%20global%2C%20hourly,and%20usability%20for%20certain%20applications..

[26] *CORDEX-ESD Domain*. https://cordex.org/domains/cordex-esd/.

[27] *CORDEX-Region-EURO-CORDEX*. https://cordex.org/domains/cordex-region-euro-cordex/.

[28] X. Costoya, A. Rocha, and D. Carvalho. "Using bias-correction to improve future projections of offshore wind energy resource: A case study on the Iberian Peninsula". In: *Applied Energy* 262 (Mar. 2020), p. 114562. DOI: 10.1016/j.apenergy.2020.114562.

[29] A. Dabbaghiyan et al. "Evaluation of wind energy potential in province of Bushehr, Iran". In: *Renewable and Sustainable Energy Reviews* 55 (2016), pp. 455–466. DOI: 10.1016/j.rser.2015.10.148. URL: http://doi.org/10.1016/j.rser.2015.10.148.

[30] Appsolutely Digital. *Chapter 11: Global Climate Models (GCMs)*. URL: https://www.appsolutelydigital.com/ModelPrimer/chapter11_section2.html.

[31] Eadaoin Doddy Clarke et al. "Climate change impacts on wind energy generation in Ireland". In: *Wind Energy* 25 (2021), pp. 300–312. DOI: 10.1002/we.2673.

[32] John Doe and Jane Roe. *20% Wind Energy by 2030: Increasing Wind Energy's Contribution to U.S. Electricity Supply*. Tech. rep. DOE/GO-102008-2567. National Renewable Energy Laboratory (NREL), July 2009. URL: https://www.nrel.gov/docs/fy09osti/38060.pdf.

[33] Ember Climate. *European Wholesale Electricity Price Data*. https://ember-climate.org/data-catalogue/european-wholesale-electricity-price-data/. Accessed: 2024-06-09. 2024.

[34] EPRI, Palo Alto, CA and Con Edison, New York, NY and National Grid, Waltham, MA and Oglethorpe Power Corp., Tucker, GA and Progress Energy, Raleigh, NC and Tri-State G&T, Denver, CO. *Review of General Circulation Models and Downscaling Techniques*. Tech. rep. 1019488. Palo Alto, CA: EPRI, 2009.

[35] EURO-CORDEX community. *Guidance for EURO-CORDEX climate projections data use*. Version 10. Aug. 2017.

[36] European Centre for Medium-Range Weather Forecasts (ECMWF). *Reanalysis*. European Centre for Medium-Range Weather Forecasts (ECMWF). URL: https://www.ecmwf.int/en/about/media-centre/focus/2023/fact-sheet-reanalysis#:~:text=Reanalysis%20data%20provide%20the%20most,as%20'maps%20without%20gaps'..

[37] European Commission. *Causes of Climate Change*. Accessed: 2024-05-22. 2024. URL: https://climate.ec.europa.eu/climate-change/causes-climate-change_en.

[38] J. Frost. *What is the mean and how to find it: Definition & formula*. 2023. URL: https://statisticsbyjim.com/basics/mean_average/.

[39] U. Fuentes and D. Heimann. "An improved statistical-dynamical downscaling scheme and its application to the alpine precipitation climatology". In: *Theoretical and Applied Climatology* 65 (2000), pp. 119–135.

[40] Juan Andrés García-Valero et al. "Downscaling Climate Data over Spain with a Multi-Model Ensemble of Artificial Intelligence Techniques". In: *Nonlinear Processes in Geophysics* 30 (2023), pp. 553–567. DOI: 10.5194/npg-30-553-2023. URL: https://npg.copernicus.org/articles/30/553/2023/.

[41] Geophysical Fluid Dynamics Laboratory. *Climate Model Downscaling*. https://www.gfdl.noaa.gov/climate-model-downscaling/.

[42] N Guyennon et al. "Benefits from using combined dynamical-statistical downscaling approaches – lessons from a case study in the Mediterranean region". In: *Hydrology and Earth System Sciences* 17.2 (2013), pp. 705–720.

[43] Andrea N Hahmann, Oscar García-Santiago, and Alfredo Peña. "Current and future wind energy resources in the North Sea according to CMIP6". In: *Wind Energy Science* 7.6 (2022), pp. 2373–2391. DOI: 10.5194/wes-7-2373-2022.

[44] Jonathan Herman and Magdalena Balmaseda. "ERA5: The new reanalysis dataset from ECMWF and what it means for climate research". In: *Quarterly Journal of the Royal Meteorological Society* 146.731 (2020), pp. 1505–1516. DOI: 10.1002/qj.3803. URL: https://rmets.onlinelibrary.wiley.com/doi/full/10.1002/qj.3803.

[45] Alfonso Hernanz et al. "Evaluation of statistical downscaling methods for climate change projections over Spain: Present conditions with perfect predictors". In: *International Journal of Climatology* 40.4 (2020), pp. 2493–2513. DOI: 10.1002/joc.7271.

[46] HKO. *Summary of Climate Change Risk Assessment*. https://www.arcadisost1.com/assets/uploads/pdfs/A01_Summary_CCRA.pdf. Accessed: 2024-03-18. 2023.

[47] Taiwan Climate Change Projection Information and Adaptation Knowledge Platform. "Shared Socioeconomic Pathway Introduction". In: (). URL: https://tccip.ncdr.nat.gov.tw/ds_02_06_ar6_eng.aspx.

[48] Intergovernmental Panel on Climate Change (IPCC). *IPCC Fifth Assessment Report (AR5) Synthesis Report*. Intergovernmental Panel on Climate Change (IPCC). 2014. URL: https://www.ipcc.ch/report/ar5/syr/.

[49] Intergovernmental Panel on Climate Change (IPCC). *IPCC Sixth Assessment Report (AR6) Synthesis Report - Longer Report*. Intergovernmental Panel on Climate Change (IPCC). URL: https://www.ipcc.ch/report/ar6/syr/downloads/report/IPCC_AR6_SYR_LongerReport.pdf.

[50] International Actuarial Association (IAA). *Introduction to Climate Scenarios*. International Actuarial Association (IAA). URL: https://www.actuaries.org/IAA/Documents/Publications/Papers/CRTF_Introduction_Climate_Scenarios.pdf.

[51] IPCC Data Distribution Centre. *Guide to General Circulation Models (GCMs)*. [Online; accessed 2024-03-18]. 2024. URL: https://www.ipcc-data.org/guidelines/pages/gcm_guide.html.

[52] P.C. Johnston. *Climate Risk and Adaptation in the Electric Power Sector*. Tech. rep. Manila, Philippines: Asian Development Bank - Publications, 2012.

[53] D. Kang, K. Ko, and J. Huh. "Determination of extreme wind values using the Gumbel distribution". In: *Energy* 86 (2015), pp. 51–58. DOI: 10.1016/j.energy.2015.03.126. URL: http://doi.org/10.1016/j.energy.2015.03.126.

[54] T. Kara and A. D. Şahin. "Implications of Climate Change on Wind Energy Potential". In: *Sustainability* 15 (2023), p. 14822. DOI: 10.3390/su152014822. URL: https://doi.org/10.3390/su152014822.

[55] *KNMI - CMIP6 Project*. https://www.knmi.nl/kennis-en-datacentrum/project/cmip6.

[56] J. Lee, M. Fields, and J. Lundquist. “Assessing variability of wind speed: comparison and validation of 27 methodologies”. In: *Wind Energy Science* 3 (2018), pp. 845–868.

[57] Raymond S Martinez et al. “The development of the predictive algorithms in the Simple Calculators in Assisted Reproductive Technology (SCART) software”. In: *Journal of Human Reproductive Sciences* 5.4 (2012), pp. 369–377. DOI: 10.4103/0974-1208.106342. URL: https://www.ncbi.nlm.nih.gov/pmc/articles/PMC3261962/.

[58] Edwin P Maurer. “Uncertainty in hydrologic impacts of climate change in the Sierra Nevada, California, under two emissions scenarios”. In: *Clim Change* 82 (2007), pp. 309–325.

[59] Edwin P Maurer and Philip B Duffy. “Uncertainty in projections of streamflow changes due to climate change in California”. In: *Geo Res Ltrs* 32 (2005), p. L03704.

[60] Domenico Mazzeo, Giuseppe Oliveti, and Ester Labonia. “Estimation of wind speed probability density function using a mixture of two truncated normal distributions”. In: *Renewable Energy* 115 (2018), pp. 1260–1280. ISSN: 0960-1481. DOI: 10.1016/j.renene.2017.09.043. URL: https://www.sciencedirect.com/science/article/pii/S0960148117309059.

[61] Linda O Mearns et al. *Guidelines for Use of Climate Scenarios Developed from Regional Climate Model Experiments*. Tech. rep. DDC of IPCC TGCIA, 2003.

[62] MIT Climate Portal. *Climate Models*. URL: https://climate.mit.edu/explainers/climate-models.

[63] Mott MacDonald. *Arcadis Ost 1 Offshore Wind Farm Climate Change Risk Assessment*. Assessment report. 2021.

[64] A. Mroz, J. Holnicki-Szulc, and T. Kärnä. “Mitigation of ice loading on off-shore wind turbines: feasibility study of a semi-active solution”. In: *Comput Struct* 86 (2008). DOI: 10.1016/j.compstruc.2007.01.039.

[65] Murakami, Hiroyuki and Takayabu, Yukari N. and Nakamura, Hisashi and Ishiwatari, Masaki. “Towards the development of a regional climate model for East Asia”. In: *Journal of the Meteorological Society of Japan* 82.6 (2004), pp. 1599–1623. URL: https://www.jstage.jst.go.jp/article/jmsj/82/6/82_6_1599/_pdf/-char/ja.

[66] J. Najac, J. Boé, and L. Terray. “A multi-model ensemble approach for assessment of climate change impact on surface winds in France”. In: *Clim. Dyn.* 32.5 (Apr. 2009), pp. 615–634. DOI: 10.1007/s00382-008-0440-4.

[67] National Centers for Environmental Information (NCEI). *Reanalysis*. National Centers for Environmental Information (NCEI). URL: https://www.ncei.noaa.gov/products/weather-climate-models/reanalysis.

[68] National Ocean Service. *National Ocean Service*. National Oceanic and Atmospheric Administration. URL: https://oceanservice.noaa.gov/.

[69] Nicolis, C. and Nicolis, G. “The Weather and Climate: Emergent Laws and Multifractal Cascades”. In: *Wiley Interdisciplinary Reviews: Climate Change* 1.2 (2010), pp. 168–171. DOI: 10.1002/wcc.8. URL: https://wires.onlinelibrary.wiley.com/doi/full/10.1002/wcc.8?casa_token=xfIThjHEUmwAAAAA%3AnTfyiowgwm6peD8K0MmylhEJESHb14qdxPHk0Qhzgv_ACEhhrjC4A1G0T7U4o0AoxrFBYMNMoo9rA3G8Bg.

[70] NOAA Geophysical Fluid Dynamics Laboratory. *Climate Modeling*. https://www.gfdl.noaa.gov/climate-modeling/. Accessed: 2024-03-18. 2023.

[71] National Oceanic and Atmospheric Administration (NOAA). *Climate Models*. 2023. URL: https://www.climate.gov/maps-data/climate-data-primer/predicting-climate/climate-models.

[72] hydroGOF package. *Percent bias (PBIAS)*. Accessed: 2024-05-21. 2024. URL: https://rdrr.io/cran/hydroGOF/man/pbias.html.

[73] S. C. Pryor and R. J. Barthelmie. “Assessing climate change impacts on the near-term stability of the wind energy resource over the United States”. In: *Proceedings of the National Academy of Sciences* 108.20 (2011), pp. 8167–8171. DOI: 10.1073/pnas.1019388108. URL: https://www.pnas.org/content/108/20/8167.

[74] S.C. Pryor and R.J. Barthelmie. "Assessing the vulnerability of wind energy to climate change and extreme events". In: *Clim Change* 121 (2013). DOI: 10.1007/s10584-013-0889-y.

[75] S.C. Pryor and R.J. Barthelmie. "Climate change impacts on wind energy: a review". In: *Renew Sustain Energy Rev* 14 (2010). DOI: 10.1016/j.rser.2009.07.028.

[76] K. Rao. *r or r² - when to use what*. Accessed: 2023-04-28. 2020. URL: https://towardsdatascience.com/r%C2%B2-or-r%C2%B2-when-to-use-what-4968eee68ed3.

[77] Mattia Righi et al. "Climate and carbon cycle changes from 1850 to 2100 in MPI-ESM simulations for the coupled model intercomparison project phase 5". In: *Geoscientific Model Development* 9 (May 2016), pp. 1937–1957. DOI: 10.5194/gmd-9-1937-2016. URL: https://doi.org/10.5194%2Fgmd-9-1937-2016.

[78] Rijksdienst voor Ondernemend Nederland (RVO). *Wind Resource Assessment Report,IJmuiden Ver Wind Farm Zone*. Project No WOZ222001. Nov. 2023. URL: https://offshorewind.rvo.nl/file/download/c8846f21-3f1e-4e80-abae-74596c13a409/ij56_20231218_dhi_wra-report-f.pdf.

[79] Gordon Scott. "Wind Energy and Power Calculations". In: *Wind Energy Systems* 1 (2019), pp. 77–102.

[80] L. P. Seaby et al. "Assessment of robustness and significance of climate change signals for an ensemble of distribution-based scaled climate projections". In: *Journal of Hydrology* 486.0 (2013), pp. 479–493.

[81] John Smith, Emma Johnson, and David Williams. "Assessment of wind energy potential and capacity factor over Bangladesh using Weather Research and Forecasting (WRF) model and MERRA-2 reanalysis data". In: *International Journal of Energy Research* 46.10 (2022), pp. 18630–18646. DOI: 10.1002/er.6382.

[82] Pedro M. M. Soares et al. "Climate change impact on Northwestern African offshore wind energy resources". In: *Environmental Research Letters* 14 (2019), p. 124065.

[83] Statistics4u. *Fractiles and Quantiles*. n.d. URL: http://www.statistics4u.com/fundstat_eng/cc_fractile.html.

[84] Suwarno and M. Fitra Zambak. "The Probability Density Function for Wind Speed Using Modified Weibull Distribution". In: *Department of Electrical Engineering, Universitas Muhammadiyah Sumatera Utara, Indonesia* (2021). DOI: 10.32479/ijeep.11625. URL: https://doi.org/10.32479/ijeep.11625.

[85] Indeed Editorial Team. *What Is a Rolling Average? (With Examples)*. Accessed: 2024-05-15. URL: https://www.indeed.com/career-advice/career-development/what-is-rolling-average.

[86] Gil Tertre. *The Impact of Supply Shortages on Electricity Prices*. Accessed: 2024-05-21. 2023. URL: https://www.ecb.europa.eu/press/conferences/ecbforum/shared/pdf/2023/Gil_Tertre_paper.pdf.

[87] The Pennsylvania State University. *Wind Energy and Power Calculations*. The Pennsylvania State University. 2023. URL: https://www.e-education.psu.edu/emsc297/node/649.

[88] Kevin E Trenberth. "Climate change caused by human activities is happening and it already has major consequences". In: *Journal of energy & natural resources law* 36.4 (2018), pp. 463–481.

[89] U.S. Energy Information Administration. *Prices and Factors Affecting Prices*. Accessed: 2024-05-21. 2024. URL: https://www.eia.gov/energyexplained/electricity/prices-and-factors-affecting-prices.php.

[90] United Nations. *What is Climate Change?* https://www.un.org/en/climatechange/what-is-climate-change. Accessed: 2023-03-18. 2023.

[91] University of Reading. *Regional vs Global Models: From the Perspective of a Polar Climate Scientist*. URL: https://blogs.reading.ac.uk/weather-and-climate-at-reading/2021/regional-vs-global-models-from-the-perspective-of-a-polar-climate-scientist/.

[92] Frauke Urban and Tom Mitchell. *Climate change, disasters and electricity generation*. Strengthening climate resilience discussion paper 8. Available at Institute of Development Studies. Institute of Development Studies, 2011.

[93] USDA Northwest Climate Hub. *What are Climate Model Phases and Scenarios?* USDA Northwest Climate Hub. URL: https://www.climatehubs.usda.gov/hubs/northwest/topic/what-are-climate-model-phases-and-scenarios.

[94] D. Viner. *Spatial Downscaling*. Retrieved from http://www.cccsn.ec.gc.ca/?page=downscaling. 2012.

[95] Jing Wang and Hong Li. "The Impact of Electricity Price on Power-Generation Structure: Evidence From China". In: *Frontiers in Environmental Science* 9 (2021), p. 733809. URL: https://www.frontiersin.org/articles/10.3389/fenvs.2021.733809/full.

[96] *WCRP-CMIP*. https://wcrp-cmip.org/.

[97] *WGCM-CMIP*. https://www.wcrp-climate.org/wgcm-cmip. Accessed: insert date here.

[98] Wikipedia contributors. *Haversine formula — Wikipedia, The Free Encyclopedia*. 2023. URL: https://en.wikipedia.org/wiki/Haversine_formula.

[99] R.L. Wilby et al. *Guidance for use climate scenarios developed from statistical downscaling methods*. Unpublished material. Supporting material for IPCC. 2004.

[100] J. Wu, J. Wang, and D. Chi. "Wind energy potential assessment for the site of Inner Mongolia in China". In: *Renewable and Sustainable Energy Reviews* 21 (2013), pp. 215–228. DOI: 10.1016/j.rser.2012.12.060. URL: http://doi.org/10.1016/j.rser.2012.12.060.

[101] Seleshi G. Yalew et al. "Impacts of climate change on energy systems in global and regional scenarios". In: *Nature Energy* 5 (2020), pp. 793–798. DOI: 10.1038/s41560-020-0664-z. URL: https://www.nature.com/articles/s41560-020-0664-z.

[102] Eduardo Zorita and Hans von Storch. "The analog method as a simple statistical downscaling technique: comparison with more complicated methods". In: *Journal of Climate* 12.8 (1999), pp. 2474–2489.

A

Appendix A

A.1. Models list

The GCMs have been statistically diwnscaled to a resolution of 3km.

A.1.1. Downscaled CMIP6 GCMs

Given below is the list of the downscaled CMIP6 models that have been used in this study as the statistically downscaled GCMs for Sites NS2,FR,IT,UK1 for SSP2-4.5 and SSP5-8.5 with exceptions given after the table.

Table A.1: List Downscaled CMIP 6 models used in this report

CMIP 6 Model	Institution	Country	Resolution (km)	Citation
ACCESS-CM2	CSIRO-ARCCSS CSIRO and Austr. Res. Council Centre of Excellence for Climate System Science	Australia	140	Dix et al. (2019a)
BCC-CSM2-MR	BCC Beijing climate centre, china	China	100	Xin et al. (2018)
CESM2-WACCM	NCAR National Center for Atmospheric Research (USA)	USA	100	Danabasoglu (2019s)
CMCC-CM2-SR5	CMCC Centro Euro-Mediterraneo sui Cambiamenti Climatici (Italy)	Italy	100	Gopinathan et al. (2019a)
CMCC-ESM2	CMCC Centro Euro-Mediterraneo sui Cambiamenti Climatici (Italy)	Italy	100	Lovato and Peano (2020a)
CanESM5	CCCMa Canadian Centre for Climate Modelling and Analysis	Canada	250	Swart et.al. (2019d)
EC-Earth3	EC-Earth Consortium	Europe	80	EC-Earth Consortium (EC-Earth) (2019a)
FGOALS-g3	CAS Chinese Academy of Sciences China	China	190	Li (2019a)

GFDL-CM4	NOAA-GFDL National Oceanic and Atmospheric Administration, Geophysical Fluid Dynamics Laboratory USA	USA	100	Guo et.al. (2018a)
GFDL-ESM4	Geophysical Fluid Dynamics Laboratory (USA)	USA	100	Krasting et al. (2018b)
IITM-ESM	Centre for climate change Research,Indian Institute of Tropical Meteorology India	India	170	Gopinathan et al.(2019a)
INM-CM4-8	INM Institute of Numerical Mathematics (Russia)	Russia	150	Volodin et al. (2019a)
INM-CM5-0	INM Institute of Numerical Mathematics (Russia)	Russia	150	Volodin et al. (2019d)
MIROC6	Japan Agency for Marine-Earth Science and Technology	Japan	250	Tatebe and Watanabe (2018)
MPI-ESM1-2-HR	MPI-M Max Planck Institute for Meteorology	Germany	80	Jungclaus et.al. (2019a))
MPI-ESM1-2-LR	MPI-M Max Planck Institute for Meteorology	Germany	170	Wieners et al. (2019b)
MRI-ESM2-0	MRI Meteorological Research Institute	Japan	100	Yukimoto et al. (2019e)
NorESM2-LM	NCC Norwegian Climate Centre	Norway	190	Seland et al. (2019a)
NorESM2-MM	NCC Norwegian Climate Centre	Norway	100	Bentsen et al. (2019b)
TaiESM1	AS-RCEC Research Center for Environmental Changes, Academia Sinica Taiwan	China	100	Lee and Liang (2019)

Exception: GCM IITM-ESM has only been used in NS2,FR SSP5-8.5, UK1.

A.1.2. Downscaled CMIP5 GCMs

Given below is the list of the downscaled CMIP5 models that have been used in this study as the statistically downscaled GCMs for Sites NS1, UK2, UK3, NA1 and NA2 under RCP4.5 and RCP8.5 with exceptions given after the table.

Table A.2: List of downscaled CMIP5 Models used in this study

CMIP5 Model	Institution	Country	Resolution (degrees)
ACCESS1-0	Commonwealth Scientific and Industrial Research Organisation - Bureau of Meteorology	Australia	1.25° x 1.875°
CMCC-CESM	Centro Euro-Mediterraneo sui Cambiamenti Climatici	Italy	3.75° x 3.75°
CMCC-CM	Centro Euro-Mediterraneo sui Cambiamenti Climatici	Italy	3.75° x 3.75°
CMCC-CMS	Centro Euro-Mediterraneo sui Cambiamenti Climatici	Italy	3.75° x 3.75°

CNRM-CM5	Centre National de Recherches Météorologiques - Centre Européen de Recherche et Formation Avancée en Calcul Scientifique	France	1.4° x 1.4°
CSIRO-Mk3-6-0	Commonwealth Scientific and Industrial Research Organisation - Queensland Climate Change Centre of Excellence	Australia	1.865° x 1.875°
CanESM2	Canadian Centre for Climate Modelling and Analysis	Canada	2.8125° x 2.8125°
GFDL-CM3	Geophysical Fluid Dynamics Laboratory	USA	2.5° x 2°
GFDL-ESM2G	Geophysical Fluid Dynamics Laboratory	USA	2.5° x 2°
GFDL-ESM2M	Geophysical Fluid Dynamics Laboratory	USA	2.5° x 2°
HadGEM2-AO	Met Office Hadley Centre	UK	1.875° x 1.25°
HadGEM2-CC	Met Office Hadley Centre	UK	1.875° x 1.25°
HadGEM2-ES	Met Office Hadley Centre	UK	1.875° x 1.25°
IPSL-CM5A-LR	Institut Pierre-Simon Laplace	France	3.75° x 1.875°
IPSL-CM5A-MR	Institut Pierre-Simon Laplace	France	3.75° x 1.875°
IPSL-CM5B-LR	Institut Pierre-Simon Laplace	France	3.75° x 1.875°
MIROC5	Model for Interdisciplinary Research on Climate	Japan	1.4° x 1.4°
MPI-ESM-LR	Max Planck Institute for Meteorology	Germany	1.875° x 1.875°
MPI-ESM-MR	Max Planck Institute for Meteorology	Germany	1.875° x 1.875°
MRI-CGCM3	Meteorological Research Institute	Japan	1.125° x 1.125°
inmcm4	Institute of Numerical Mathematics	Russia	2° x 2.5°

Exception: CMCC-CESM and HadGEM2-AO were used under climate change scenario RCP8.5.

B

Results

B.1. CORDEX analysis

The plote below represent the long term mean wind speed during operational years by 11 CORDEX models under RCP4.5. Wind speeds with same colour represent same GCM used by different RCMs.

NS1

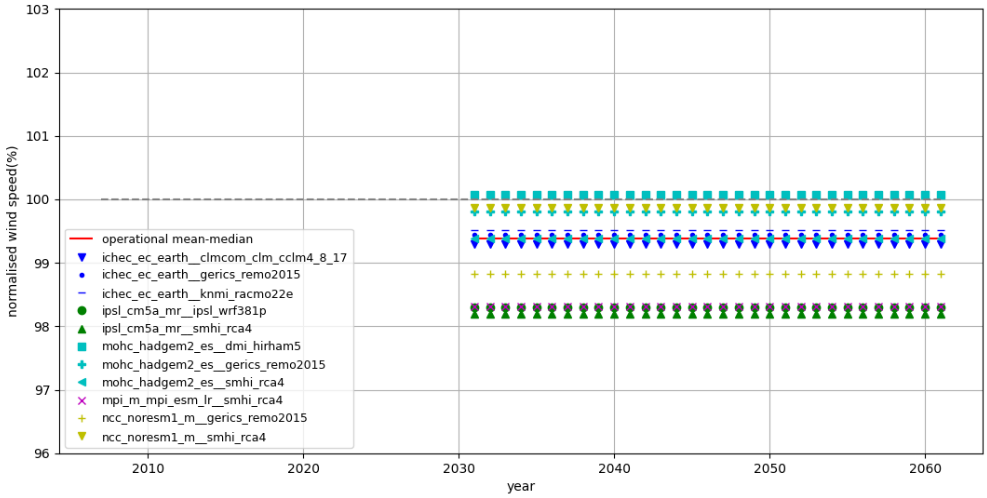

Figure B.1: Mean wind speed projected by 11 CORDEX models at site: NS1

NS2

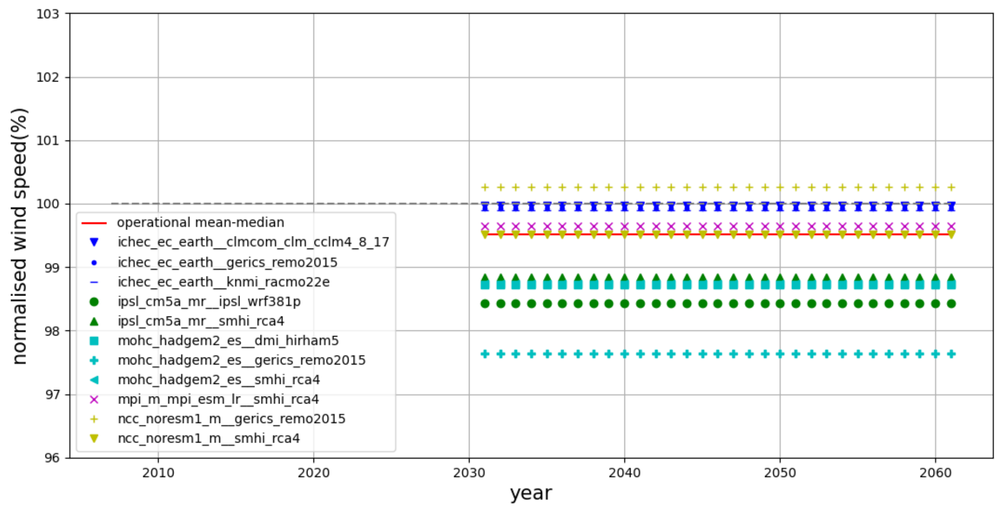

Figure B.2: Mean wind speed projected by 11 CORDEX models at site: NS2

FR

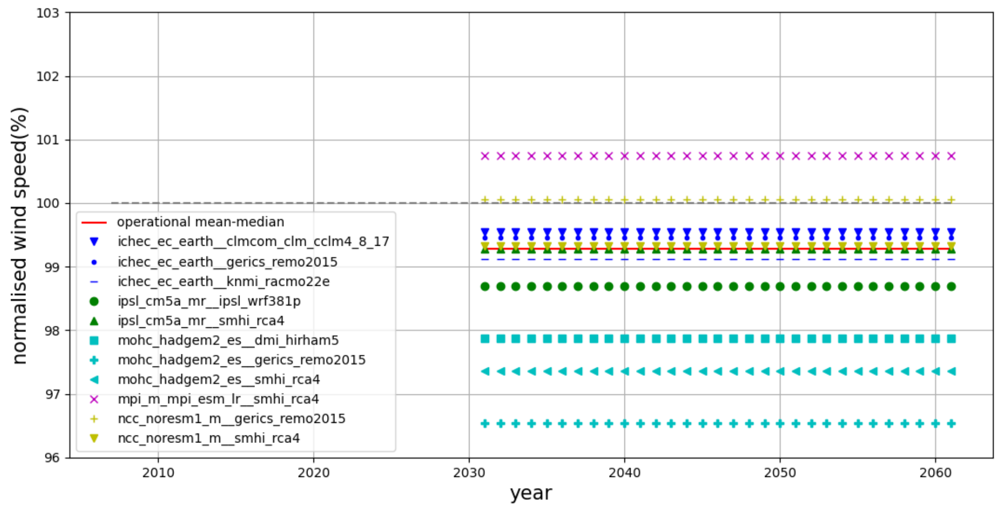

Figure B.3: Mean wind speed projected by 11 CORDEX models at site: FR

IT

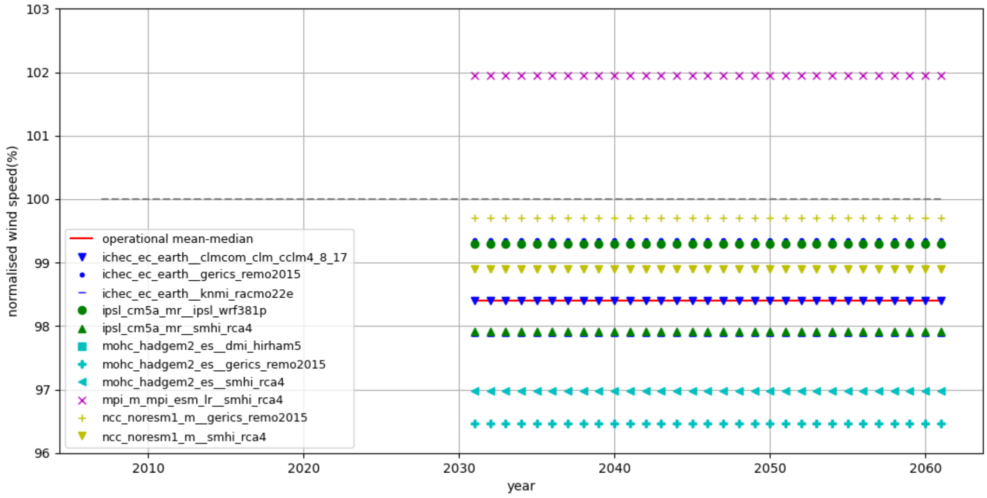

Figure B.4: Mean wind speed projected by 11 CORDEX models at site: IT

UK1

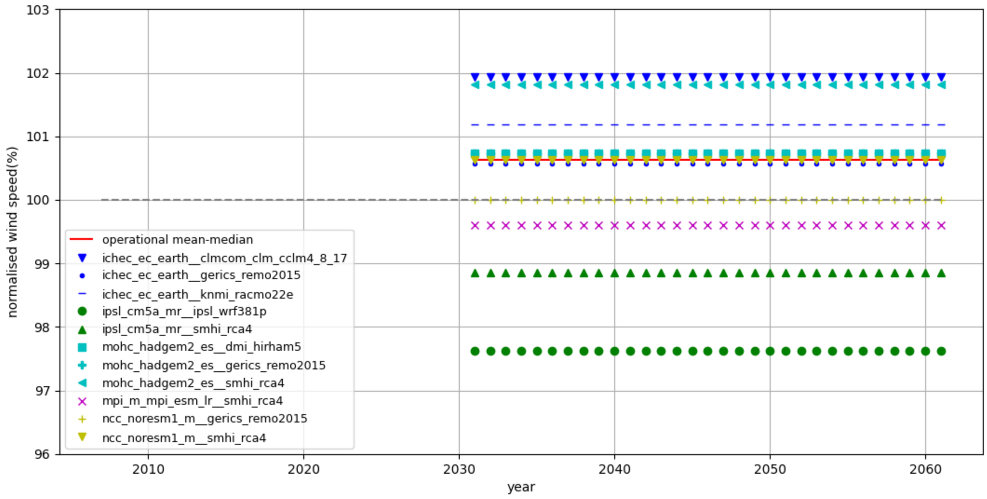

Figure B.5: Mean wind speed projected by 11 CORDEX models at site: UK1

UK2

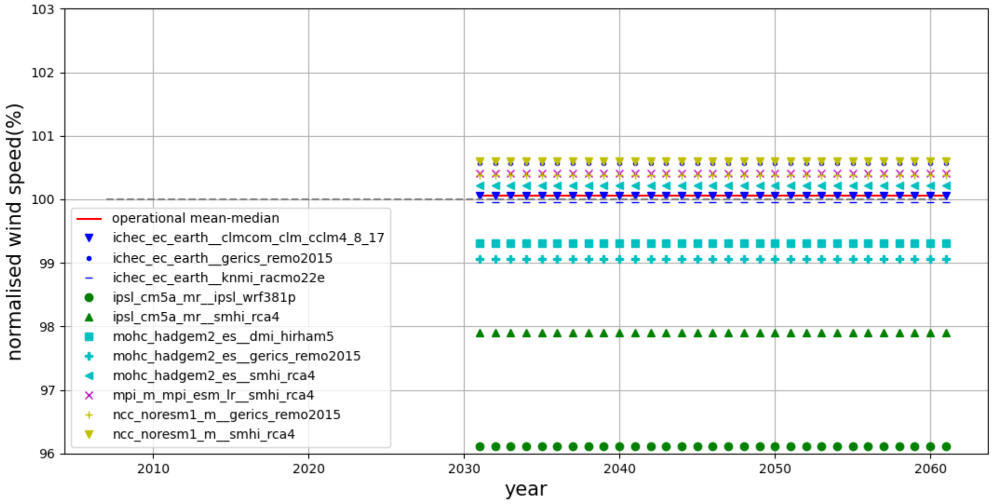

Figure B.6: Mean wind speed projected by 11 CORDEX models at site: UK2

UK3

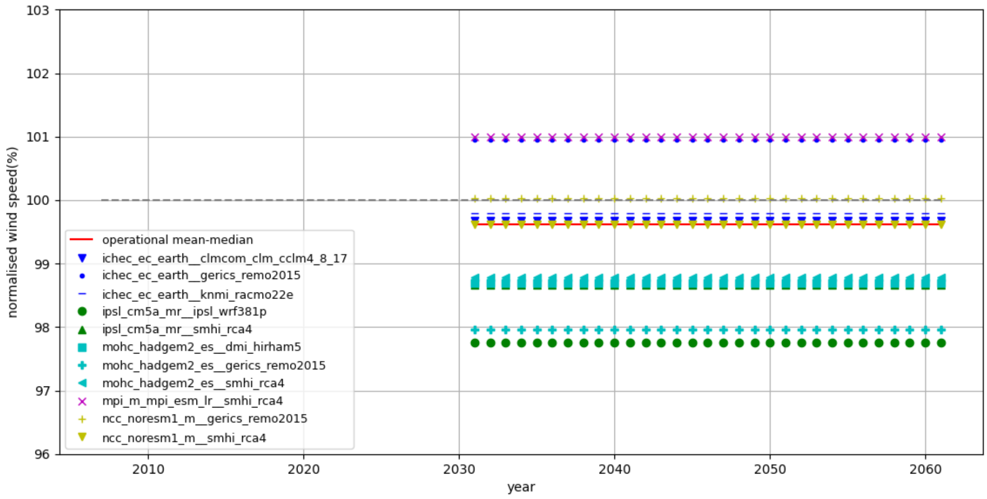

Figure B.7: Mean wind speed projected by 11 CORDEX models at site: UK3

B.2. PDF for wind speeds at site NS2 and FR

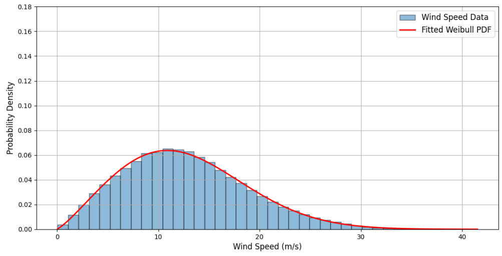

(a) PDF for wind speeds at site NS2

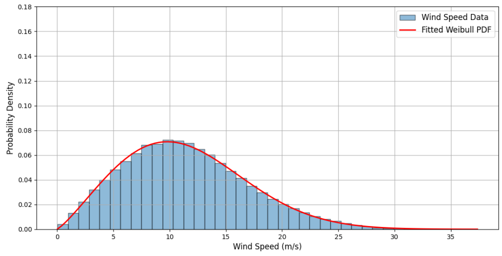

(b) PDF for 10% lower wind speeds at site NS2

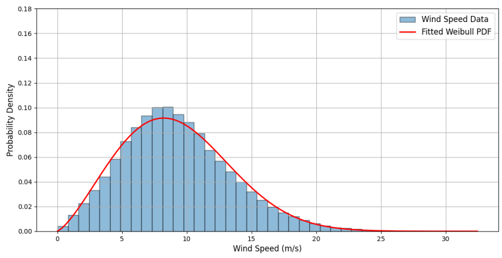

(c) PDF for wind speeds at site FR

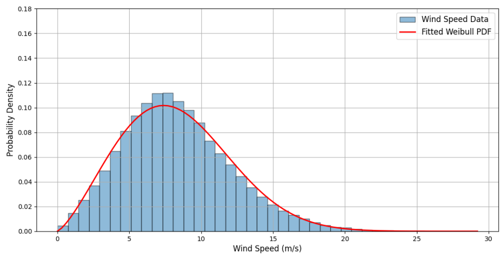

(d) PDF for 10% wind speeds at site FR

Figure B.8: PDF for wind speeds at site NS1 and IT before and after 10% decline

Table B.1: Scale and shape factor and AEP values based on decline in wind speed

Parameter	NS1	NS2	FR	IT
% change	1%	1%	1%	1%
k	2.32	2.20	2.33	1.75
a	10.88	10.30	7.49	5.13
AEP	25.29	23.36	13.59	6.24
% change	3%	3%	3%	3%
k	2.32	2.20	2.33	1.75
a	10.66	10.09	7.34	5.03
AEP	24.69	22.76	12.99	5.91
% change	5%	5%	5%	5%
k	2.32	2.20	2.33	1.75
a	10.44	9.89	7.19	4.93
AEP	24.07	22.14	12.38	5.59
% change	10%	10%	10%	10%
k	2.32	2.20	2.33	1.75
a	9.89	9.37	6.81	4.67
AEP	22.40	20.51	10.87	4.82
historic				
k	2.32	2.20	2.33	1.75
a	10.99	10.41	7.57	5.19
AEP	25.58	23.65	13.90	6.40

B.3. Distance vs MAPE values

Table B.2: Comparison of Distance and Bias for Wind Speed Change Factors across Different Sites

Site	NS1		NS2		FR		IT	
GCM	Distance (km)	MAPE (%)	Distance (km)	MAPE (%)	Distance (km)	MAPE (%)	Distance (km)	MAPE (%)
$pe - access_c m2$	81.27	44.65	75.40	10.74	47.40	16.20	50.08	37.72
$pe - BCC - CSM2 - MR$	43.50	34.89	71.48	10.14	19.55	57.57	41.87	91.46
$pe - CESM2$	25.01	30.43	49.63	14.56	30.42	15.12	2.77	58.39
$pe - CMCC - CM2 - SR5$	25.01	31.49	49.63	10.80	30.42	27.01	2.77	27.06
$pe - CMCC - ESM2$	25.01	33.32	49.63	9.59	30.42	26.93	2.77	29.35
$pe - GFDL - ESM4$	36.14	44.04	50.52	11.21	52.91	22.30	61.83	15.30
$pe - HadGEM3 - GC31 - LL$	81.27	37.38	75.40	10.20	47.40	10.99	50.08	42.85
$pe - IITM - ESM$	16.87	34.23	41.15	20.38	92.14	16.68	56.64	103.74
$pe - INM - CM4 - 8$	15.44	48.60	58.06	13.75	77.23	17.78	59.87	90.18
$pe - INM - CM5 - 0$	15.44	48.99	58.06	16.89	77.23	14.16	59.87	95.86
$pe - IPSL - CM6A - LR$	55.09	34.47	99.80	10.27	96.60	28.11	123.62	85.89
$pe - KACE - 1 - 0 - G$	81.27	16.15	75.40	31.73	47.40	51.56	50.08	128.62
$pe - KIOST - ESM$	58.15	51.67	95.81	41.73	55.87	33.01	43.60	65.72
$pe - MIROC6$	69.32	51.50	40.08	39.88	11.51	25.97	31.22	25.97
$pe - MPI - ESM1 - 2 - LR$	72.80	40.81	45.55	10.68	57.47	37.08	122.81	142.09
$pe - MRI - ESM2 - 0$	43.50	45.14	71.48	12.08	19.55	16.44	41.87	55.30
$pe - NorESM2 - LM$	42.44	35.52	111.01	13.14	103.01	39.79	115.89	46.45
$pe - NorESM2 - MM$	25.01	31.30	49.63	12.72	30.42	16.70	2.77	36.46
$pe - UKESM1 - 0 - LL$	81.27	41.92	75.40	10.92	47.40	13.52	50.08	46.39
$pe - MIROC - ES2L$	114.34	59.49	45.55	10.68	136.25	16.53	54.54	34.72